8-31-2020

# The Effect of a Leading Sound on the Local-Field Potentials Elicited by a Trailing Sound in the Rat's Inferior Colliculus

Syed Anam Asim
*University of Windsor*

# THE EFFECT OF A LEADING SOUND ON THE LOCAL-FIELD POTENTIALS ELICITED BY A TRAILING SOUND IN THE RAT'S INFERIOR COLLICULUS

by

Syed Anam Asim

A Thesis
Submitted to the Faculty of Graduate Studies
through the Department of Integrative Biology
in Partial Fulfillment of the Requirements for
the Degree of Master of Science at the
University of Windsor

Windsor, Ontario, Canada

# THE EFFECT OF A LEADING SOUND ON THE LOCAL-FIELD POTENTIALS ELICITED BY A TRAILING SOUND IN THE RAT'S INFERIOR COLLICULUS

by
Syed Anam Asim

APPROVED BY:

_____

K. Milne
Department of Kinesiology

_____

J. Dason
Department of Biomedical Sciences

_____

H. Zhang, Advisor
Department of Biomedical Sciences

July 28, 2020

## DECLARATION OF ORIGINALITY

I hereby certify that I am the sole author of this thesis and that no part of this thesis has been published or submitted for publication.

I certify that, to the best of my knowledge, my thesis does not infringe upon anyone's copyright nor violate any proprietary rights and that any ideas, techniques, quotations, or any other material from the work of other people included in my thesis, published or otherwise, are fully acknowledged in accordance with the standard referencing practices. Furthermore, to the extent that I have included copyrighted material that surpasses the bounds of fair dealing within the meaning of the Canada Copyright Act, I certify that I have obtained a written permission from the copyright owner(s) to include such material(s) in my thesis and have included copies of such copyright clearances to my appendix.

I declare that this is a true copy of my thesis, including any final revisions, as approved by my thesis committee and the Graduate Studies office, and that this thesis has not been submitted for a higher degree to any other University or Institution.

## ABSTRACT

The perception of one sound can be influenced by another sound in the environment, with the effect dependent on the spectrotemporal and spatial relationship between the sounds. Mechanisms responsible for this perceptual phenomenon is dependent on the integration of neural signals driven by the two ears in brain centers responsible for hearing. The inferior colliculus (IC) as a midbrain structure is important for the processing of acoustic information. To understand why/how the perception of one sound is influenced by another sound, it is important to study how the two sounds interact with each other in generating responses in the IC.

In this study, I examined the effect of a leading sound on the responses elicited by a trailing sound in an ensemble of neurons in the IC. Local-field potentials (LFPs) were recorded to reflect responses of neural ensembles. The two sounds were first colocalized at the ear that was contralateral to the recording site. Then the two sounds were then spatially separated. I evaluated whether the influence generated by a leading sound was dependent on the spatial relationship as well as the time gap between the leading and trailing sounds.

Results indicated that the LFPs elicited by a trailing sound were suppressed by a leading sound no matter whether the leading sound was at the contralateral or ipsilateral ear. The suppressive effect was larger when a leading sound was presented at the contralateral than the ipsilateral ear. Furthermore, the effect was larger when the two sounds were separated by a short time gap. Inhibitory neurotransmitter antagonists, gabazine and strychnine significantly decreased the suppression produced by the leading sound but did not eliminate it. These results suggest that local inhibitory interaction in the inferior colliculus may not be the only factor that is responsible for the suppressive effect produced by the leading sound. Results from this study are important for understanding neural mechanisms responsible for hearing in a real-world situation.

## ACKNOWLEDGMENTS

Firstly, I want to sincerely thank Dr. Zhang for being my academic mentor. There are several skills I have been able to develop under his guidance such as critical thinking skills, effective scientific and personal communication, and being an effective leader. There were endless challenges I faced at every turn of my early research career, and it was comforting knowing that Dr. Zhang was there to help me deal with them objectively. I will always be indebted to you for all the help you have provided me including filling out countless references for work-study applications, medical school references, and also multiple national scholarships such as OGS and NSERC, both, of which I was awarded. I can confidently say that without your help I would not have the opportunity to pursue my academic aspirations. I could not have asked for a better mentor to introduce me to the academic realm.

I am extremely grateful to have a supportive family who has been so caring and loving. They have supported me since day one and continue to support me in every step of my personal and academic life. Both of my parents have sacrificed so much for me so that I can pursue my dreams. I want to sincerely thank my mom for selflessly waking up every morning and packing me delicious lunches and always being someone who I can share my thoughts with.

I am thankful for all the lab members who have helped me in my research journey. Sarah Tran has been very helpful in developing computer circuits and macros which have been instrumental to my research. Nicholas Reynolds and Olivia Sauve have both been very helpful in analyzing data and running some parts of my experiments. I want to thank Mathiang G. Chot for teaching me his elite surgical skills and sharing some of the workload of Excitable Cells while I run my experiments. I always felt open to asking you questions without feeling judged. Also, thanks for answering my last-minute questions during my thesis writing.

# TABLE OF CONTENTS

## LIST OF FIGURES

## LIST OF ABBREVIATIONS

| Abbreviations | Full form |
|---|---|
| AAF | Anterior auditory field |
| A1 | Primary auditory cortex |
| ALF | Amplitude level function |
| AVCN | Anteroventral cochlear nucleus |
| CF | Central frequency |
| CIC | Central nucleus of the inferior colliculus |
| CN/CNC | Cochlear nucleus |
| DCIC | Dorsal cortex of the inferior colliculus |
| DCN | Dorsal cochlear nucleus |
| DNLL | Dorsal nucleus of lateral lemniscus |
| FTC | Frequency tuning curve |
| IC | Inferior colliculus |
| ILD | Interaural level difference |
| ISI | Interstimulus interval |
| ITD | Interaural time difference |
| LCIC | Lateral cortex of the inferior colliculus |
| LFP | Local-field potential |
| LSO | Lateral superior olive |
| MGB/MGN | Medial geniculate nucleus/body |
| MNTB | Medial nucleus of trapezoid body |
| MSO | Medial superior olive |
| NLL | Nucleus of lateral lemniscus |
| NR | Normalized ratio |
| SD | Standard deviation |
| SO/SOC | Superior olivary complex |
| SPON | Superior paraolivary nucleus |

# CHAPTER I. INTRODUCTION

## 1.1 Hearing in an acoustic environment with multiple sounds

Animals including humans normally live in a complex acoustic environment that contains multiple sounds with different qualities, intensities, timing, and locations. It is of critical importance for survival, communication, and many other behavioral needs of animals to analyze information from the acoustic environment and find “what” and “where” each sound is. The perception of one sound can be affected by another sound in the environment. For instance, the sound of one's speech can be difficult to interpret when there are other sounds in the environment, a phenomenon termed masking (Bronkhorst 2000). Although the perception of one sound being affected by another sound has been examined in human behavioural studies (Crocker 1997; Fastl and Zwicker 2007; Litovsky 2005), neurophysiological studies on animal models serve to bridge the gap between the observed behaviour and their potential neural correlates (Chot et al. 2019; Flammino and Clopton 1975; Palmer and Kuwada 2005; Zhang and Kelly 2009). This study seeks to examine how the responses to one sound are affected by another sound in the auditory midbrain by varying the frequency, timing, and location of the sounds.

## 1.2 Human psychoacoustics

Psychoacoustics describes the relationship between the physical stimuli of the sound and the sensory perception of a sound (Fastl and Zwicker 2007). An example of a psychoacoustic procedure in humans is the method of adjustment where subjects may be asked to vary the stimulus frequency until they perceive it matches a reference tone (Crocker 1997; Fastl and Zwicker 2007; Pulkki and Karjalainen 2015).

### *1.2.1 Perception of spectral, temporal, and directional cues generated by a single sound*

The frequency range of human hearing is between 20 Hz and 20 kHz (Fastl and Zwicker 2007). The sound pressure level for detecting low-frequency sounds is high and reaches about 40 dB at 50 Hz (Fastl and Zwicker 2007). Human hearing is most sensitive to sounds between 2 and 5 kHz reaching threshold levels below 0 dB (Fastl and Zwicker 2007). Sound pressure levels stay between 0 and 15 dB for frequencies below 12 kHz and rise rapidly for frequencies beyond this point (Fastl and Zwicker 2007).

Studies have indicated that humans are unable to perceive differences in sound durations which are below 200 ms (Fastl and Zwicker 2007). The subjective duration of the sound is longer than the physical duration of the sound for sounds shorter than 200 ms long (Fastl and Zwicker 2007). In sound paradigms, where tones are presented separated by a pause, subjects are unable to distinguish the physical durations of the tone and pauses when the duration of either one varies by less than a 100 ms (Burghardt 1973).

There are three planes of symmetry that can be used to describe the location of the sound: the frontal plane, the horizontal plane, and the median plane (Figure 1) (Fastl and Zwicker 2007). In the horizontal plane, any non-zero value of $\varphi$ will result in differences in the time and intensity of the sound between the two ears which helps subjects localize the direction of a sound (also referred to as interaural time and interaural level differences) (Fastl and Zwicker 2007).

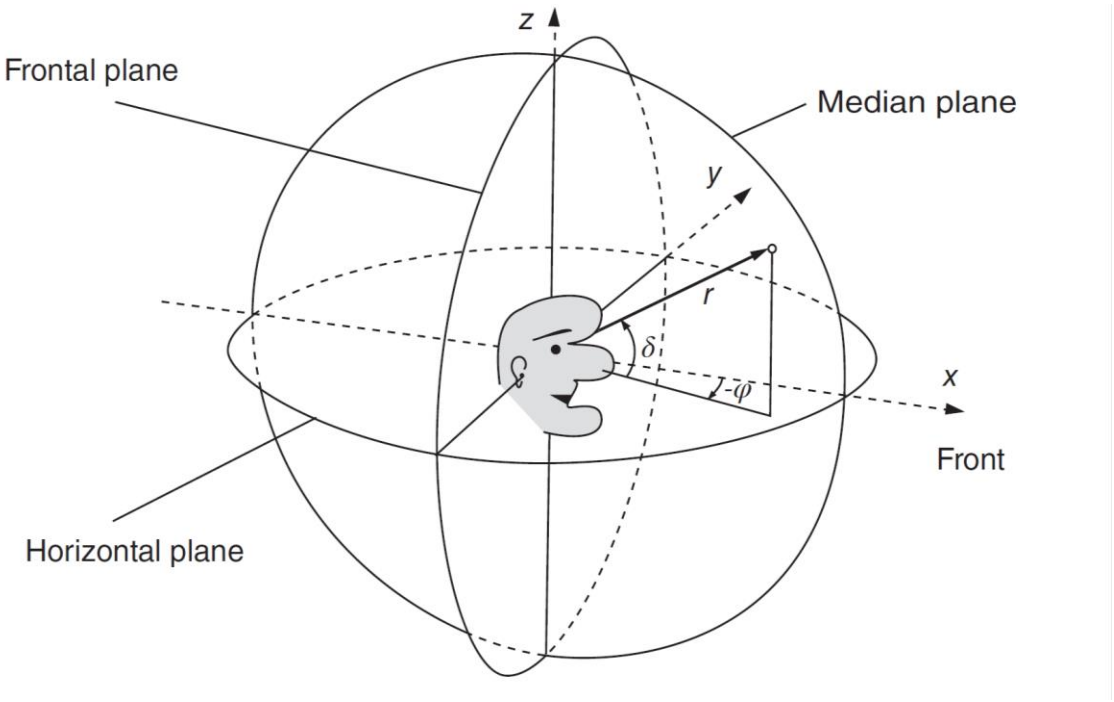


**Figure 1.** The coordinate system used to describe the spatial location of a sound. Adapted from Pulkki and Karjalainen 2015. The $\varphi$ symbol is showing the angle between the sound in the horizontal plane while the $\delta$ is showing the angle of the sound in the median plane.

### *1.2.2 Masking*

The most important perceptual phenomenon related to this study is masking. This is a perceptual phenomenon in which the perception of one sound (test) is affected by the presence of another sound (masker) (Crocker 1997). A masker may make the test sound inaudible, decrease its loudness, or make it hard to discern (Crocker 1997). For instance, a listener may find it difficult to hear a person's speech (signal) if there is also the sound of an ambulance siren (mask) nearby. Masking can be influenced by the temporal, spectral, and spatial aspects (Pulkki and Karjalainen 2015).

*1.2.2.1 Temporal masking*

The three types of temporal masking are forward, simultaneous, and backward masking (Fastl and Zwicker 2007). In forward masking, the masker is presented before the test sound and its' effect decreases 5-10 ms after its offset and can last between 100-200 ms (Fastl and Zwicker 2007). Moreover, the forward masking effect is also dependent on the level and duration of the masker (Figure 2) (Pulkki and Karjalainen 2015). As the level of the masker increases, the masked threshold (level of the test sound to become audible) of the test sound increases and it needs to be presented at higher levels or increase time delays to be perceived (Figure 2A) (Fastl and Zwicker 2007). If the duration of the masker is increased from 5 ms to 200 ms, the masked threshold of the test tone also increases (Figure 2B) (Fastl and Zwicker 2007).

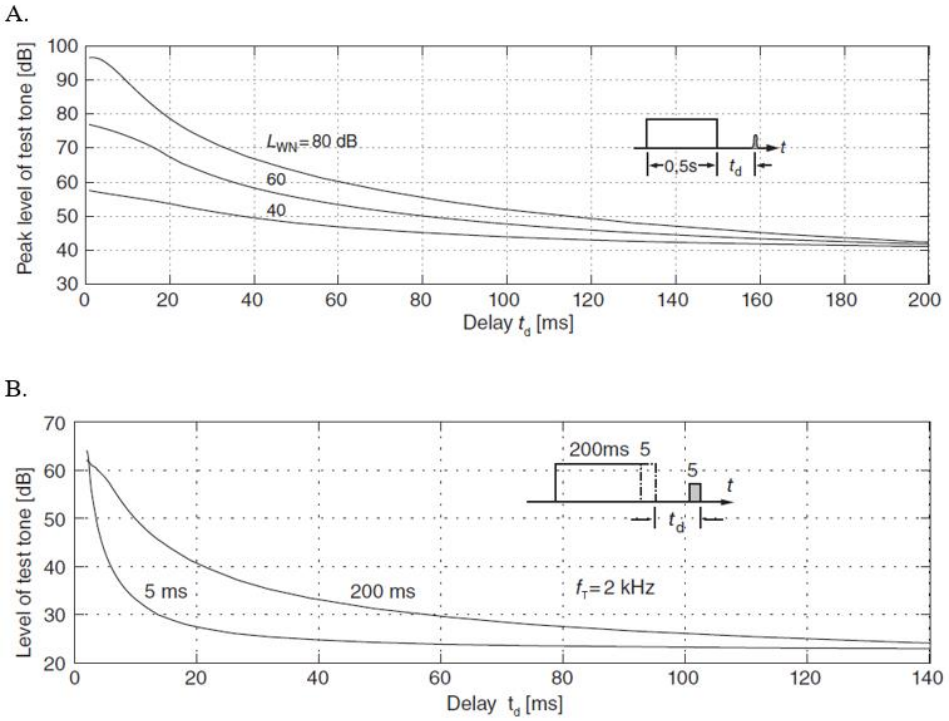


**Figure 2.** A conceptual illustration of the forward masking effect. **A.** A 0.5s long white noise (WN) masker was presented at 80, 60, and 40 dB before a test sound at various delays between the two sounds, $t_d$. The peak level of the test tone is associated with its detection threshold. **B.** A

200 ms and 5 ms masker was presented before a test sound. Adapted from Pulkki and Karjalainen (2015).

Another temporal condition of masking is simultaneous masking in which the test sound is overlapped with the masker sound presentation (Figure 3) (Fastl and Zwicker 2007). The effect of masking is dependent on the duration of the test sound, the delay between the onset of the masker and test sound, and frequencies of the two sounds (Fastl and Zwicker 2007). At shorter delays, Δt, the masked threshold is more elevated than at longer delays.

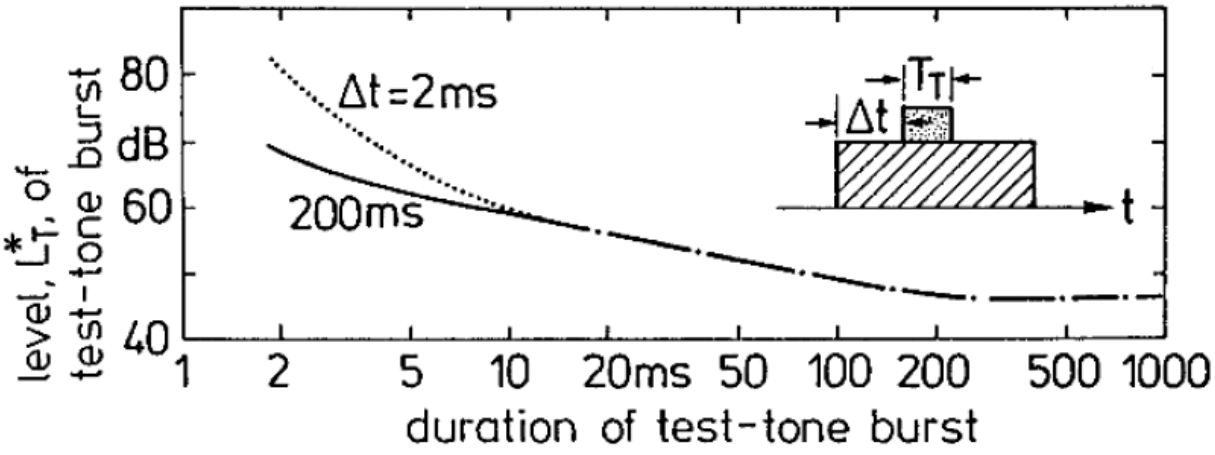


**Figure 3.** A conceptual illustration of simultaneous masking. Test sound with a duration of $T_T$ is presented simultaneously with a masker after a delay of 2 ms and 200 ms from the onset of the masker sound. Modified from Fastl and Zwicker (2007).

Backward masking is when the masker affects the perception of test sounds presented before it. This type of masking is shown to affect sounds only 5-10 ms before the onset of the masker and effects low-level sounds (Pulkki and Karjalainen 2015). All three types of temporal masking are dependent on spectral characteristics of the sounds involved (Fastl and Zwicker 2007).

*1.2.2.2 Spectral masking*

Spectral masking is when a sound with a certain spectral content makes the detection of another sound with a different spectral content difficult (Pulkki and Karjalainen 2015). In spectral masking, the masker can be a noise (broadband or narrowband) or pure tone. Broadband noise masker is composed of a large number of frequencies and the level of the noise can affect the detection threshold of the test sound (Pulkki and Karjalainen 2015). In contrast, pure tone masker is composed of a single frequency (Pulkki and Karjalainen 2015). For a narrowband noise masker, the threshold of test tone detection increases for tones within the noise band and is the highest for the test tone corresponding to the central frequency of the masker (Figure 4) (Pulkki and Karjalainen 2015). Similarly, the masking threshold is the highest for pure tone maskers with a frequency closest to that of the test sound (Small 1959).

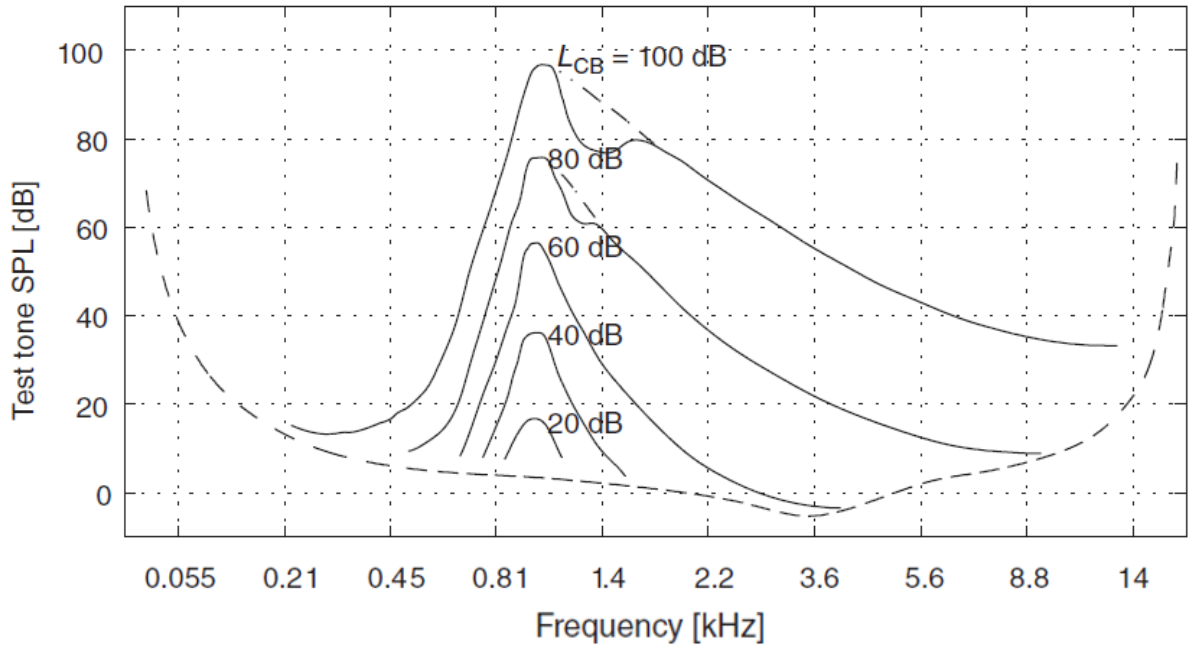


**Figure 4.** The masking threshold curve resulting from a narrowband noise masker centered at 1kHz with different levels (*L*). Modified from Pulkki & Karjalainen (2015).

*1.2.2.3 Spatial masking*

A change in direction of a masker source can change the effect it has on the test sound. For instance, studies examining the perception of speech in noise first present both the masker and test sound from a colocalized position (Figure 5A). Next, the masker is separated from the test sound (Figure 5B). The results reported from multiple studies indicate that subjects showed an improvement in word identification in the separated condition with monaural or binaural masker cues (Figure 5C) (Freyman et al., 1999; Litovsky, 2005; Plomp & Mimpen, 1981).

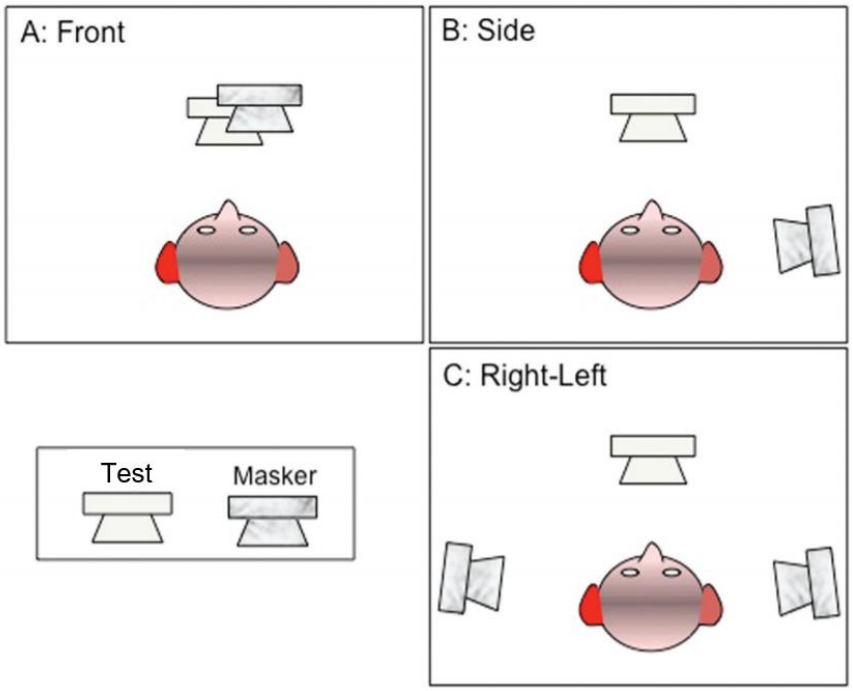


**Figure 5.** An experimental setup of a study examining the role of spatial cues in speech perception. **A.** The masker and the test sound are presented from a colocalized position in front of the subject. **B.** The masker is moved to the right ear while the test sound is presented from the front. **C.** A masker is placed in front of both ears while the test is presented from the front of the subject. Modified from Litovsky (2012).

### 1.3 Human neurophysiological studies

To find the neural correlates of psychoacoustic phenomena such as masking, neurophysiological studies serve as a gateway. Some studies have examined neural responses in human subjects to different sound in the environment (Ahveninen et al. 2014; Bernstein 1999). However, the neurophysiological studies conducted in humans have been limited to non-invasive procedures such as using electroencephalographic equipment to record event-related potentials (ERP) (Alho et al., 1990; Frey et al., 2015; Leppänen et al., 1997). ERP is scalp recording electrical potentials that reflect the summed activity of groups of neurons in the brain (Regan 1972). Some ERP studies in humans have focused on the mismatch negativity component of the ERP recording. Mismatch negativity is referred to a negative peak on an ERP recording which has shown to be elicited during stimulus irregularities such as changes in loudness (Näätänen et al., 1987), pitch (Näätänen et al. 1978; Sams et al. 1985), duration (Jacobsen & Schröger, 2003; Kaukoranta et al., 1989), and sound location (Paavilainen et al., 1989; Schröger & Wolff, 1996). However, the EEG studies are limited in scope because they lack spatial resolution and it becomes difficult to evaluate the contribution by different areas of the brain (Pulkki and Karjalainen 2015).

### 1.4 Animal behavioural studies

Since hearing is considered a behaviour, many behavioural studies have been conducted to validate animal models for hearing research (Fay and Popper 1994). Psychoacoustic studies in animals serve as a bridge between animal neurophysiology and human hearing (see Fay & Popper, 1994 for a review). With the use of classical and operant conditioning, animals can be trained to recognize certain tones and elicit a specific behaviour (Cowles and Pennington 1943; Gourevitch et al. 1960; Gourevitch and Cole 1963; Hack 1971; Kelly and Masterton 1977;

Talwar and Gerstein 1998). Studies have shown that difference acoustic measures such as audiograms, intensity and frequency discrimination thresholds, temporal discriminations, auditory filters, gap detections thresholds critical bandwidths, and psychophysical tuning curves show a similarity between humans and nonhuman mammals such as chinchilla, cat, various primates, mouse and rats (Fay and Popper 1994; Hack 1971; Kelly and Masterton 1977).

### *1.4.1 Animal behavioural tests show that the perception of a sound can be affected by another sound*

Using operant conditioning, auditory masking has been demonstrated in rats (Gourevitch 1965). Rats were trained to press a bar for water after a tone (which they had been previously trained to recognize) had ended. The tone was then presented simultaneously with different noise levels and the rat would press the bar after it could no longer hear the tone due to masking (Gourevitch 1965). The major finding of this study was that the masked threshold in rats increased linearly with the level of the noise, a finding which reflected in human studies (Gourevitch 1965). However, it is unclear whether the rat perceived a qualitatively different sound when the noise and test tone were simultaneously played.

Another study examined the influence of one sound on the perception of another sound in rats (Hoeffding and Harrison 1979). The study focused on precedence effect, an acoustic phenomenon which aids in the localization of the sound source by suppressing the perception of echoes in a reverberant acoustic environment (Pulkki and Karjalainen 2015). The rat was trained to press a lever in response to a click emitted by a sound source in the presence of a second click, which served as an artificial echo, from a sound source located opposite of the first sound source (Hoeffding and Harrison 1979). The time between the first click and the artificial click was varied, and the results showed that the majority of the correct responses (rat pressing the lever

corresponding to the first sound) were at a higher time delay between the two clicks (Hoeffding and Harrison 1979). This study shows that one sound can affect the perception of another sound in a time-dependent manner. However, it is unclear whether the rat was responding to the second sound rather than the first sound.

### *1.4.2 Sound localization in rats*

Rat's have demonstration spatial acuity in discrimination sound location (Beecher and Harrison 1971; Harrison and Beecher 1969). In one study, rats were reinforced if they pressed a lever closest to the speaker delivering a 4kHz tone burst (Beecher and Harrison 1971). The results showed that the rats rapidly acquired the ability to discriminate between the two speakers and press the lever closest to the speaker delivering the sound stimulus within the first session (Beecher and Harrison 1971).

### *1.4.3 Binaural cues and sound localization in rats*

Binaural cues such as interaural time (difference in the time of sound arrival at the two ears) and interaural level differences (difference in the level of sound arriving at the two ears) are reflected in the anatomy and physiology of the mammalian auditory pathway (Fay and Popper 1994). Rat and many other small rodents predominantly use interaural level difference (ILD) in sound localization (Inbody and Feng 1981; Kelly et al. 1991; Potash and Kelly 1980).

Binaural cues, or differences in sound arriving at two ears, play an important role in sound localization (Kelly et al. 1987; Potash and Kelly 1980). A study tested the tendency of three groups of rat infants to approach a target sound. Group 1 had one ear blocked with an earplug, group 2 had both ears blocked, and group 3 had no ear blocked (Potash and Kelly 1980). The purpose of the plug was to attenuate the sound by approximately 10dB. The results showed that only group 2 and group 3 approached the target sound with above chance levels (Potash and

Kelly 1980). The failure of the monoaural group 1 infant was probably due to a disruption in binaural cues (Potash and Kelly 1980).

## 1.5 Overview of the auditory system

### *1.5.1 Peripheral auditory system and transduction of sound to neural signals in the inner ear*

In mammals, hearing is dependent on the peripheral auditory system and the central auditory pathway (Pulkki and Karjalainen 2015). The ear, or the peripheral auditory system, consists of an external ear which receives sound waves, middle which mechanically conducts sound waves through vibrations of the tiny bones called ossicles, and the inner ear which transduces mechanical stimuli to neuronal signals (Figure 6) (Pulkki and Karjalainen 2015). Signals are then carried up via various nuclei to the auditory cortex for higher-level processing (Pulkki and Karjalainen 2015).

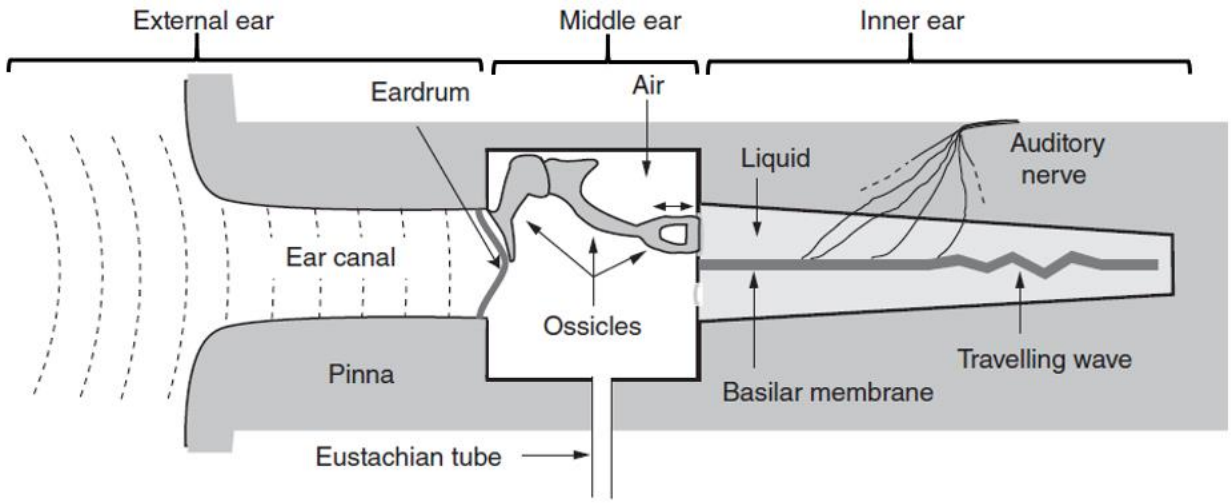


**Figure 6.** A cross-section of an ear showing the external ear (blue), the middle ear (green), and inner ear (yellow) (modified from Pulkki and Karjalainen, 2015).

Transduction of sound occurs in the cochlea, a spiral-shaped structure in the inner ear that contains the basilar membrane. The organ of Corti resides on the basilar membrane and it

contains sensitive hair cells known as inner hair cells which converts mechanical vibration of sound to neural impulses in the auditory nerve fibers (Pulkki and Karjalainen 2015). Different parts of the basilar membrane vibrate maximally to certain frequencies of sound. The basel part of the basilar membrane is stiffer and responds optimally to high-frequency sounds, while while the apical part of basilar membrane is floppy and responds optimally to low-frequency sounds (Pulkki and Karjalainen 2015). This positioning of frequencies along the basilar membrane is referred to as the tonotopic organization and it is preserved throughout neural processing stages (Pulkki and Karjalainen 2015). Generally, the anatomy and physiology in the inner ear is generally the same between the human and rat. However, there are key differences in the length and width of the basilar membrane, the length of the inner and outer hair cells, and the number of inner and outer hair cells between the two species (Nadol 1988).

### *1.5.2 The overall organization of the central auditory system*

#### *1.5.2.1 Major central auditory structures*

The auditory system is composed of six major structures as shown in the top schematic diagram of Figure 7: the cochlear nucleus (CN), superior olivary complex (SO/SOC), the nucleus of the lateral lemniscus (NLL), inferior colliculus (IC), medial geniculate nucleus (MGN), and the auditory cortex (AC). The detailed descriptions of all these structures are provided below. The ascending auditory pathway starts with at the CN and converges towards the IC which then sends signals to the AC (Figure 7). The descending auditory pathway starts at the AC and ends at the Organ of Corti.

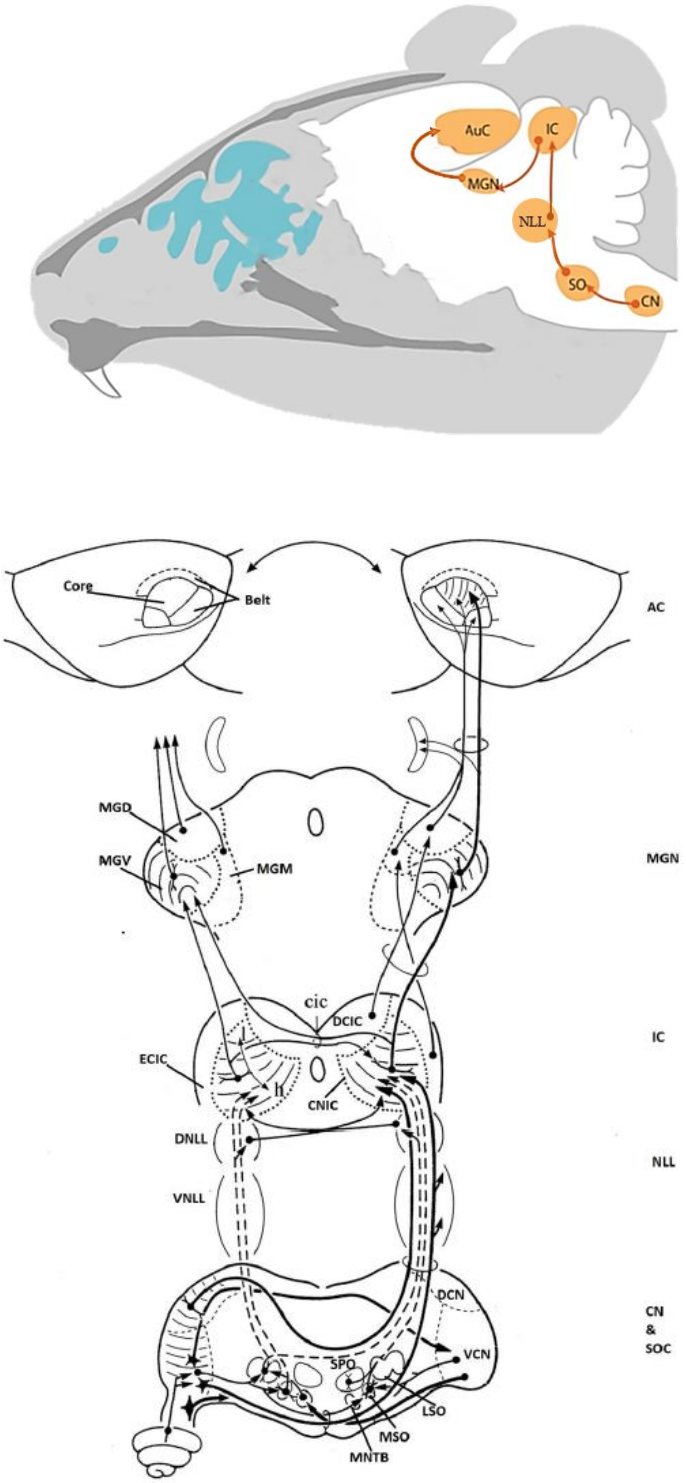


**Figure 7.** Schematic representation of the auditory pathways in a rodent. The top figure shows the major structures within the auditory pathways (modified from Asaba et al., 2014). The

bottom figure shows the connections between the major auditory structures (adapted from (Malmierca 2015). Please see the list of abbreviations for the full form of the words in the figures.

*1.5.2.2 Ascending Auditory pathway*

*1.5.2.2.1 The cochlear nucleus (CN)*

The first relay station for signals carried by the auditory nerve fibers is the cochlear nuclear complex (CNC/CN) (Figure 7). The CN is composed of a dorsal cochlear nucleus (DCN) ventral cochlear nucleus (VCN). The ventral nucleus is further composed of anteroventral (AVCN) and posteroventral (PVCN) nucleus. Cochlear nerve fibers terminate tonotopically in the CN where fibers carrying low-frequency sound signals terminate ventrally and fibers carrying high-frequency sounds terminate progressively dorsally. There is also a topographic projection from the VCN to the DCN where low frequency projections are relatively more ventral in the DCN compared to high frequency signals which are more dorsal (Doucet and Ryugo 1997). As shown by Figure 7 (bottom diagram), the CN receives projections from the ipsilateral cochlea and is thus considered a monoaural structure.

The cell types that comprise the VCN include bushy cells. There are two kinds of bushy cells, spherical and globular, which differ based on cell morphology and physiology (Young et al. 1988). These cells have a primary like firing pattern, which means they have a strong response to the onset of a sound and then reduced sustained firing (Blackburn and Sachs 1989; Young et al. 1988). Moreover, they are key in transmitting temporal information for sound localization (Young et al. 1988). Spherical bushy cells project bilaterally to medial superior olive (MSO) and ipsilaterally to the lateral superior olive (LSO) (Friauf and Ostwald 1988; Harrison

and Warr 1962). The globular bushy cells project to the medial nucleus of the trapezoid body (MNTB).

Other notable cell types of the VCN include the octopus cells which have been suggested to encode pitch period and they project bilaterally to the superior paraolivary nucleus (SPON) and contralaterally to ventral nucleus of the lateral lemniscus (VLL) (Thompson and Schofield 2000). The multipolar cells may convey frequency-specific excitatory information about the stimulus level and innervate the central nucleus of the inferior colliculus (CIC) (Doucet and Ryugo 1997). The radiate cells are the sole source of inhibitory projections in the CN (Alibardi 1998; Doucet et al. 1999).

The main projection fibers of the DCN are from the pyramidal cells which innervate the IC and MNTB. These projections may serve a role in sound localization and head orientation to sound (May, 2000; Young et al., 1992).

*1.5.2.2.2 Superior olivary complex (SOC)*

The superior olivary complex is subdivided into LSO, MNTB, MSO, SPON, and periolivary nuclei (PO) (Malmierca 2015; Osen et al. 1984). SOC lesions have shown to disrupt sound localization in the albino rat (Van Adel and Kelly 1998). In cats, MSO has shown to respond mainly to low-frequency sounds while LSO responds to all frequencies with an emphasis on high-frequency tones (Heffner and Masterton 1990).

*1.5.2.2.2.1 Lateral superior olive (LSO)*

The LSO is the lateral most part of the SOC. The major cell types found in the LSO are bipolar and multipolar cells (Rietzel and Friauf 1998). The inputs to the LSO are from AVCNs from both sides. The excitatory ipsilateral inputs are from the spherical bushy cells and

multipolar planar cells (Doucet and Ryugo 2003; Warr 1966). Indirect inhibitory inputs are from the globular bushy cells of the contralateral AVCN (Henkel and Gabriele 1999; Moore and Caspary 1983). These inputs first innervate the MNTB which then project glycinergic inputs to the LSO on the same side (Henkel and Gabriele 1999; Moore and Caspary 1983). LSO neurons are binaural because they are excited by ipsilateral inputs and inhibited by contralateral inputs. Their binaural property helps them encode interaural intensity differences (Shu Hui Wu and Kelly 1992).

LSO projections are to the central nucleus of the inferior colliculus where ipsilateral inputs have been suggested to be glycinergic and inhibitory while the contralateral inputs are excitatory (Glendenning and Baker 1988; Saint Marie and Baker 1990; Shneiderman and Henkel 1987). Additionally, the LSO also sends projections to the dorsal nucleus of the lateral lemniscus (DNLL) bilaterally (Brodal A 1981).

*1.5.2.2.2.2 Medial superior olive (MSO)*

The MSO is located in between MNTB and LSO. MSO processes low frequency sounds (Goldberg and Brown 1969). In rats, the MSO is unusually small because they are more receptive to high frequency sounds relative to larger mammals such as humans and cats (Moore and Moore 1971). MSO is comprised largely of principal cells and fewer non-principal cells (marginal and multipolar) (Lindsey 1975; Smith 1995). The MSO receives excitatory inputs bilaterally from both VCN and inhibitory inputs from ipsilateral MNTB (Banks and Smith 1992). The MSO projects excitatory inputs to the CIC and DNLL (Kelly et al. 2009; Oliver and Shneiderman 1989). Moreover, MSO is involved in sound localization and is sensitive to interaural time differences (ITD) (difference in the timing of the sounds arriving at the two ears) (Malmierca 2015). However, some studies have suggested MSO responses are too crude for

sound localization and may play a role in suppressing echoes and reverberations from the environment (Grothe and Neuweiler 2000).

*1.5.2.2.2.3 Superior paraolivary nucleus (SPON)*

The SPON is a conspicuous nucleus in rodents as compared to humans (Malmierca and Ryugo 2011). It contains the largest multipolar GABAergic neurons in the SOC (Kulesza Jr. and Berrebi 2000). It receives excitatory inputs from the globular bushy, octopus, and multipolar cells of the contralateral VCN and the from the multipolar and globular bushy cells of the ipsilateral VCN (Saldaña et al., 2009). It receives major glycinergic inputs from the ipsilateral MNTB (Banks and Smith 1992; Sommer et al. 1993). SPON projects to the ipsilateral inferior colliculus in a topographic manner which may indicate its tonotopic organization (Saldaña et al. 2009).

Even though the circuitry exists for SPON to respond to binaural cues, it is only shown to be excited by contralateral stimulation (except in a gerbil) (Behrend et al., 2002; Saldaña et al., 2009). Neurons in the SPON respond to the offset of pure tones (Kadner and Berrebi 2008)

*1.5.2.2.2.4 Periolivary nuclei (PO)*

PO nuclei are composed of neurons with different projection patterns (Adams 1983; Faye-Lund 1986; Osen et al. 1984). The most prominent nucleus within the rat's PO is the ventral nucleus of the trapezoid body (VTz) (Osen et al. 1984). The VTz projects to the to the cochlear nucleus, the contralateral SOC, and the ipsilateral IC (Faye-Lund 1986). The PO nuclei, as a group, receive inputs from many auditory and non-auditory regions and they may function in multiple aspects of hearing (Kulesza 2008).

The periolivary nuclei include the medial nucleus of the trapezoid body (MNTB). The MNTB is the most medial nuclei in the SOC and it is comprised of principal and non-principal cells (Banks & Smith, 1992; Sommer et al., 1993). The principal cells resemble globular cells from the VCN and project within the ipsilateral SOC to LSO, MSO, and SPON (Banks and Smith 1992; Sommer et al. 1993). The responses from the primary cells show that they may play a role in encoding sound duration (Tolnai el al., 2008). The strong excitatory inputs received by the principal cells from the contralateral VCN are relayed as strong inhibitory inputs to the ipsilateral LSO with minimal synaptic delay (Banks and Smith 1992; Kopp-Scheinpflug et al. 2008; Sommer et al. 1993). The non-principal cells may project to the VNLL (Banks and Smith 1992).

*1.5.2.2.3 Nuclei of the lateral lemniscus (NLL)*

The NLL is subdivided into dorsally and ventrally into DNLL and VNLL respectively (Brodal A 1981). Based on cat studies, DNLL neurons have shown to respond to binaural cues while VNLL neurons have only shown to respond to monoaural cues (Aitkin et al. 1970; Brugge et al. 1970). However, some rat VNLL studies have supported its role in binaural processing (Nayagam et al. 2005; Zhang and Kelly 2006a).

*1.5.2.2.3.1 The ventral nucleus of the lateral lemniscus (VNLL)*

The cells that comprise the VNLL include bushy and stellate cells (Zhao and Wu 2001). The bushy cells exhibit an onset firing pattern while the stellate cell types exhibit various firing patterns including onset-pause, adaptive firing, and burst to fire (Zhang and Kelly 2006a, 2006b). The VNLL receives excitatory inputs from the contralateral VCN and inhibitory inputs from the ipsilateral MNTB and SPON (Kelly et al. 2009; Saldaña et al. 2009). The VNLL functions to rapidly relay information from lower brainstem structures to the ipsilateral IC and also integrates

binaural inputs (Irfan et al. 2005; Whitley and Henkel 1984). The majority of the cells in the VNLL are glycine or GABA immunoreactive (González-Hernández et al. 1996; Riquelme et al. 2001).

*1.5.2.2.3.2 Dorsal nucleus of the lateral lemniscus (DNLL)*

DNLL sends bilateral projections to the IC with most of the inputs being sent to the contralateral IC (Bajo et al. 1993; Chen et al. 1999; Merchán et al. 1994; Zhang et al. 1998). There are 4 cell types in the DNLL including large and multipolar, large and bipolar, and medium-sized with round cell bodies, and small round neurons (Bajo et al. 1993). These cells are GABAergic and inhibit responses in the IC and the contralateral DNLL (Chen et al., 1999; Riquelme et al., 2001; Zhang et al., 1998). Excitation of the DNLL neurons can be quick via AMPA receptors or slow and long-lasting due to NMDA receptors (Kelly & Kidd, 2000). Moreover, stimulation of the ipsilateral ear produces long-lasting inhibition of the DNLL cells which suggests it may function in the localization of multiple sound sources (Kelly & Kidd, 2000).

Unlike VNLL, DNLL neurons receive binaural inputs from the contralateral DNLL through the commissure of the lateral lemniscus, ipsilaterally from MSO, SPON, and VNLL, and bilaterally from the LSO (Van Adel and Kelly 1998; Bajo et al. 1993; Chen et al. 1999; Zhang et al. 1998). Thus, DNLL may play a crucial role in the localization of sound with the help of binaural cues (Bajo et al., 1998; Kelly et al., 1998). Studies that lesioned the commissure of Probst in rats observed behavioural deficits in their ability for sound localization (Ito et al., 1996; Kelly et al., 1996). This could be because DNLL may play a role in relaying information about interaural time (ITD) and ILD to its target structure, the IC (Li and Kelly 1992).

*1.5.2.2.4 Inferior colliculus (IC)*

The rat IC has an ellipsoid shape with diameters of 3.5 and 2 mm and considered a major relay station for auditory signals (Faye-Lund and Osen 1985). It is subdivided into the central nucleus (CIC), the dorsal cortex (DCIC), the lateral cortex (LCIC), and the rostral cortex (RCIC) (Bartlett and Smith 1999a; Loftus et al. 2008; Malmierca et al. 1993). Figure 8 shows the inhibitory and excitatory connections to the CIC.

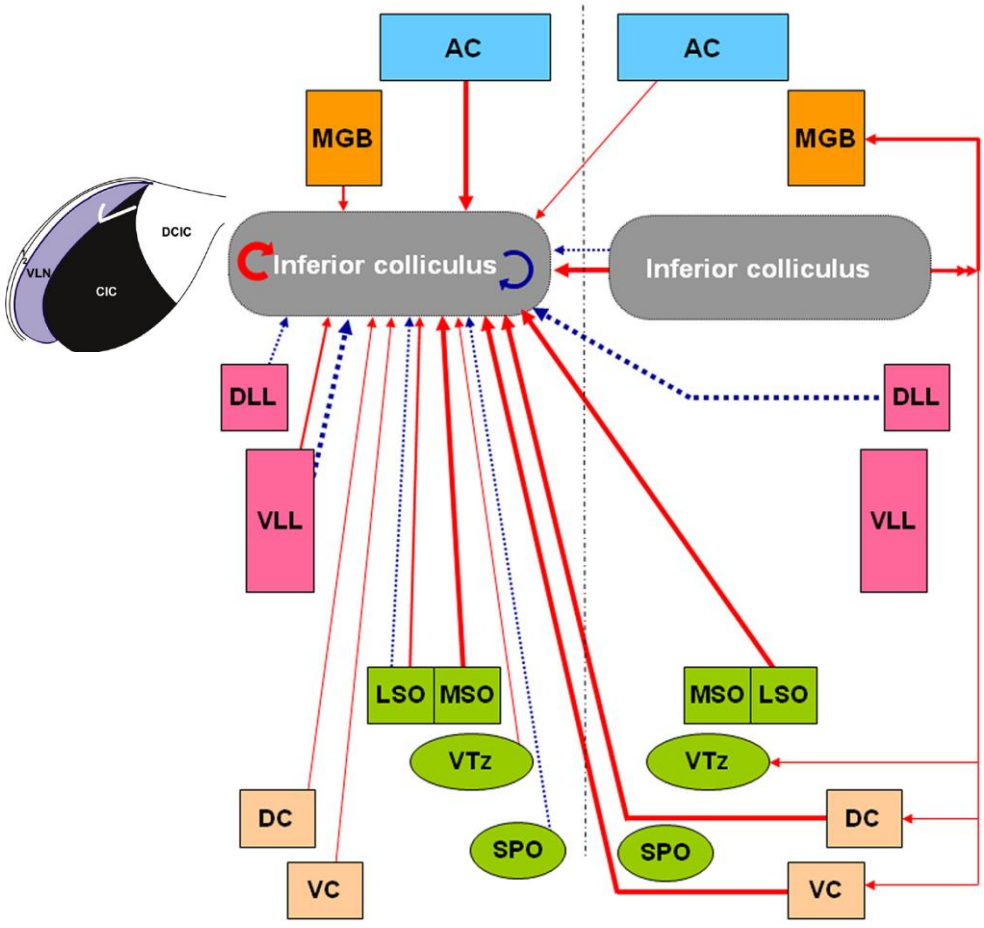


**Figure 8.** Schematic representation of the ascending and descending projections to and from the left inferior colliculus. Red lines represent excitatory inputs and blue lines represent inhibitory inputs. The thickness of the lines represents the strength of innervation. (Adapted from

(Malmierca 2015). The there main areas within the IC are shown in the small figure next to the left IC (Modified from Loftus et al. 2008).

*1.5.2.2.4.1 The central nucleus of the inferior colliculus (CIC)*

The CIC is made up of discontinuous laminae (fibrodendritic laminae) which are comprised of neurons with flattened dendritic arbors (Faye-Lund and Osen 1985; Loftus et al. 2008; Malmierca and Merchán 1991). These laminae are organized in a tonotopic manner where laminae responding best to low frequencies are dorsal while laminae responding best to high frequencies are ventral (Friauf 1992; Loftus et al. 2008). The two types of cells that characterize the CIC are flat and less flat neurons (Malmierca et al. 1993, 1995). These two types of cells differ in dentric branching, dendritic thickness, and their location and orientation about the laminae. The flat cells make up the laminae around 1 cell layer thick while the less flat cells are found in compartments in between the laminae (Faye-Lund and Osen 1985; Malmierca et al. 1993). The dendritic arbors of most cells are oriented parallel to the laminae along the ventrolateral to the dorsomedial axis, however, the dendritic arbors of a few flat cells are oriented more rostrocaudally (Malmierca et al. 1993). Although firing patterns observed with extracellular recordings differ from firing patterns observed with patch clamp recordings, patch clamp studies have categorized the firing patterns of the CIC neurons into six groups: sustained-regular, onset, pause/build, rebound-regular, rebound-adapting, and rebound transient (Peruzzi et al. 2000; Tan et al. 2007). This diversity in firing patterns could mean that the neurons not only have the potential to merely relay signals but also process temporal and intensity differences between sound signals (Peruzzi et al. 2000; Tan et al. 2007).

The bilateral ascending inputs to the CIC are from DNLL and LSO, ipsilateral inputs are from VLL and MSO, and contralateral inputs are from AVCN, PVCN, and DCN (Bajo et al.

1993; Beyerl 1978; Coleman and Clerici 1987; González-Hernández et al. 1996; Loftus et al. 2008; Malmierca et al. 2005b; Merchán et al. 1994; Merchán and Berbel 1996; Oliver et al. 1999). Axons from the DCN and LSO have been shown to overlap in the contralateral CIC, however, the axons from the DCN projected more dorsally compared to the projections from LSO (Malmierca et al., 2005; Oliver et al., 1997). Moreover, projections from the VCN and DCN remain segregated and innervate separate regions in the CIC (Malmierca et al., 2005). Furthermore, the CN projections to the IC can either terminate in large or small axonal boutons which may be confined to specific functional zones in the CIC and play a role in processing different acoustic information (i.e. temporal, spectral, or intensity related) (Malmierca et al. 2005b).

The CIC projects mainly to the ipsilateral ventral MGB with fewer projections to the medial and dorsal subdivisions (Peruzzi et al. 1997). The projections are mainly glutamatergic with a few GABAergic projections (Peruzzi et al. 1997; Winer et al. 1996).

*1.5.2.2.4.2 The lateral cortex of the inferior colliculus (LCIC)*

The LCIC is subdivided into three layers. Layer 1 is a continuation of the DCIC's fibrodentritic laminae (discussed below), layer 2 is an aggregate of small to medium-sized neurons, and layer 3 is the largest and has a topographical relationship with the commissural fibers (Faye-Lund and Osen 1985; Loftus et al. 2008). Layer 3 contains flat neuron cell types however they differ structurally from their counterpart in the CIC with respect to dendritic arbor thickness and orientation (Faye-Lund and Osen 1985; Loftus et al. 2008).

LCIC receives projections from lower brainstem structures such as the CN (Faye-Lund and Osen 1985). It also receives inputs from other regions near the ipsilateral primary auditory cortex (Faye-Lund and Osen 1985). LCIC also receives inputs from non-auditory structures such

as cuneate and substantia niagra which are involved in processing somatosensory information (Coleman and Clerici 1987). LCIC sends projections to the medial and dorsal regions of the MGB (Brodal A 1981).

*1.5.2.2.4.3 The rostral cortex of the inferior colliculus (RCIC)*

RCIC is comprised of multipolar cells of different sizes and without orientation. Thus, there is no indication of layering in the RCIC (Malmierca & Ryugo, 2011). The arborization of the neurons differs substantially from the neurons found in CIC and LCIC (Malmierca & Ryugo, 2011).

*1.5.2.2.4.4 The dorsal cortex of the inferior colliculus (DCIC)*

The DCIC is made up of three layers. Layer 1 is a thin fibrocellular capsule composed of flattened neurons and covers part of the LCIC layer 1 (Faye-Lund and Osen 1985; Malmierca and Ryugo 2011). Layer 2 is composed of multipolar neurons and layer 3 (largest layer) is composed of small and medium-sized cells. The DCIC receives bilateral topographic inputs from the primary auditory cortex as well as inputs from lower brainstem structures (Faye-Lund and Osen 1985; Malmierca et al. 2005b). Cells in this region fire phasic firing to the stimulus of increasing intensity and then tonic firing as the level is increased more (Banks and Smith 1992; Li et al. 1998).

*1.5.2.2.4.5 Commissural and intrinsic fibers of the inferior colliculus*

Commissural fibers connect the IC on both sides of the midline while intrinsic fibers connect the subdivisions within each IC (González-Hernández et al. 1991; Malmierca et al. 2009; Okoyama et al. 2006; Saldaña and Merchán 2005). Neurons contributing to the commissural inputs are mainly glutamatergic and about 20% are GABAergic (Hernández et al. 2006). Due to this, commissural projections can have both an excitatory or inhibitory effect on

the contralateral IC and may play a role in the binaural processing of sound (Malmierca et al. 2005a).

*1.5.2.2.5 Medial geniculate body (MGB)*

The MGB is located on the posterolateral part of the thalamus (Winer et al. 1999b). Within the MGB, there are three subdivisions: ventral (MGBV), medial (MGBM), and dorsal (MGBD) (LeDoux et al. 1985a).

*1.5.2.2.5.1 Ventral medial geniculate body (MGBV)*

The MGBV has a tonotopic and laminar arrangement of fibers belonging to the principal neurons which project tufted dendritic arbors (Bordi and LeDoux 1994a, 1994b). High frequencies are found more ventrally while low frequencies are found more dorsally (Bordi and LeDoux 1994a). Moreover, there are three subdivisions within the MGBV with a different laminar organization: ventral nucleus, ovoid nucleus, and the marginal zone (Clerici et al. 1990; Winer et al. 1999a). The major input to the MGBV is from the ipsilateral CIC (González-Hernández et al. 1991) and to a weaker extent from the contralateral CIC (Chernock and Winer 2001). The IC projects both glutamatergic and GABAergic inputs to the MGBV tufted neuronal dendrites (Bartlett and Smith 1999b). Additionally, the primary auditory cortex is reciprocally connected with the MGBV and only projects glutamatergic inputs onto the tufted neurons (Bartlett and Smith 1999a). MGBV also received GABAergic inputs from the thalamic reticular nucleus, which envelops the lateral MGBV may play a role in modulating auditory signals (Arcelli et al. 1997). The role of MGBV is only limited to the processing of acoustic signals (Ledoux et al. 1987). Although neurons in the MGBV respond to binaural stimuli, there were no differences found in sound localization in rats after MGBV was lesioned (Kelly and Judge 1985).

*1.5.2.2.5.2 Dorsal medial geniculate body (MGBD)*

Five subnuclei within the MGBD do not have a tonotopic organization: the dorsal superficial, dorsal, deep dorsal, suprageniculate, and ventrolateral subdivisions (Clerici and Coleman 1990). The major inputs are from cortical regions of the IC (DCIC, RCIC, and LCIC), excitatory inputs from the cortex, and inhibitory inputs from the thalamic reticular nuclei (Bartlett et al. 2000; Bartlett and Smith 1999a). It mainly projects to secondary auditory cortical areas, the insular cortex, and the lateral nucleus of the amygdala (Doron and Ledoux 1999). The two main neurons found in MGBD are stellate and tufted neurons which differ slightly from the MGBV tufted neurons (Clerici et al. 1990).

*1.5.2.2.5.3 Medial division of the medial geniculate body (MGBM)*

Relative to the other subdivisions of the MGB, MGBM is the smallest and contains diverse cell types (Clerici et al. 1990). It receives diverse ascending inputs including from the RCIC, LCIC, VNLL, SOC, CN, and the spinal cord (Ledoux et al. 1987; Malmierca et al. 2002). It projects to the IC and the auditory cortex and also to nonauditory regions such as the caudate-putamen and the amygdala (LeDoux et al. 1985b; Malmierca 2015; Ottersen and Ben-Ari 1979; Senatorov and Hu 2002). Due to a convergence of input from diverse sources, MGBM may be involved in multisensory arousal and emotional auditory learning (Bordi and LeDoux 1994b, 1994a).

*1.5.2.2.6 Auditory Cortex*

The auditory cortex is the highest sound processing center in the ascending auditory pathway. The auditory cortex is comprised of three temporal areas: Te1, Te2, and Te3 (Zilles et al. 1980). Based on physiological responses, five cortical auditory fields have been mapped within the three temporal areas: primary auditory cortex (A1), the posterior auditory field (PAF),

the anterior auditory field (AAF), the ventral auditory field (VAF), and the suprarhinal auditory field (SRAF) (Polley et al. 2007). Te1 corresponds to A1, AAF, and VAF (Polley et al. 2007; Smith et al. 2012; Storace et al. 2010). Te2 corresponds to PAF and Te3 corresponds to SRAF (Polley et al. 2007; Smith et al. 2012; Storace et al. 2010).

So far studies have examined the neuroal architecture of A1. The A1 is comprised of six distinct layers. Layer 1 occupies 13% of the cortical thickness and has the fewest neurons (Games and Winer 1988). Layer II occupies 11% of the cortical thickness and densely packed with neurons (Games and Winer 1988). Layer III occupies 17% of the cortical thickness and is comprised of pyramidal and non-pyramidal neurons whose dendritic arbors have a random orientation (Games and Winer 1988). Layer IV occupies a bit more than 10% of the cortical thickness and contains mostly small stellate neurons which are smaller and more densely packed than neurons in layer III (Games and Winer 1988). Layer V is the thickest by occupying 26% of the cortical thickness and it contains large pyramidal cells (Games and Winer 1988). Layer VI occupies 22% of the cortical thickness and comprised of pyramidal and non-pyramidal cells (Games and Winer 1988).

There are two types of pyramidal cells within the cortices, intrinsically bursting and regular spiking (McCormick et al., 1985; Kawaguchi, 1993; Kasper et al., 1994). Intrinsically bursting neurons receive less GABAergic inputs and fire more readily while the regular spiking neurons receive more inhibition and show variable degree of adaptation (Hefti and Smith 2000). The layer V is predominantly comprised of the intrinsically firing neurons and send projections to the thalamus, subthalamic nuclei (including IC), and contralateral cortex (Feliciano et al. 1995; Games and Winer 1988; Hefti and Smith 2000; Moriizumi and Hattori 1991; Weedman and Ryugo 1996; Winer 1992). The neurons in the A1 and AAF are sharply tuned to specific

frequencies and intensities and responses have a shorter latency (Polley et al. 2007; Wu et al. 2006). The neurons in the SRAF and PAF are broadly tuned and responses have a longer latency (Polley et al. 2007; Wu et al. 2006). Neurons in the VAF respond to nonmonotonic intensity-tuned responses (Polley et al. 2007; Wu et al. 2006). Behavioural studies involving rats have shown that the auditory cortex is not necessary for sound localization (Kelly 1980; Kelly and Glazier 1978).

*1.5.2.3 Descending auditory pathway*

The descending auditory pathway starts at the auditory cortex and ends at the organ of Corti (Brodal A 1981; Herbert et al. 1991). Three tracts that orginate at the AC are: corticogeniculate, corticocollicular, and corticopontine projections (Faye-Lund 1985; Herbert et al. 1991; Saldaña et al. 1996; Winer and Larue 1987). The three pathways may have feedback loops or be comprised of a descending chain (Spangler and Warr 1991). Projections in the feedback loop would start at the cortex and innervate subcortical structures (such as the thalamus) which would then send projections back to the cortex either directly or indirectly (Spangler and Warr 1991). In the descending pathway, the cortical projections will innervate subcortical structures which will only send projections to other lower structures (Spangler and Warr 1991).

The corticogeniculate pathway is a reciprocal loop between the auditory cortex and the MGB (Winer and Larue 1987). The corticocollicular projection innervates the IC and has both excitatory and inhibitory effects on the IC neurons (Faye-Lund 1985; Herbert et al. 1991; Saldaña et al. 1996). Moreover, this pathway may play a role in plasticity in the IC in response to sensory experiences (Clarkson et al. 2010b, 2010a, 2012; Yan and Suga 1998). The corticopontine projection innervates the nuclei below the IC (Faye-Lund 1985; Herbert et al.

1991; Saldaña et al. 1996). This pathway sends input to areas around the NLL, ipsilateral, and bilateral inputs to the CNC and SOC, DCN, and VCN (Doucet and Ryugo 2003; Saldaña et al. 1996).

In the descending pathway, there are also two projections originating in the IC and innervating lower auditory structures: colliculoolivary and colliculocochleonuclear projections (Malmierca 2015). Colliculoolivary projections originate specifically from the ventral part of CIC, LCIC, and RCIC and indirectly supply the outer hair cells of the cochlea (Caicedo and Herbert 1993; Faye-Lund 1986; Saldaña 1993). The colliculocochleonuclear projections originate in the LCIC and CIC and terminate at the DCN and VCN (Caicedo and Herbert 1993; Faye-Lund 1986; Saldaña 1993).

## 1.6 CIC is a major auditory integration center

The CIC is a hub of auditory processing because it receives multiple ascending and descending inputs (Figure 8). This study is related to neural processing of acoustic information in the CIC. The CIC plays a major role in converging binaural inputs which enables it to process temporal, spectral, and directional information of sounds (Malmierca 2015).

### *1.6.1 Spectral processing in the CIC*

Neurons in the CIC can be characterized based on their curves (FTC). These curves are plotted by varying the frequency and intensity of a tone systematically and recording the firing pattern (Ehret and Schreiner 2005). These curves convey several key pieces of information about a neuron such as the characteristic frequency (CF) (frequency resulting in a response at the lowest sound pressure level (SPL)), best frequency (BF) (frequency resulting in the highest number of spikes from the neuron at a certain SPL), and minimum threshold (MT) (the SPL at CF) (Ehret and Schreiner 2005). The CIC neurons can be highly specific to detect sounds of

specific frequencies (Kelly et al. 1991). A tone that lies outside the FTC of a neuron can have an inhibitory effect on its firing. Studies using a two-tone sound paradigm first examine the responses in the CIC to a single-tone played at the CF of the recording site. Next, the single-tone at CF is played with another tone of variable frequency simultaneously which can inhibit the response from the first tone (Egorova et al. 2001; LeBeau et al. 2001). Moreover, pharmacological experiments have shown that iontophoretic application of bicuculine and strychnine (antagonists for $GABA_A$ and glycinergic receptors respectively) have changed the FTCs of certain neurons by eliminating their inhibitory sidebands (LeBeau et al. 2001). It is suspected that the glycinergic projections are from the SOC and the VNLL (LeBeau et al. 2001).

### *1.6.2 Temporal processing in the CIC*

Approximately half of the neurons in the IC show duration sensitivity to sound, however, most of these neurons are found outside the central nucleus (Pérez-González et al. 2006). Some of these neurons responded to sound exceeded a certain duration threshold while others were only sensitive to restricted sound durations (Pérez-González et al. 2006). It is suggested that convergence of inhibitory and excitatory inputs may play a role in shaping response properties to temporal characteristics of sound (Brand et al. 2000). Pharmacological studies have shown that inhibition is essential for temporal encoding in the CIC. For instance, the application of $GABA_A$ or glycine antagonists eliminated duration timing in bats (Casseday et al. 1994).

### *1.6.3 Directional dependence of CIC neurons*

Most neurons in the CIC are excited by a sound when it is presented in the hemifield contralateral to the neurons and inhibited by the sound when it is presented in the hemified ipsilateral to the neurons (Cant 2005; Finlayson and Adam 1997; Flammino and Clopton 1975; Kelly et al. 1991). Moreover, the firing latency of most neurons is the shortest when the sound is

presented at the contralateral ear relative to the ipsilateral ear (Flammino and Clopton 1975). An interesting phenomenon was found in bats where 85% of the CIC neurons were excited following a contralateral stimulation, however, there was a persistent inhibition that outlasted the initial tone by tens of milliseconds. Moreover, this inhibition acted through $GABA_A$ because application of bicuculine reduced or eliminated the inhibition. The duration of the persistent inhibition increased as the sound level increased as well as when the stimulus duration was increased (Bauer et al. 2000).

### *1.6.4 Binaural convergence in the CIC*

Binaural hearing is an underpinning of spatial localization of sounds in the CIC. The convergence of multiple inputs from bilateral sound processing structures such as LSO and MSO, both cochlear nuclei, and NLL in the CIC makes it a suitable structure to process binaural cues (Palmer and Kuwada 2005).

Studies have used dichotic stimulation to identify neurons in the CIC which are excited by contralateral stimuli and inhibited by ipsilateral stimuli (Irvine and Gago 1990). Moreover these studies have shown that the neurons in the CIC respond to ILD (Irvine et al. 1995; Wenstrup et al. 1988a, 1988b; Zhang and Kelly 2009).

### *1.6.5 Forward masking in the CIC*

A study by Finlayson and Adam (1997) used forward masking paradigms to compare monaural and binaural processing in the CIC. The results showed that in the monaural contralateral condition, the responses to the test tone (30 ms in duration) were suppressed by 25% or more in 85% ($n$ = 28) of the neurons examined following a masking tone (200 ms in duration). The maximum suppression occurred when the test sound was delayed by 8 ms (Finlayson and Adam 1997). The recovery time of the responses was approximately 226.9 ms

(Finlayson and Adam 1997). However, four neurons did not show any significant changes in response (Finlayson and Adam 1997). In neurons which exhibited a bimodal response pattern which fires 12-20 ms after the stimulus onset, pause firing for 20-30 ms, and then resume firing to a sustained level, test tone response was maximal in the 2 ms delay condition and progressively decreased as the delay between the masker and test increased (Finlayson and Adam 1997).

In binaural conditions, neurons sensitive to binaural cues were examined. A test tone was presented at the contralateral ear following a leading masker at the ipsilateral ear. 4/10 of the neurons showed immediate facilitation because they fired more, 1 neuron was excited at a short delay, while the other 5 neurons did not show significant changes.

### *1.6.6 Time-dependence of ipsilateral inhibition*

A study by Zhang and Kelly (2009) examined the time course of ipsilateral inhibition on contralaterally elicited responses. They compared CIC neuronal responses to a contralateral tone presented either simultaneous with an ipsilateral tone or after various delays. Both tones were 200 ms in duration and presented simultaneously. The interaural level differences between the two tones were also varied. The results showed that 20 out of the 24 neurons showed an excitatory/inhibitory (EI) interaction which means that they were excited by the contralateral test tone but suppressed by the ipsilateral tone (Zhang and Kelly 2009).

Next, the onset of the ipsilateral and contralateral tone bursts were changed to 100 ms and the aftereffects of the leading ipsilateral tone burst were studied. Results showed that when the trailing contralateral tone burst was delayed by 100 ms and there was no overlap with the ipsilateral tone, 8 out of the fourteen neurons displayed inhibitory aftereffects, 2 displayed excitatory aftereffects, and 4 neurons showed no aftereffects (Zhang and Kelly 2009).

The study also found that excitatory/inhibitory aftereffects can influence responses within a short time window. For instance, the responses from one neuron were suppressed when a contralateral tone was presented simultaneously with an ipsilateral tone, however, the degree of suppression was the largest when the tone was delayed by 50 ms (Zhang and Kelly 2009). The study indicated that ipsilateral stimulus could generate an aftereffect to enhance or suppress the response elicited by a subsequent contralateral stimulus.

### 1.7 A study: response of one sound can be influenced by another sound in a space-dependent manner

This study address some of the major questions raised by a study from Chot et al. (2019) which examined the interaction between two independently recurring sounds in the generation of responses in the CIC. One of the major questions we focus on is whether the effect of spatial separation is dependent on change in the level of adaptation or the level of inhibition. The study compared the responses of an equal probability two-tone sequence, $T_L$ and $T_H$, when both sounds were colocalized at the contralateral ear (c90°) versus when one sound (either $T_L$ or $T_H$) was at c90° (also called the location-fixed sound) and when one sound was at a non-c90° azimuth (also called the location changeable sound) (Chot et al. 2019).

The results showed that the responses to the location fixed sound at c90° (whether $T_L$ or $T_H$) was enhanced when the location-changeable sound was at a non-c90° azimuth (Figure 9) (Chot et al. 2019). Specifically, there was an increase in the strength of the response when the location-changeable sound was at 0°, i45°, and i90°.

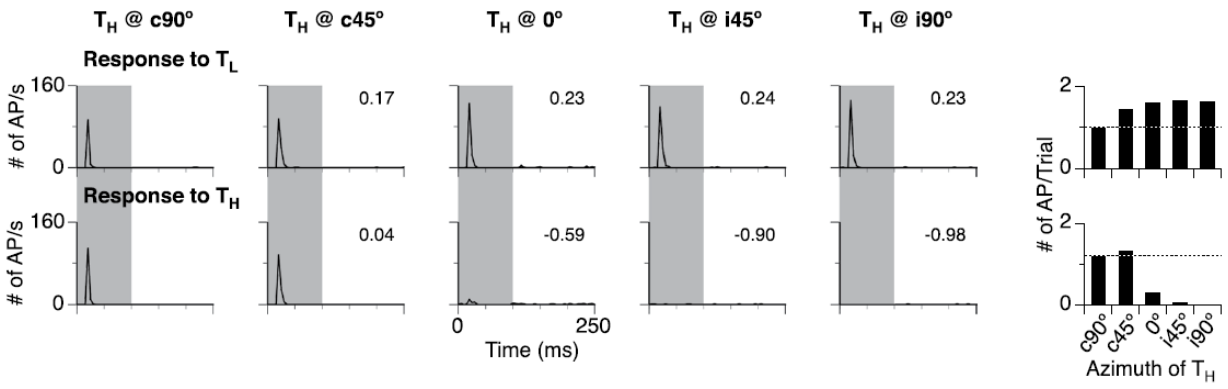


**Figure 9.** An individual neuron's responses to a two-tone equal probability sequence with various spatial conditions. The bar chart at the top shows the responses to the location-fixed $T_L$ sound at c90° while the bottom bar chart shows the responses to a location-changeable $T_H$ sound at various azimuths. The shaded areas show the duration of the two sounds. Modified from Chot et al. (2019).

The study also examined how the response to the sound at c90° was affected by a second colocalized sound. The responses of the first sound were compared in the presence and absence of the second (Chot et al. 2019). The results showed an increase in responses when the second sound was omitted (Chot et al. 2019). Moreover, neurons that were irresponsive to the ipsilateral i90° sound showed a response enhancement to the sound at c90° condition when the i90° sound was omitted (Chot et al. 2019).

The increase in the strength of responses to the location-fixed sound upon spatial separation of the second sound may indicate spatial release from masking (Chot et al. 2019). It is not fully understood as to why the location-fixed sound showed a response enhancement when the other sound was spatially separated, however, one explanation could be changes in the level of inhibition by the neurons in the SPON in response to the first sound (Chot et al. 2019). SPON is excited by contralateral stimulation and sends offset inhibitory signals to the ipsilateral CIC

(Behrend et al. 2002; Chot et al. 2019; Kulesza et al. 2003). Consequently, these offset inhibitory inputs to the CIC may be generated after the first contralateral tone and inhibit the responses to the second colocalized tone (Chot et al. 2019). When the second sound was spatially separated to the ipsilateral side, SPON inhibition would have been prevented (Chot et al. 2019).

Another finding of this study was that the responses were more enhanced following the location-fixed sound at c90° when the second sound was omitted compared to when there was an ipsilateral i90° sound even in neurons irresponsive to i90° stimulation (Chot et al. 2019). This suggests that ipsilateral inhibitions may have shaped the responses to the c90° sound when the second sound was presented at i90° (Chot et al. 2019).

To evaluate the role of inhibition in shaping the separation-dependent enhancement of response to the location-fixed sound at c90° and inhibition by ipsilateral sound, our study incorporates pharmacological manipulations to study some potential inhibitory mechanisms which shape responses in the CIC. Using inhibitory neurotransmitter antagonists, inhibitory effects can be eliminated and the interaction between the responses to a location-fixed and location-changeable sound can be observed.

## 1.8 Neurotransmission in the IC

The main excitatory neurotransmitter of the IC is glutamate while the two inhibitory neurotransmitters are γ-aminobutyric acid (GABA) (main inhibitory neurotransmitter) and glycine (Kelly and Caspary 2005).

### *1.8.1 Glutamatergic inputs into the IC*

Glutamate acts on N-methyl-D-aspartate (NMDA) and α-amino-3-hydroxy-5-methyl-4-isoxazolepropionic acid (AMPA) receptors (Kelly and Caspary 2005). AMPA receptors are

responsible for the initial early response component while NMDA receptors have been responsible for the slow-developing late response (Kelly and Caspary 2005).

The main glutamatergic inputs to the IC is from the VCN (Kelly and Caspary 2005). There are direct excitatory inputs sent by the contralateral DCN to the CIC (Davis 2002). LSO is a binaural processor which also send contralateral glutamatergic inputs to the IC neurons shaping responses to ILD typically for high-frequency sound (Kelly and Caspary 2005; Sally and Kelly 1992). Another binaural processor, MSO, sends ipsilateral glutamatergic inputs to the IC neurons conveying information about ITD related to low-frequency sounds (Kelly and Caspary 2005; Sally and Kelly 1992). Descending excitatory inputs from the auditory cortex to the DIC and CIC may also be excitatory, however, the physiological significance of these inputs is not yet certain (Kelly and Caspary 2005). *In vivo* pharmacology studies have shown that glutamate antagonist (±)-2-amino-5-phosphonovaleric acid (APV) reduces firing rates of most neurons in the IC (Kelly and Caspary 2005). Injection of glutamate agonist increases spontaneous firing of CIC neurons (Faingold et al. 1989).

### *1.8.2 GABAergic and glycinergic inputs into the IC*

GABA can act on $GABA_A$ as well as $GABA_B$ receptors. Both $GABA_A$ and glycine receptors have been shown to play a role in influencing the frequency tuning curves of IC neurons and the duration sensitivity of neurons to tones (Casseday et al. 1994; Faingold et al. 1991; LeBeau et al. 2001). $GABA_A$ receptor seems to play a more dominant inhibitory role in the IC (Milbrandt et al. 1996; Moore et al. 1998). $GABA_B$ receptors may influence inhibition by controlling the amount of transmitter acting on the $GABA_A$ receptors sites through presynaptic modulation (Ma et al., 2002). They may also facilitate the release of glutamate (Zhang and Wu 2000).

$GABA_A$, $GABA_B$, and glycine terminals are differentially distributed in the IC (Choy Buentello et al. 2015). Immunohistochemistry sections of the rat's IC targeting GAD67 (an enzyme that decarboxylates glutamate to GABA) and GLYT2 (glycine reuptake transporter) have shown that GAD67 was found throughout the IC, however, GLYT2 was only found in the CIC (Choy Buentello et al. 2015). Within the CIC, the GAD67 signals were relatively higher in the dorsomedial regions while GLYT2 signals were relatively higher in the ventrolateral region (Choy Buentello et al. 2015). Similarly, other studies using western blotting and immunohistochemical procedures have indicated that $GABA_B$ receptors are more abundant in the dorsomedial regions than the ventral regions (Fubara et al. 1996; Jamal et al. 2012; Milbrandt et al. 1994).

The IC receives extrinsic, intrinsic, and commissural GABAergic inputs (Helfert et al. 1989; Huffman and Henson 1990; Peruzzi et al. 1997; Shneiderman et al. 1988). Around 20-40% of the neurons in the rat's IC produce GABA (Kelly and Caspary 2005). Extrinsic sources of the GABAergic inputs include small ipsilateral DNLL projection and a large contralateral DNLL projection to mainly the dorsal CIC (Kelly and Caspary 2005; Shneiderman et al. 1988). The SPON also sends direct ipsilateral GABAergic inputs to the CIC and these projections may be more diffuse (Choy Buentello et al. 2015; Kulesza et al. 2003). Half of the inputs from the LSO to the ipsilateral CIC are glycinergic (Glendenning et al. 1992; Helfert et al. 1989; Marie et al. 1989; Vater et al. 1992b). These projections may be concentrated in the ventral CIC (Cant and Benson 2006). VNLL also projects glycinergic inputs into the CIC and these inputs may be more diffuse (Choy Buentello et al. 2015; Riquelme et al. 2001; Vater et al. 1997). Application of $GABA_A$ antagonists, bicuculline, and gabazine, increase the firing rate of most neurons in the IC (Kelly and Caspary 2005; Pérez-González et al. 2012). Similarly, the application of glycine

antagonists, strychnine, reduces postsynaptic inhibition in most IC neurons (Kelly and Caspary 2005). The application of $GABA_B$ antagonist, phaclofen, slightly increases postsynaptic firing (Ma et al. 2002). $GABA_A$ receptors also seem to process excitatory-inhibitory binaural interactions since blocking both $GABA_A$ and glycinergic receptors by bicuculline and strychnine, respectively, reduced ipsilateral inhibition in the IC neurons (Klug et al. 1995).

The three antagonists used in this study are gabazine (to block $GABA_A$ receptors), CGP 35348 (to block $GABA_B$ receptors), and strychnine (to black glycine receptors). Gabazine can bind to $GABA_A$ sites with relatively high affinity (McCabe et al. 1988). Saturation of binding to tissue showed that gabazine had a dissociation constant of 42.4 nM. Similarly, CGP 35348 has similar affinities of binding to $GABA_B$ sites only shown in studies where it was tested on a variety of receptor binding essays (Olpe et al. 1990). Strychnine is also a highly specific antagonist for glycine receptors (Faingold et al. 1989).

**1.9 Influence of anesthetics on the neuronal responses of the IC**

This study uses a ketamine-xylazine combination to keep the rat under anesthesia. Ketamine acts as a non-competitive antagonist of one of the glutamate receptors, N-methyl-D-aspartate (NMDA) (Lima et al. 2012). Xylazine is an agonist for alpha 2 adrenergic receptors which reduce noradrenaline release (Lima et al. 2012). Physiologically, a ketamine-xylazine combo increases the latency of IC neurons relative to the other anesthetics such as pentobarbital (Astl et al. 1996). However, the number of spontaneously firing neurons is higher with the ketamine-xylazine combo than with other drugs (Lima et al. 2012). Moreover, the threshold of sustained neurons was significantly lower compared to the threshold of onset neurons with ketamine-xylazine combo relative to other drugs (Lima et al. 2012).

## 1.10 Objectives

The main objective of the present study is to examine how a location-changeable leading sound affects the LFPs elicited by a location-fixed trailing sound. Specifically, I examined how the effect produced by a leading sound was dependent on:

I. The interstimulus interval (ISI) between the leading and trailing sound.

II. The spatial location of the leading sound.

III. Neurotransmission mediated by the $GABA_A$, $GABA_B$, and glycine receptors.

I hypothesized that the response to a trailing sound would be more suppressed at shorter ISIs and less suppressed at longer ISIs. The response to the trailing sound would be more suppressed when the leading-trailing sounds were colocalized and less suppressed when the leading sound was spatially separated from the trailing sound. The suppression of the response to a trailing sound was partly due to inhibition.

# CHAPTER II. MATERIALS AND METHODOLOGY

## 2.1 Subject and anesthetics

Experiments were conducted using fifteen 2-4 months old male albino Wistar rats (*Rattus novgicus*)) obtained from Charles River Canada Inc. The rat was chosen as the model organism as their auditory system has been studied extensively in previous studies (King et al., 2015; Zhang & Kelly, 2009).

Anesthesia was induced with a combination of ketamine hydrochloride (60mg/kg, i.m.) and xylazine hydrochloride (10mg/kg, i.m.). Anesthesia was maintained using supplementary injections of ketamine hydrochloride (20 mg/kg, i.m.) and xylazine hydrochloride (3.3 mg/kg, i.m.) at 45-min intervals for the duration of the experiment (see Appendix for calculations). During surgical procedures, feet and tail pinch reflexes were tested regularly using a pair of forceps to ensure that an animal was deeply anesthetized.

Upon completion of a recording session, the rat was euthanized using pentobarbital (300 mg/kg, i.p.) and transcardially perfused for histological processing of the brain (See Appendix for calculations).

## 2.2 Acoustic stimulation

Two free-field magnetic speakers (Tucker-Davis Technologies Model FF1 free-field speakers, Alachua, FL) were used to elicit neural responses. The speakers were calibrated at five azimuths (Fig. 1) over a frequency range between 1kHz and 40kHz using a condenser model 4134 microphone and model 2608 measuring amplifier (Brüel & Kjær, Dorval, QC). These five azimuths included the midline of the frontal field (denoted by 0° in Fig. 1) and 90° and 45° on the contra- and ipsilateral side of the recording site (denoted by c90°, c45°, i45°, and i90° in Fig. 1). The speakers were 50 cm away from the midpoint of a rat's interaural line. Sound waveforms

were generated digitally using a System 3 real-time signal processing system controlled by a personal computer running OpenEx software (Tucker-Davis Technologies, Alachua, FL).

**2.3 Surgical procedures**

When a rat was deeply anesthetized, the hair at the top of the head was removed using an electric trimmer. The rat was placed onto a thermal heating pad throughout the surgery.

The surgical procedure was similar to that described in a previous publication by Zhang and Kelly (2009). Briefly, a midline incision was made on the scalp and the skin was retracted laterally using a spatula. The retracted muscles were held in place using hemostats. Small bone screws were placed in the skull. The head along with the bone screws was fixed to a stainless-steel rod with dental acrylic (Dentsply Repair Material Power and Repair material liquid, York, PA). The stainless-steel rod served as a head bar to hold the head stationary during the procedures when a craniotomy was made and when neurophysiological signals were recorded. The craniotomy was a small hole (approximately 3 mm in diameter) which allowed for the insertion of the recording/drug injection electrode assembly into the inferior colliculus. The centre of the craniotomy was about 4 mm to the right of the lambda point (Fig. 1).

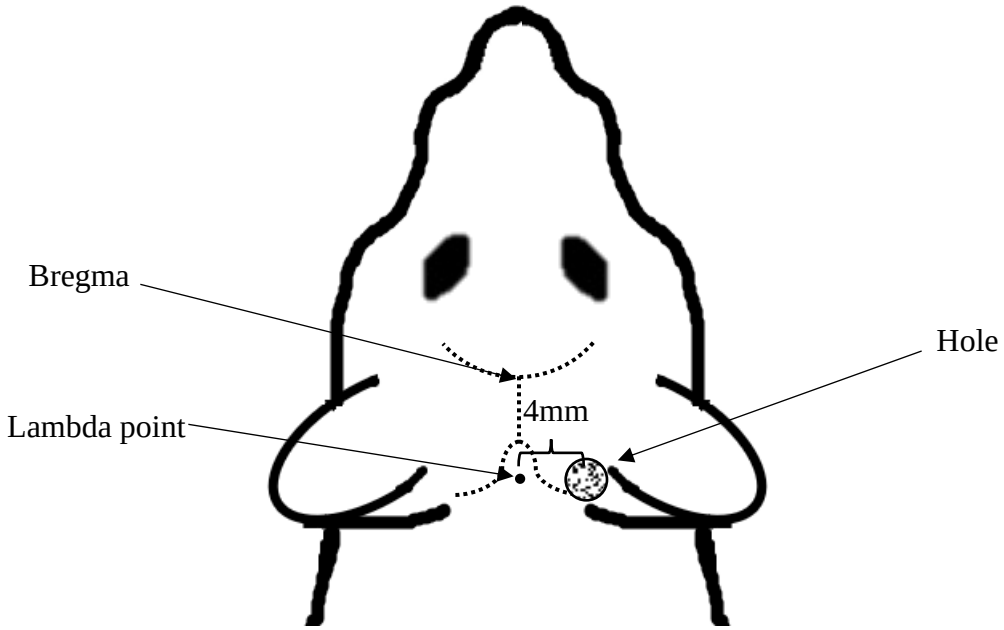


**Figure 10.** Location of craniotomy. The diagram shows the bregma, lambda, midline sutures (dotted lines), and the hole (circle with dots). The centre of the craniotomy was about 4 mm lateral to the lambda point.

All procedures were approved by the University of Windsor Animal Care Committee and were in accordance with the guidelines of the Canadian Council on Animal Care.

**2.4 Setup of the rat in a recording chamber**

Upon completion of the surgery, the rats was transferred into a recording chamber (Eckel Industries Model CL-15A LP, Morrisburg, ON) for a neurophysiological recording/ pharmacological manipulation experiment. The recording chamber was a single-wall sound-attenuated booth (Eckel Industries, Inc. Morrisburg, ON). Over the entire duration of neurophysiological recording/pharmacological manipulation, the body temperature of the animal was maintained at 37°C using a homeothermic system (Harvard Apparatus Model 50-7061-F Unit, Montreal, QC) with an anal temperature probe. A 3-dimensional small animal stereotaxic

instrument (David Kopf Model 902, Tujunga, CA) and a dissection microscope (Olympus Model SZM-45T-STL2 7X-45X, Cleveland, OH) was used to align the head of a rat and guide the placement of a recording probe into the rat's IC. For aligning the rat's head, a glass pipette was attached to the micromanipulator of the stereotaxic instrument and the tip of the pipette was placed at the bregma and the lambda to measure the coordinates of points. The head was considered aligned if the differences in coordinates between the bregma and the lambda point were within 20 μm in both medial-lateral and dorsal-ventral dimensions.

After the rat's head was aligned, a piggy-back microelectrode assembly was positioned stereotaxically into the brain to record LFP signals from the IC. The electrode was in the coronal plane and tilted by 30° relative to the sagittal plane. The electrode was lowered into the CIC from a dorsolateral to ventromedial location. The orientation of the electrode was perpendicular to the fibrodendritic laminae of the CIC and along the tonotopic axis of the structure (Kelly et al., 1991; Zhang & Kelly, 2009). The electrode was moved to a coordinate that was 3.8-4.2 mm lateral and 0.3-0.5 mm rostral in reference to the Lambda point. The tip of the electrode assembly was advanced into the CIC at a depth between 2500 and 4500 μm in reference to the surface of the brain using a micropositioner (David-Kopf Instruments Model 650, Tujunga, CA). A reference electrode was placed in the muscle surrounding the cranium.

**2.5 Neurophysiological recording and pharmacological manipulation**

A "piggy-back" multi-barrel electrode assembly was used to record LFPs from an ensemble of neurons and to release neuropharmacological agents onto the neuron ensemble from which neural signals were recorded. The electrode assembly consisted of a single-barrel glass pipette (tip diameter ~15-20 μm) and a multi-barrel glass pipette (tip diameter ~15 μm – 20 μm). The tip of the single-barrel pipette protruded the tip of the multi-barrel pipette by about 20-25 μm. The

single-barrel pipette was used to record LFP signals. It will was filled with 0.5 M sodium acetate with 3% Chicago sky blue. The dye was released upon completion of recording to label the site of recording. The electrode had an impedance in the range between 100 kΩ – 300 kΩ. Signals registered by the electrode were amplified by 1,000 times by an amplifier (2400A preamplifier, Minneapolis, MN). The bandpass filter of the amplifier was set at 0.3 – 300 Hz. These signals were registered using a System 3 real-time signal processing system controlled by a personal computer running OpenEx software (Tucker-Davis Technologies, Alachua, FL). They were sampled at a rate of 3.1 kHz. Such a sampling rate ensured that enough temporal details of an LFP waveform were revealed. Under each condition of stimulation, LFP signals elicited by 61 presentations of a stimulus (either a single sound or paired sounds) were registered and an averaged waveform was obtained.

The multi-barrel pipette consisted of 5 barrels that form an "H" configuration. The four side barrels were filled with gabazine (an antagonist of the $GABA_A$ receptor), CGP 35348 (an antagonist of the $GABA_B$ receptor), and/or strychnine (an antagonist of the glycine receptor). These pharmacological agents had a concentration of 5 mM in a vehicle of 0.9% saline (pH 3.5). The central barrel was filled with 0.9% saline to balance the electrical current. The five barrels were connected with a microiontophoretic system (Neurophore BH-2, Harvard Apparatus, Holliston, MA). A retention current at between -20 to -50 nA was applied to each of the four side barrels to prevent drug leakage when the electrode assembly was in the brain before pharmacological manipulation was conducted.

## 2.6 Recording procedures

### *2.6.1 Finding and characterizing a site of recording*

Bursts of Gaussian noises with a 8-ms duration were presented from a single speaker at c90° to search for a recording area in the CIC. These noises were presented at 60 dB SPL at a rate of 4/sec. While the noise bursts were presented, a recording electrode was driven into the CIC. Neural activity collected by the electrode were monitored audio-visually using a four-channel digital storage oscilloscope (Tektronix TDS2014B, Beaverton, OR) and audio monitor (Grass AM8, West Warwick, RI).

A site of recording was selected primarily based on the amplitude of an LFP signal registered by the electrode. Such a signal had a large negative trough that follows a noise burst (See Fig. 13 for a typically averaged waveform recorded in the CIC). Neural responses were recorded only if recording traces displayed a larger signal-to-noise ratio and a stable baseline.

Once the recording site was selected, tone-bursts were used to obtain basic characteristics of the ensemble of neurons at the recording site. The tones-burst had a 8-ms duration (4 ms rise/fall time and 4 ms plateau) and was presented at 4 /sec. The frequency tuning curve (FTC) along with the characteristic frequency (CF, the frequency at which the lowest threshold of response is observed) were obtained for the neural ensemble at the recording site.

Two tone bursts with different frequencies, named as $T_L$ and $T_H$, with frequencies at $f_L$ and $f_H$, respectively, were chosen based on the CF of the recording site. One of the tone bursts will be used as a leading sound and paired with a tone burst at CF (as a trailing sound) to study how a leading sound affected the response to a trailing sound. While $f_L$ was below the CF, $f_H$ was above the CF. The centre frequency of $f_L$ and $f_H$ (i.e., $(f_L * f_H)^{1/2}$ was at CF. The difference between $f_L$ and $f_H$ (i.e., $(f_L - f_H)/(f_L * f_H)^{1/2}$) was 0.10 octave (see appendix for frequency

calculations). Both $T_L$ and $T_H$ will have an 8 ms duration (with 4 ms rise/fall phases). The sound pressure levels of both sounds will be at 30 dB above the threshold of the site of recording. A leading sound alternated between $T_L$ and $T_H$ in consecutive experiments (i.e., $T_L$ in recordings from one rat and $T_H$ in recordings from the following rat).

An amplitude-stimulus intensity function (AIF), i.e., the relationship between the amplitude of LFP and the level of stimulation, was obtained at the CF and the $f_L$ and $f_H$ of the recording site. At each frequency, a tone burst was played at multiple (typically 7) levels from below the threshold to well above (typically 30 dB above) the threshold at CF. At each level, a tone burst was presented 20 times. All the tone burst presentations at various intensities (e.g., 140 presentations if a tone burst is presented at 7 intensities) was presented in a random order.

The dependence of the response of the neural ensemble at the recording site on the direction of stimulation was examined using a leading sound (either $f_L$ or $f_H$). The LFP elicited by this sound was recorded when the sound was presented at each of the 5 azimuths used in the present study (i.e., c90°, c45°, 0°, i45°, and i90°). The tone was first presented at the c90° and gradually moved ipsilaterally in increments of 45°. At each azimuth, the tone was presented a total of 61 times.

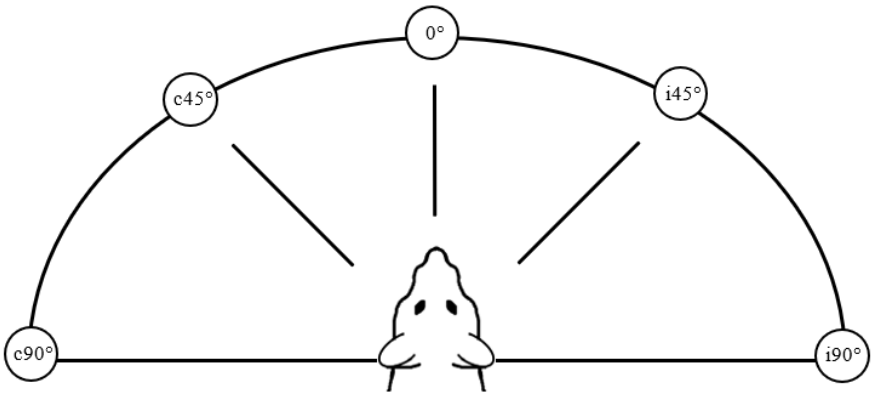


**Figure 11.** Experimental setup showing the different speaker locations.

### *2.6.2 Responses to a pair of leading-trailing sounds*

Responses to a pair of leading-trailing sounds were recorded under a pre-drug condition when the trailing sound was at c90° while the leading sound was at various locations and led the trailing sound by various amounts of time. For each animal, either $T_L$ or $T_H$ was chosen as a leading sound. A tone burst with a frequency at the CF of the recording site served as a trailing sound. The frequency relationship between the leading and trailing sounds were maintained throughout the entire experiment, including all recordings conducted under pre-drug, pharmacological manipulation, and recovery conditions.

Responses to the leading and the trailing sound alone were collected to provide references for evaluating how the two sounds interact with each other to shape responses to the two sounds in a pair (Figure 12).

Responses to a pair of leading-trailing sounds were first recorded when the leading sound was at c90° (i.e., when leading and trailing sounds were colocalized at c90°, see Figure 11). The inter-stimulus interval (ISI, the time gap between the onset of a leading sound and the onset of a trailing sound) was systematically varied (Table 1) to evaluate the effect of a leading sound on the response to a trailing sound. Logarithmic increments was used to change the ISI. A pair of leading-trailing sounds was presented 61 times to elicit responses. To ensure that the trailing sound of one pair did not affect the response elicited by the leading sound of the following pair, the time gap between the onset of a trailing sound and the onset of the next leading sound was 1500 ms.

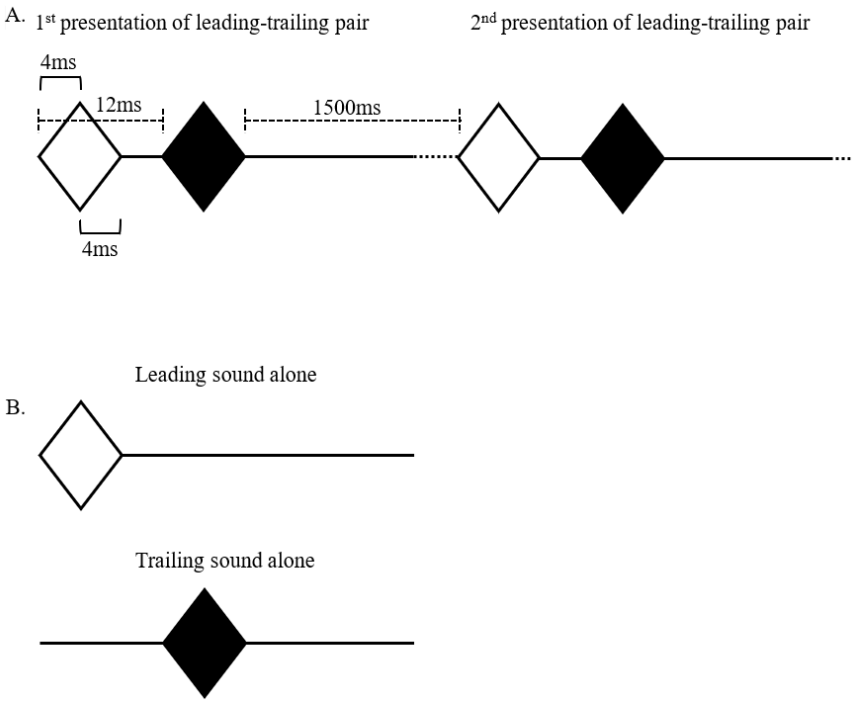


**Figure 12. Diagram showing acoustic paradigms. A.** Two presentations of a pair of leading-trailing sounds. The leading sound is white while the trailing sound is black. The inter-stimulus interval shown in the figure is 12 ms. However, in an experiment is was systematically varied. The time gap between the offset of the trailing sound of one presentation and the onset of the leading sound of the next presentation was 1500 ms. Leading and trailing sounds was both 8 ms long (4 ms rise/fall phases). **B.** The bottom panel shows the leading and trailing sound presented alone. The frequency of the leading sound was at either $f_H$ or $f_L$, while the frequency of the trailing sound was at CF.

Table 1 *ISIs and the Corresponding Acquisition Durations*

| ISIs | Signal Acquisition Duration for 1 Cycle (ms) |
|---|---|
| 12 | 1520 |
| 16 | 1524 |

| | |
|---|---|
| 24 | 1532 |
| 40 | 1548 |
| 72 | 1580 |
| 136 | 1644 |
| 264 | 1772 |
| 520 | 2028 |
| 900 | 2408 |

After the effect of a leading sound on the response to a trailing sound is evaluated when the two sounds are colocalized at c90°, the effect was examined when the two sounds were spatially separated. For this, the trailing sound was retained at c90°, while the leading sound was relocated to another azimuth (i.e., i90°, c45°, i45°, or 0°). At each angle of separation, the ISI was systematically varied (see Table 1 for a list of ISIs).

### *2.6.3 Pharmacological manipulations*

After the effect of a leading sound on the neural response to a trailing sound was evaluated under a control condition, it was evaluated under pharmacological manipulations. Gabazine (5mM, antagonist of the $GABA_A$ receptor), CGP35348 (5 mM, antagonist of the $GABA_B$ receptor), or strychnine (5 mM, antagonist of the glycine receptor) was released microiontophoretically at the recording site. A current ranging between 5 and 90 nA was used for drug release. An AIF of the response to the trailing sound at c90° was used to monitor the effect of the drug. When the effect of the drug reaches a plateau, responses to a pair of leading-trailing

sounds will be collected using the same spatial and temporal relationships as those used under a pre-drug condition. Responses to a leading and a trailing sound alone were also obtained.

After a complete set of neural responses were recorded under a pharmacological manipulation, ejection of the drug was stopped and neurons at the site of the recording were allowed to recover. An AIF of the response to the trailing sound at c90° was used to monitor the process of recovery. Upon recovery, responses to a pair of leading-trailing sounds and to leading and trailing sounds presented alone were collected using the same spatial and temporal relationships as those used under a pre-drug condition.

In a few cases, effects of more than one pharmacological agents were evaluated in a single animal. An effort was made to ensure that neurons at the recording site completely recovered from the effect of the first drug before pharmacological manipulation using the second drug was initiated.

**2.7 Labeling of a recording site**

Upon completion of neurophysiological recordings and pharmacological manipulations, the site of the recording was labeled. Chicago sky blue was released microiontophoretically using a build-in current pump of the Dagan 2400A preamplifier (Dagan, Minneapolis, MN). A continuous current of 200nA was used to deliver the dye. In addition to the site of recording, the dye was also released at two other sites, with one being 1000 μm shallower than the recording site and the other being 1000 μm deeper than the recording site. These 2 sites were labeled to assess possible shrinkage of the brain during transcardial perfusion and subsequent histological processing.

**2.8 Fixation and histological processing of brain tissue**

Upon completion of labeling of a recording site, a rat was euthanized by sodium pentobarbital (300 mg/kg, i.p.). After a rat was deeply anesthetized before the animal's heart stopped beating, a horizontal cut was made below the sternum to expose the diaphragm. A pair of iris scissors was used to cut the diaphragm and expose the lungs and the heart. A 23-gauge butterfly needle was inserted into the left ventricle of the heart and pointed towards the aorta; and the right atrium of the heart was cut. One hundred fifty to two hundred milliliters of 0.04 M phosphate buffer solution (PBS) was pumped into the left ventricle through the needle. Such an isotonic solution was used to clear the blood out of the circulation system. Paraformaldehyde (PFA) was then be pumped through the needle to fix the animal including the brain. The rat was then be decapitated with a guillotine and the head was submerged into PFA jar for postfixation.

The brain was extracted from the skull. The muscles around the cranium were removed and the skull was chipped away using a pair of rongeurs. When the brain was fully exposed, all the cranial nerves were cut and the brain was removed from the cranium using a spatula. The brain was kept in 30% sucrose in 0.04 M PBS for overnight. Once the brain is sunk to the bottom of a jar with a sucrose solution, it was ready for slicing. A midsagittal cut was made to separate the left and right sides of the brain. Coronal cuts were made to separate the part containing the right IC from the rest of the brain. The part containing the right IC was put into a vacuum chamber to remove the excess of sucrose. It was then covered with brain matrix and frozen. Starting from the caudal side of the block, the brain tissue was cut into 30 μm sections using a CM1050 S cryostat (Leica Microsystems, Heidelberg, Germany). The site of labeling was identified using a brightfield microscope.

## 2.9 Data analysis

### *2.9.1 Analysis of the response to a leading sound*

To determine whether the trailing sound in one leading-trailing sound presentation affected the response to a leading sound of the subsequent presentation, the trough amplitude and latency of the response to a leading sound were compared with those of the response to a leading sound presented alone. A normalized amplidute of response (NR) was calculated:

$$NR = \frac{A_1}{A_0}\ x\ 100$$

Where $A_1$ is the trough amplitude of the response to a leading sound in a leading-trailing pair while $A_0$ is the trough amplitude of the response to a leading sound presented alone. A value of 100% indicates that the amplitude of the response to a leading sound in a leading-trailing pair was the same as that of the response to the leading sound presented alone (see Appendix for a sample calculation).

The latency of the responses was measured from the onset of a sound to the trough amplitude of an LFP. The calculated was calculated using a macro in Excel (see Appendix for a sample calculation).

### *2.9.2 Analysis of the trailing sound*

To determine if the response to a trailing sound was influenced by a leading sound, the response was compared with the response to a trailing sound presented alone. An NR value was calculated:

$$NR = \frac{A_1}{A_0}\ x\ 100$$

Where $A_1$ is the trough amplitude of the response to a trailing sound in a leading-trailing pair while $A_0$ is the trough amplitude of the response to a trailing sound presented alone. NR values were calculated at all ISIs and angles of separation between the two sounds. The latency of the response to a trailing sound was calculated using the same method as that outlined in the Section 2.9.1.

An $ISI_{70}$ value was calculated using the responses obtained at various ISIs at a specific angle of separation between a leading and a trailing sound. At $ISI_{70}$, the amplitude of the response to a trailing sound was 70% of that of the response to a trailing sound presented alone. The $ISI_{70}$ value was obtained through interpolation using two data points immediately next to the one associated with $ISI_{70}$ (with one above while the other one below the point associated with $ISI_{70}$) (see appendix for calculations).

### *2.9.3 Statistics analysis*

As the data collected was not normally distributed, non-parametric tests were used. The Friedman's test was used as a non-parametric equivalent of a two-way ANOVA for dependent measurements. Wilcoxon singed-rank test was used as a post-hoc test. All figures based on groups results show median values with error bars showing standard error of mean.

# CHAPTER III. FINDINGS

LFP responses were recorded from 23 animals (referred to as cases in the rest of the document). All the 23 cases were used to evaluate the frequency differences in responses elicited by $T_L$ and $T_H$ when they were presented from the c90° azimuth versus the i90° azimuth. Eleven cases were used to evaluate the directional dependence of the recording site using a single tone. Fifteen cases were used to evaluate the responses to a leading-trailing sound pair colocalized at c90. Ten cases were used to evaluate the dependences of responses to the leading-trailing sound pair on the angle of separation between the sounds. Seventeen cases were used to evaluate the time course of the effect of leading sound on the response elicited by the trailing sound. The effect of gabazine on neural responses to two sounds was evaluated in six cases. The effects of CGP and strychnine were evaluated in five and seven cases, respectively.

## 3.1 Typical waveforms of LFPs

Ten cases were used to evaluate the dependences of responses to the leading-trailing sound pair on the angle of separation between the sounds. Seventeen cases were used to evaluate the time course of the effect of leading sound on the response elicited by the trailing sound. The effect of gabazine on neural responses to two sounds was evaluated in six cases. The effects of CGP and strychnine were evaluated in five and seven cases, respectively.

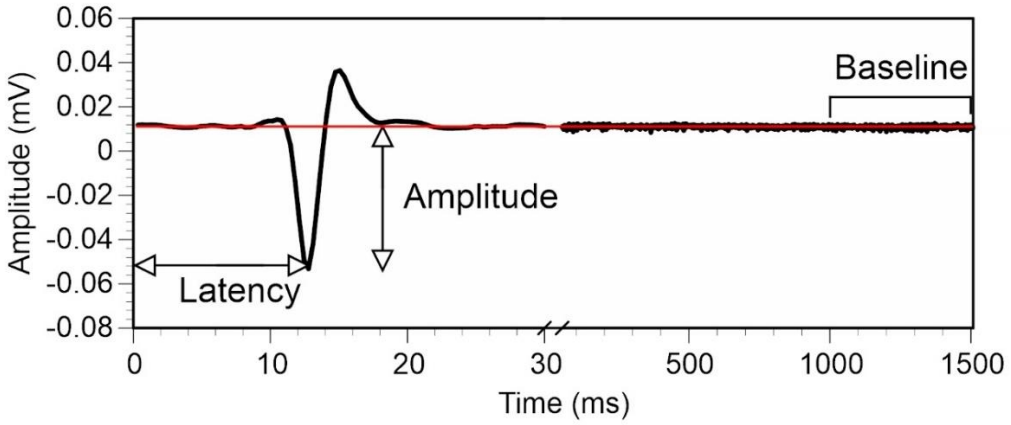


**Figure 13.** A typical LFP waveform. The baseline (red horizontal line) and the latency and the amplitude of the negative peak are indicated by the double arrows.

### 3.2 Characteristics of responses to single sounds

#### *3.2.1 Frequency-tuning curve (FTC) and amplitude-stimulus intensity functions (AIFs)*

A tone pip was presented at the contralateral ear to elicit a sound-drive response at a recording site in the IC. At a specific frequency, the sound-pressure level were varied to determine the threshold level at which a sound-drive response could be elicited. A frequency-tuning curve was obtained by evaluating thresholds at various frequencies. The frequency at which the lowest sound-pressure level was observed was the characteristic frequency of the recording site. Figure 14 shows the FTC of a sample recording site. The characteristic frequency of the recording site was 14kHz. Generally, most recording sites had FTCs similar to that shown in Figure 14, however, few sites were more broadly tuned. Once the CF of the recording site was determined, the $f_H$ and $f_L$ were calculated at 0.1-octave difference relative to CF (see appendix for calculations).

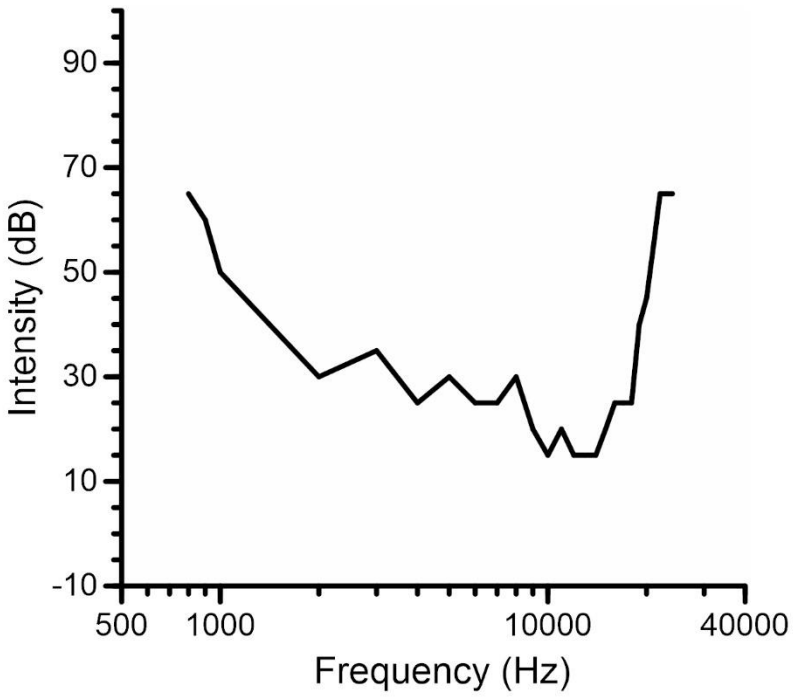


**Figure 14.** The frequency-tuning curve of a recording site. The depth of the recording site was 3437.5 μm and the CF was 10 kHz with a threshold of 15 dB.

The amplitude of an LFP recorded in the IC was dependent on the sound pressure level of a sound. An amplitude-stimulus intensity function (AIF) was used to evaluate this dependence. AIFs were acquired at CF and either $f_L$ or $f_H$ at seven different intensities. In each experiment, the trailing sound was always presented at CF while the leading sound was presented at $f_L$ in one case and switched to $f_H$ in the subsequent case. If the two frequencies used in one case were CF and $f_L$ then the two frequencies used in the next case were CF and $f_H$. In the case shown in Figure 15, the two frequencies used were CF and $f_H$.

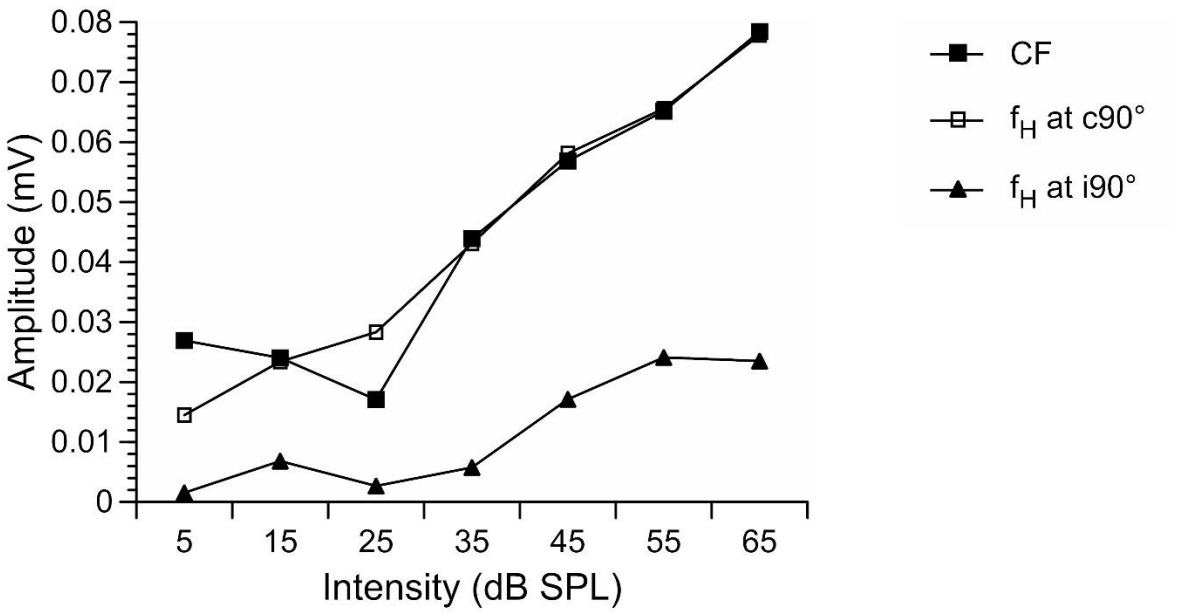


**Figure 15.** An example showing ALFs in response to a tone burst presented at CF and $f_H$ at the c90° azimuth and a tone burst presented at fH at i90° azimuth. The CF of the recording site was 10 kHz and the threshold was 35 dB. The $f_H$ of the recording site was 10,352.649 Hz.

To determine if a low-frequency tone ($T_L$) elicited a different response than a high-frequency tone ($T_H$), the effect of the frequency of a single-tone on the responses from c90° and i90° azimuth were compared across cases. The amplitudes of the LFPs elicited by $T_L$ and $T_H$ at 10, 20, and 30 dB (Figure 16A, B, and C respectively) above the minimum threshold were compared at c90° and i90° azimuths. Based on 23 cases (12 cases of $T_L$ and 11 cases of $T_H$ responses), there were no significant differences between responses to $T_L$ and $T_H$ whether they were presented at c90° or the i90° azimuth at all three sound pressure levels. In most cases, the tone intensity used to collect responses from other conditions where leading-trailing sound pairs were used was 30 dB above threshold. Based on Mann-Whitney test, there were no significant differences between the responses to $T_L$ and $T_H$ at c90° ($U$ = 0.985, $p$ = 0.347, n = 23) or at i90°

(U = 0.246, $p$ = 0.833, n = 23) when tones were played 30 dB above threshold. Thus, in the rest of the results section, the data obtained from $T_L$ and $T_H$ at each azimuth is combined.

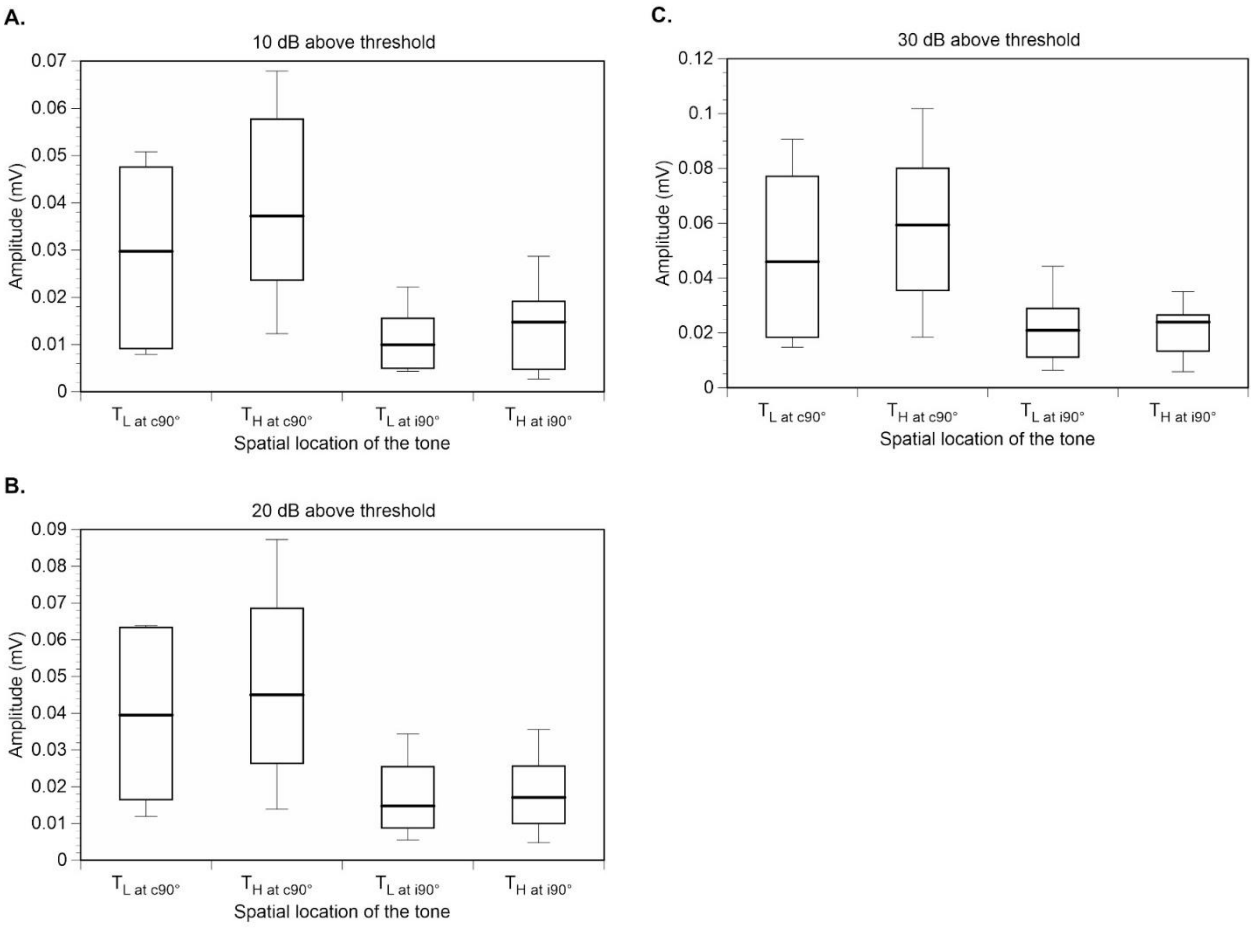


**Figure 16.** Distribution of absolute amplitudes resulting form $T_L$ and $T_H$ at c90° and i90° azimuths. **A.** Responses elicited by $T_L$ and $T_H$ when they were presented 10 dB above threshold. **B.** Responses elicited by $T_L$ and $T_H$ when they were presented 20 dB above threshold. **C.** Responses elicited by $T_L$ and $T_H$ when they were presented 30 dB above threshold.

### *3.2.2 Directional dependence of responses to a single tone*

A single tone burst was presented at the five azimuths c90°, c45°, 0°, i45°, and i90° to determine how the spatial location of a single-tone affects the LFP. In the example shown in

Figure 17, a tone burst at $f_L$ (4,829.68 Hz) and 70 dB was used to elicit a response at five azimuths c90°, c45°, 0°, i45°, and i90° (Figure 17A). The normalized ratio (NR) and latencies of those responses are shown in

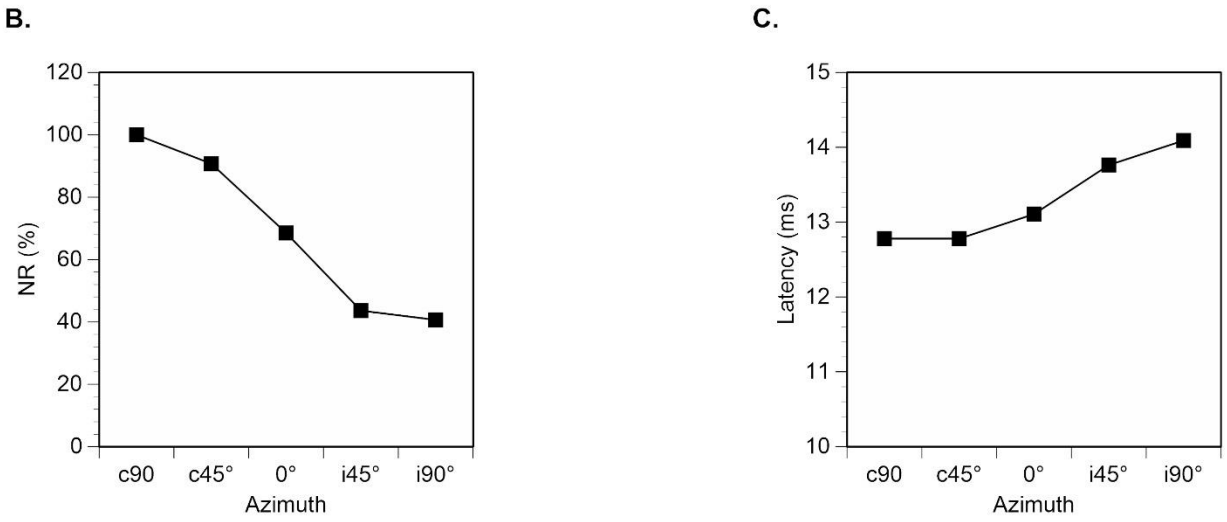


Figure 17B and C, respectively. The normalized ratio was calculated by dividing the amplitude of the negative peaks of waveforms at each azimuth by the amplitude of the negative peak of the waveform at the c90° azimuth. There was a gradual decrease in response NRs as the tone was moved from the c90° azimuth to the i90° azimuth. In contrast, the latencies of the negative peak increased gradually as the tone was moved from the c90° azimuth to the i90° azimuth.

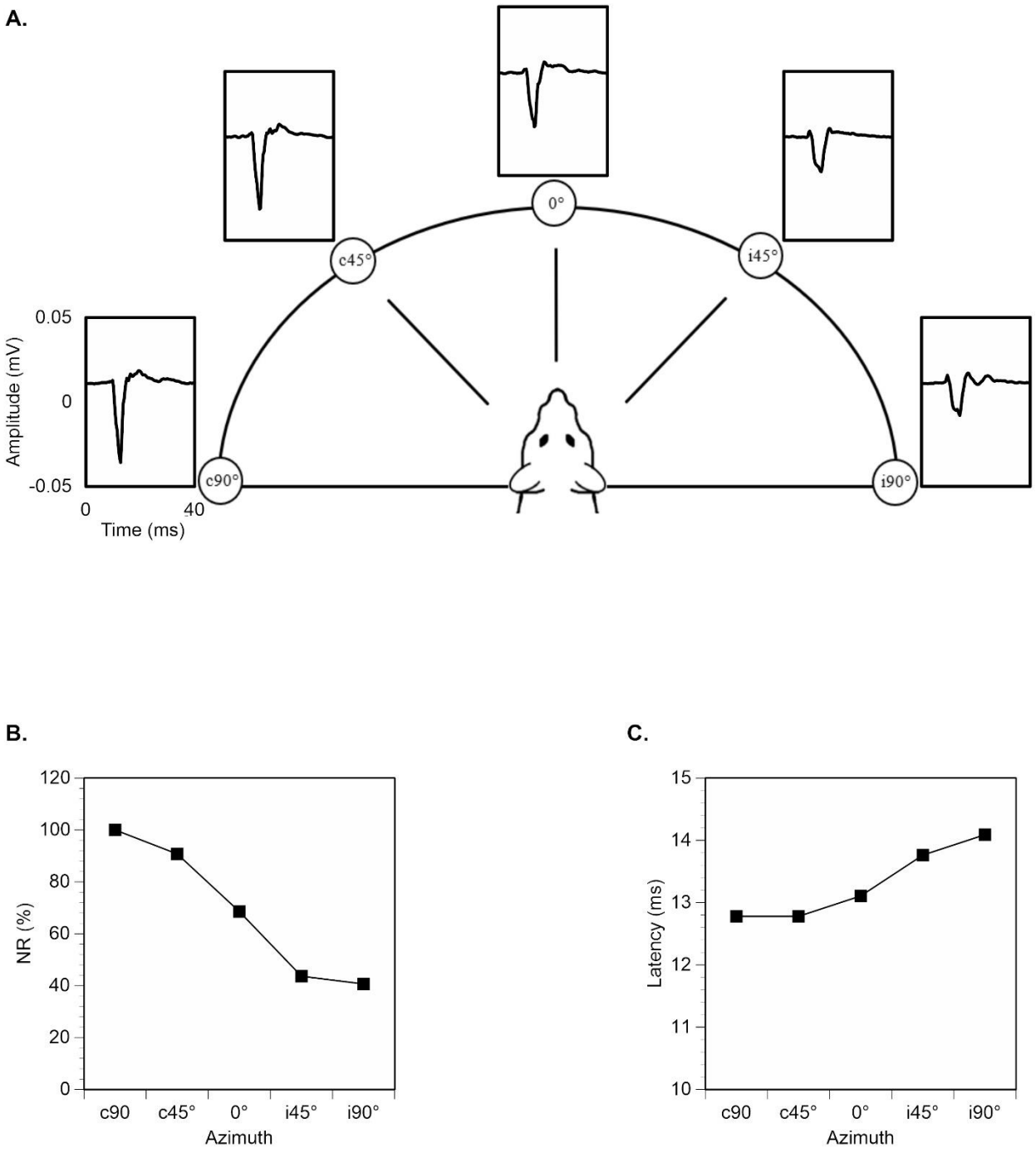


**Figure 17.** An example showing LFP signals elicited by a tone burst presented at 5 different azimuths. The tone burst was at the $f_L$ of a recording site (4,830 Hz) at 70 dB SPL (50 dB above the threshold at CF at c90°). **A.** Waveforms of LFPs elicited by the tone burst presented at 5 azimuths. **B.** Line chart showing a dependence of the amplitude of the negative peak on the

azimuth of the tone burst. **C.** Line chart showing a dependence of the latency of the negative peak on the azimuth of the tone burst.

Within each case, the amplitude of the negative peak of an LFP obtained at each azimuth was normalized against the amplitude of the response obtained at c90° to reflect the azimuth dependence of the LFP. Such an azimuth dependence was examined in 11 cases. The results are summarized in Figure 18. It is clear that the amplitude of an LFP obtained when the sound was at an ipsilateral azimuth was reduced in comparison to that obtained when the sound was at c90°. The median NR of the responses at c45°, 0°, i45°, and i90° were 95.75% (SEM = 4.16%), 82.47% (SEM = 4.87%), 48.21% (SD = 7.62%), and 40.71% (SD = 5.29%). The azimuth-dependent reduction in the amplitude of the response was significant (Friedman test, $\chi^2$ (4) = 31.273, $p < 0.001$). Wilcoxon-signed rank *post-hoc* test revealed a significant difference between results obtained at c90° and i45° ($Z = 2.091$, $p = 0.002$) and between results obtained at c90° and i90° ($Z = 3.273$, $p < 0.001$).

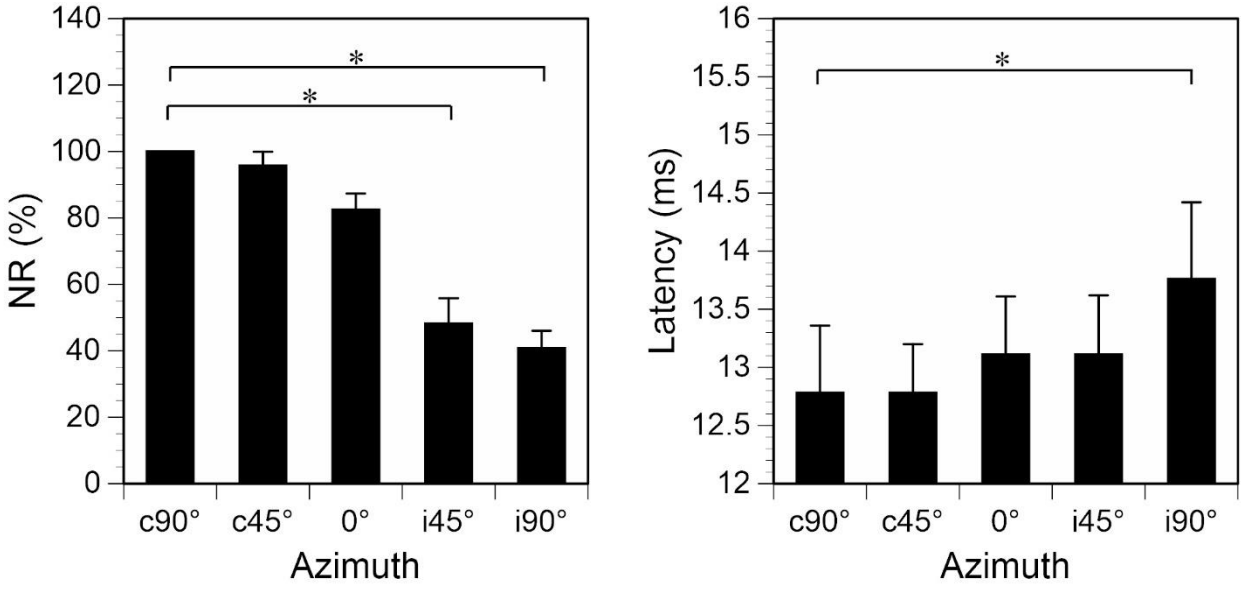

**Figure 18.** Group results (n=11) showing normalized amplitudes of the negative peak of an LFP (left) and latencies of the negative peak of an LFP (right) elicited by a single tone burst presented at various azimuths. Error bars show SEM.

The latency of the negative peak of an LFP was increased when the tone was relocated from c90° to another azimuth. The median latency at c90°, c45°, 0°, i45°, and i90° was 12.78 ms (SEM = 0.58 ms), 12.78 ms (SEM = 0.42 ms), 13.11 ms (SEM = 0.5 ms), 13.11 ms (SEM = 0.51 ms), and 13.76 ms (SEM = 0.66 ms). The increase was statistically significant (Friedman's test, $\chi^2$ (4) = 12.354, $p$ = 0.015). The Wilcoxon-signed rank *post-hoc* test revealed a significant difference between the latencies at c90° and i90° ($Z$ = -1.955, $p$ = 0.004).

### 3.3 Responses to a pair of leading-trailing sounds

#### *3.3.1 Leading-trailing sounds colocalized at c90°*

To determine how a leading sound in a leading-trailing sound pair affected the response to a trailing sound, the pair of sounds was presented when both sounds were colocalized at c90° and separated by various ISIs. Responses were collected from 15 cases.

As shown by an example in Figure 19, the negative peak of an LFP elicited by a leading sound in a leading-trailing sound pair was the same as that elicited by the sound presented alone (Figure 19A upper row). Furthermore, a leading sound in a leading-trailing sound pair elicited the same response when the two sounds were separated by nine different ISIs (Figure 19A upper row and Figure 19B top left panel). The latency of the negative peak of the LFP elicited by a leading sound in a sound pair is the same as that of the LFP elicited by a leading sound alone (Figure 19B bottom left panel). Thus, over multiple sound presentations of a sound pair the response to a leading sound of a pair was not affected by a trailing sound of a preceding pair.

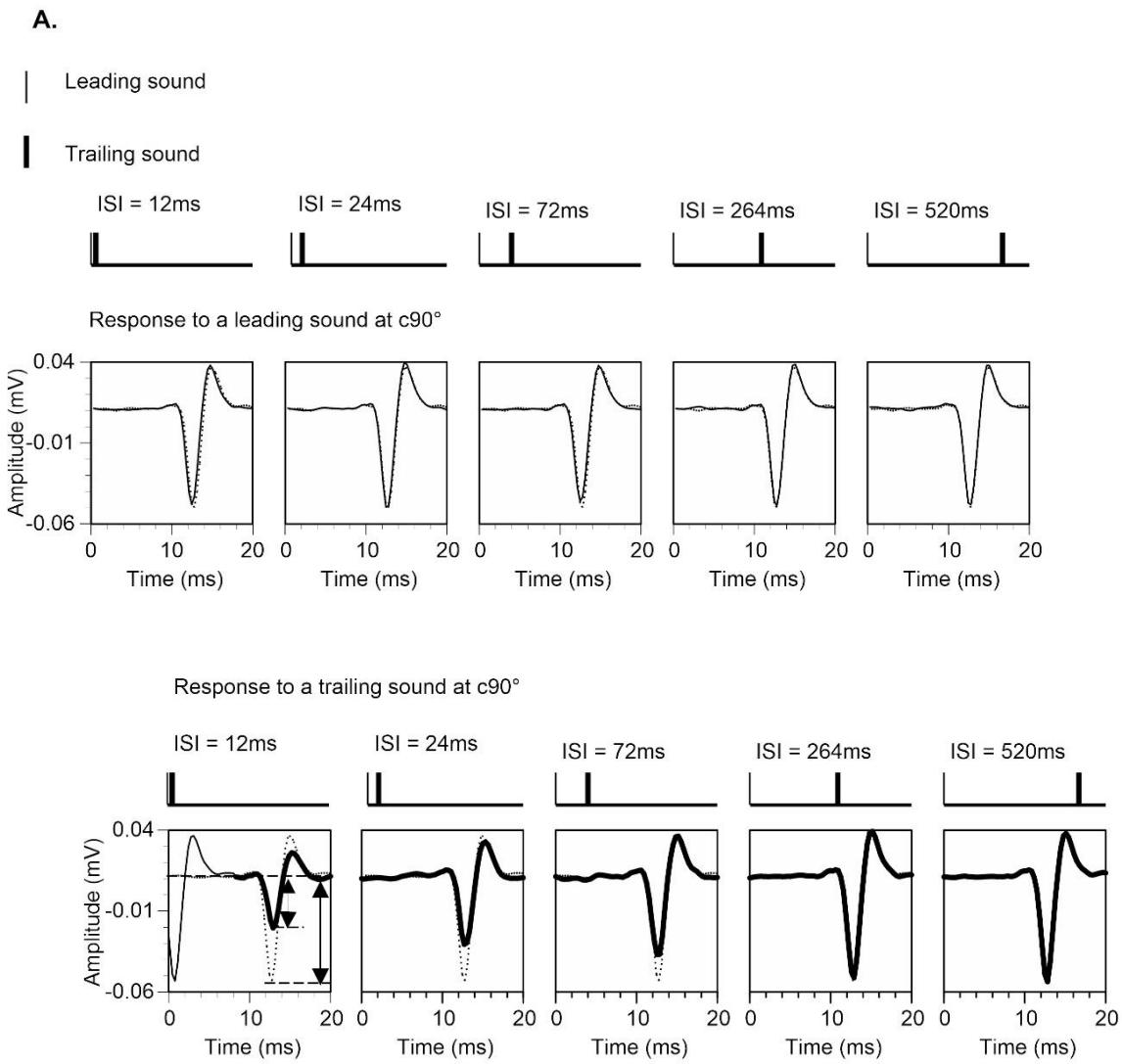
A.
Leading sound
Trailing sound
ISI = 12ms
ISI = 24ms
ISI = 72ms
ISI = 264ms
ISI = 520ms
Response to a leading sound at c90°
Amplitude (mV)
0.04
-0.01
-0.06
0
10
20
Time (ms)
Response to a trailing sound at c90°
ISI = 12ms
ISI = 24ms
ISI = 72ms
ISI = 264ms
ISI = 520ms
Amplitude (mV)
0.04
-0.01
-0.06
Time (ms)

**B.**

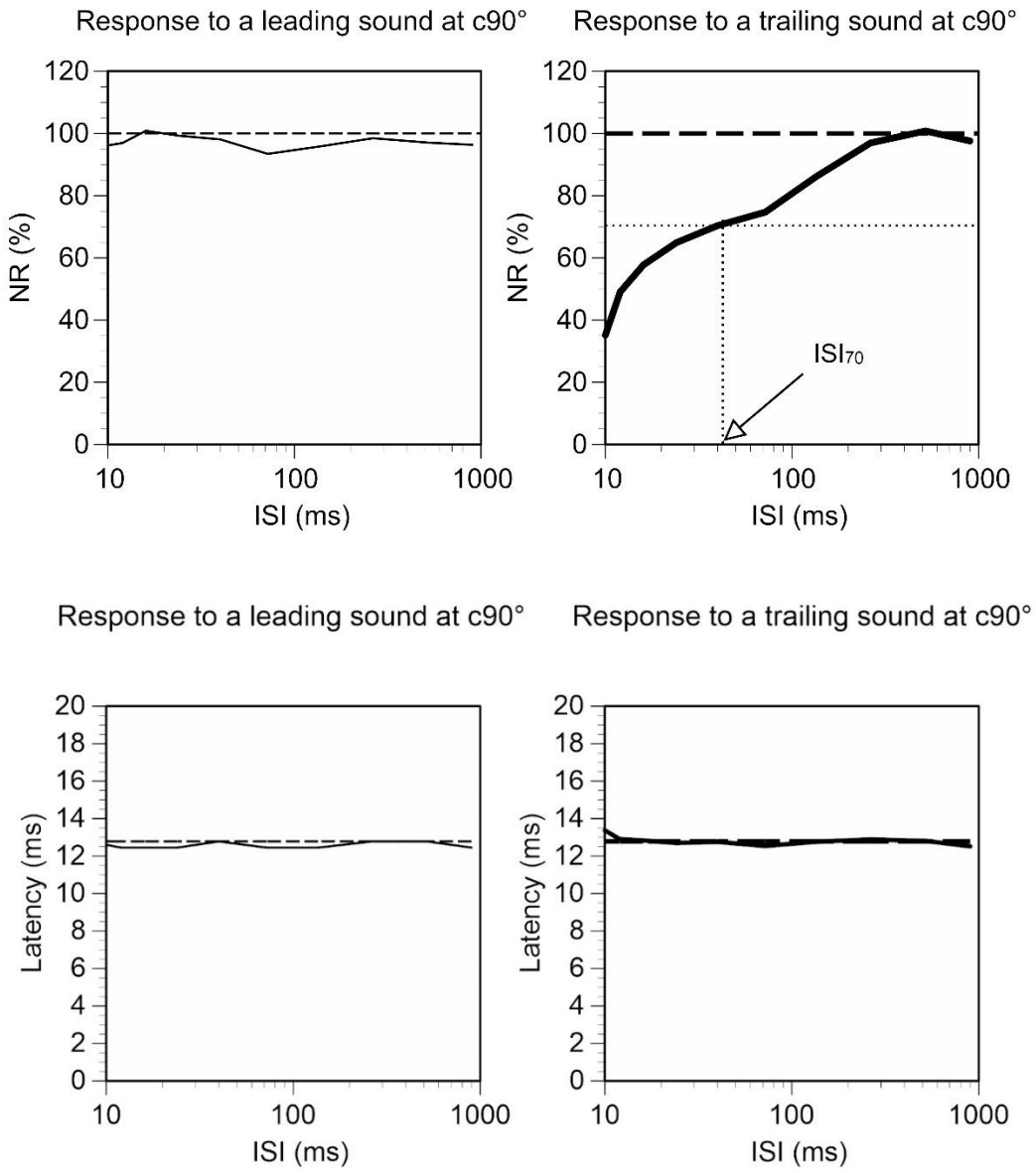


**Figure 19.** An example showing responses to a pair of leading and trailing sounds that were colocalized at c90°. **A.** Top and bottom rows show responses to the leading and trailing sounds, respectively. A leading sound and responses to a leading sound in a leading-trailing sound pair are indicated by thin lines while a trailing sound and responses to a trailing sound in a leading-trailing sound pair are indicated by the thick lines. Responses to leading and trailing sounds that were presented alone are shown by the dotted lines. **B.** Line charts that summarize responses to

leading and trailing sounds obtained at various ISIs. The left column is based on responses to a leading sound while the right column is based on responses to a trailing sound. Within each column, the top panel shows amplitudes of the negative peak of an LFP while the bottom panel shows latencies of the negative peak of an LFP. In the top panels, the horizontal dashed line shows NR of 100%. The $ISI_{70}$ shows the the time point at which the trailing sound NR recovered to 70%. The horizontal dashed line in the bottom panels shows the latency of leading sound alone (left panel) and trailing sound alone (right panel).

The response to a trailing sound was suppressed by a leading sound when the leading-trailing sounds were separated by a small ISI. When the ISI was 12 ms, the amplitude of the negative peak of an LFP elicited by a trailing sound was 49.03% of that of the LFP elicited by the same sounds presented alone (Figure 19A left panel of the bottom row). The suppressive effect was reduced at larger ISIs (Figure 19A bottom row and Figure 19B right panel). The ISI at which the amplitude of the response elicited by a trailing sound in a sound pair was 70% of that of the response elicited by the sound presented alone was calculated using the curve shown in Figure 19B right panel. Such an $ISI_{70}$ value was obtained through interpolation using two data points immediately next to the one associated with $ISI_{70}$ (with one above while the other one below the point associated with $ISI_{70}$) (see appendix for a sample calculation). For the example shown in Figure 19, the $ISI_{70}$ is 38.92 ms. A further analysis was made on the latency of the negative peak of the LFP elicited by a trailing sound in a leading-trailing sound pair. The latency was unchanged over the entire range of the ISIs.

Figure 20 shows group results from a total of 15 cases in which the responses to a pair of leading-trailing sounds colocalized at c90° were examined for ISIs up to 520 ms. The amplitude of the response to a leading sound was not different across the entire range of ISIs (Friedman’s

test, $\chi^2$ (7) = 1.822, $p$ = 0.969) (Figure 20 left panel). In contrast, the amplitude of the response to a trailing sound was lowest at short ISIs and gradually increased to 100% NR. The response to a trailing sound was significantly different across the different ISIs (Friedman's test, $\chi^2$ (7) = 73.444, $p < 0.001$). Wilcoxon-signed rank *post-hoc* analysis showed that there was a significant reduction in NRs between the shorter ISIs (12 ms to 72 ms) and ISI 520 ms. For each of the 15 cases, an $ISI_{70}$ value was calculated using the amplitude-ISI curve based on the LFP elicited by a trailing sound. The median $ISI_{70}$ was 38.93 ms (SEM = 24.66 ms).

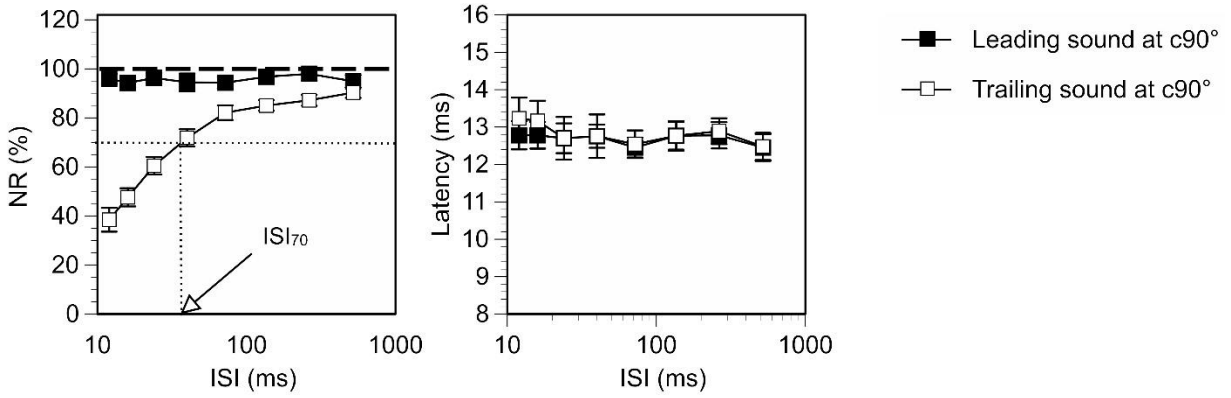


**Figure 20.** Group results showing the dependence of responses to a leading and a trailing sound on the ISIs between the two sounds. The left figure is based on the normalized amplitude of the negative peak of an LFP while the right figure is based on the latency of the negative peak of an LFP. The dashed line shows NR values of 100% . The $ISI_{70}$ shows the the time point at which the trailing sound NR recovered to 70%. Error bars show the SEM.

Group results did not reveal a significant difference in the latency of the negative peak of the LFP elicited by a leading sound across different ISIs (Friedman's test, $\chi^2$ (7) = 7.845, $p$ = 0.346) (Figure 20 right panel). There was a significant difference in the latency of the negative peak of the LFP elicited by a trailing sound across different ISIs ($\chi^2$ (7) = 49.556, $p < 0.001$).

Wilcoxon-signed rank *post-hoc* analysis showed that the latencies at ISIs 12 ms to 136 ms were significantly higher than the latency at ISI 520 ms.

### *3.3.2 Leading-trailing sounds spatially separated*

The effect of relocating a leading sound from c90° to another azimuth on the response to a trailing sound that remained at c90° was examined in ten cases. Shown in Figure 21 is an example. Responses to a pair of leading-trailing sounds were obtained when the two sounds were temporally separated by an ISI of 24 ms. Relocating a leading sound from c90° to another azimuth reduced the amplitude and increased the latency of the negative peak of the LFP elicited by the sound. This is apparent when comparing the responses to the leading sounds (thin black lines) in each panel to the reference waveform of the leading sound alone (dotted line) at c90°. In Figure 21, the amplitude of the leading sound was 0.0394 mV at c90° and was reduced to 0.0146 mV at i90°. In contrast, the latency of the leading sound was increased when the sound moved away from the c90° azimuth from 13.11 ms to 14.09 ms at the i90° azimuth. This increase in latency is reflected by the increase in the duration of the leading sound LFP trough as the sound is moved towards the i90° azimuth. Such relocation of a leading sound also changed the response to a trailing sound (thick black lines) (Figure 21). The amplitude of the negative peak of the LFP elicited by the trailing sound was increased from 0.0197 mV when the leading sound was at c90° to 0.0223mV when the leading sound was at i90°. The latency of the response to a trailing sound was reduced from 13.03 ms when a leading sound was at c90° to 12.70 ms when the leading sound was at i90°.

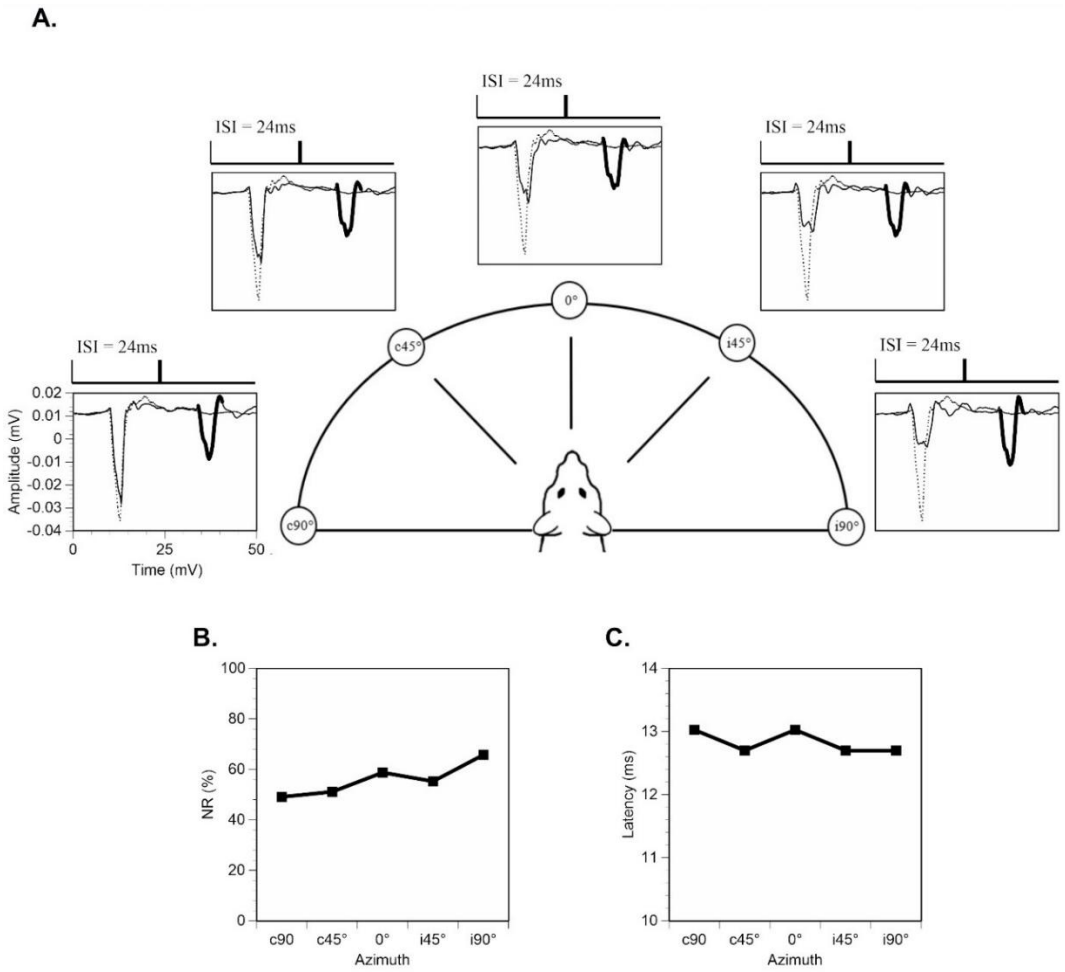


**Figure 21.** An example showing that relocation of a leading sound from c90 to another azimuth changed responses to both leading and trailing sounds. Responses shown in this figure were obtained when a leading and a trailing sound were separated by an ISI of 24 ms. The leading sound was presented at various azimuths, while the trailing sound was always presented at c90°. **A.** This panel shows waveforms of LFPs elicited by a leading sound and a trailing sound. The response to the leading sound is shown in the thin black line while the response to the trailing sound is shown by the thick black line. A reference response (dotted line) to a leading sound alone at c90° is shown in all panels. **B.** A line chart showing the dependence of the amplitude of the negative peak of an LFP elicited by the trailing sound on the location of the leading sound. **C.**

A line chart showing the dependence of the latency of the negative peak of an LFP elicited by the trailing sound on the location of the leading sound.

Figure 22 shows the group results of responses to a trailing sound obtained at ISIs 12, 16 ms, and 24 ms. At each ISI, there was a general increase in the NRs based on responses to a trailing sound when the leading sound was relocated away from the c90° azimuth. The latency of response was also increased when the leading sound was relocated. The NR values were significant different across angles of separation at ISIs 16 ms (Friedman's test, $\chi^2$ (4) = 13.600, $p$ = 0.009) and 24 ms (Friedman's test, $\chi^2$ (4) = 10.640, $p$ = 0.031) (Figure 22). No statistical significance was obtained at 12 ms (Friedman's test, $\chi^2$ (4) = 5.067, $p$ = 0.281). Wilcoxon-signed rank *post hoc* test showed that at 16 ms ISI there was a significant increase in NR (based on responses to a trailing sound) when the leading sound was moved from c90° to i45° ($Z$ = -1.667, $p$ = 0.025) and i90° ($Z$ = -1.778, $p$ = 0.017). At 24 ms ISI, there was a significant increase in NR when a leading sound was moved from c90° to i45° ($Z$ = -1.500, $p$ = 0.034) and i90° ($Z$ = -2.100, $p$ = 0.003). There were no significant differences in the latency of the trailing sound responses under any condition of spatial change.

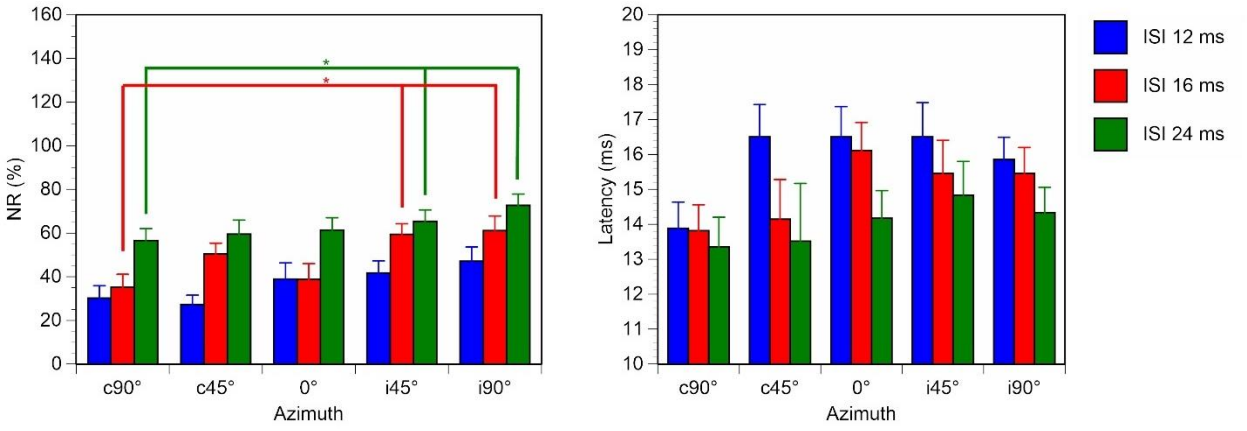

**Figure 22.** Group results showing dependences of the amplitude (left panels) and latency (right panels) of the LFP elicited by a c90° trailing sound on the location of a leading sound at 12, 16, and 24 ms ISIs. The error bars show SEM.

### 3.4 The time course of the effect of a leading sound on the response to a trailing sound

In 17 cases, we compared the time courses of the effect of a leading sound on the response to a trailing sound obtained when the leading sound was at c90° and i90°. For the example shown in Figure 23, the response to a trailing sound was suppressed by a leading sound at short ISIs relative to the trailing sound alone condition. The relocation of the leading sound from the c90° azimuth to the i90° azimuth made the response to the trailing sound slightly less suppressed. The effect of the relocation of a sound from c90° to i90° on the amplitude of the response to a trailing sound was observed at nine other ISIs (Figure 23A left panel and Figure 23B). The $ISI_{70}$ value of the trailing sounds NRs was 23.63 ms when the leading sound was at c90° and it was 13.28 ms when the leading sound was at i90°. In contrast to the effect on the amplitude of the response, the relocation of a leading sound did not change the latency of the response elicited by a trailing sound (Figure 23A right panel).

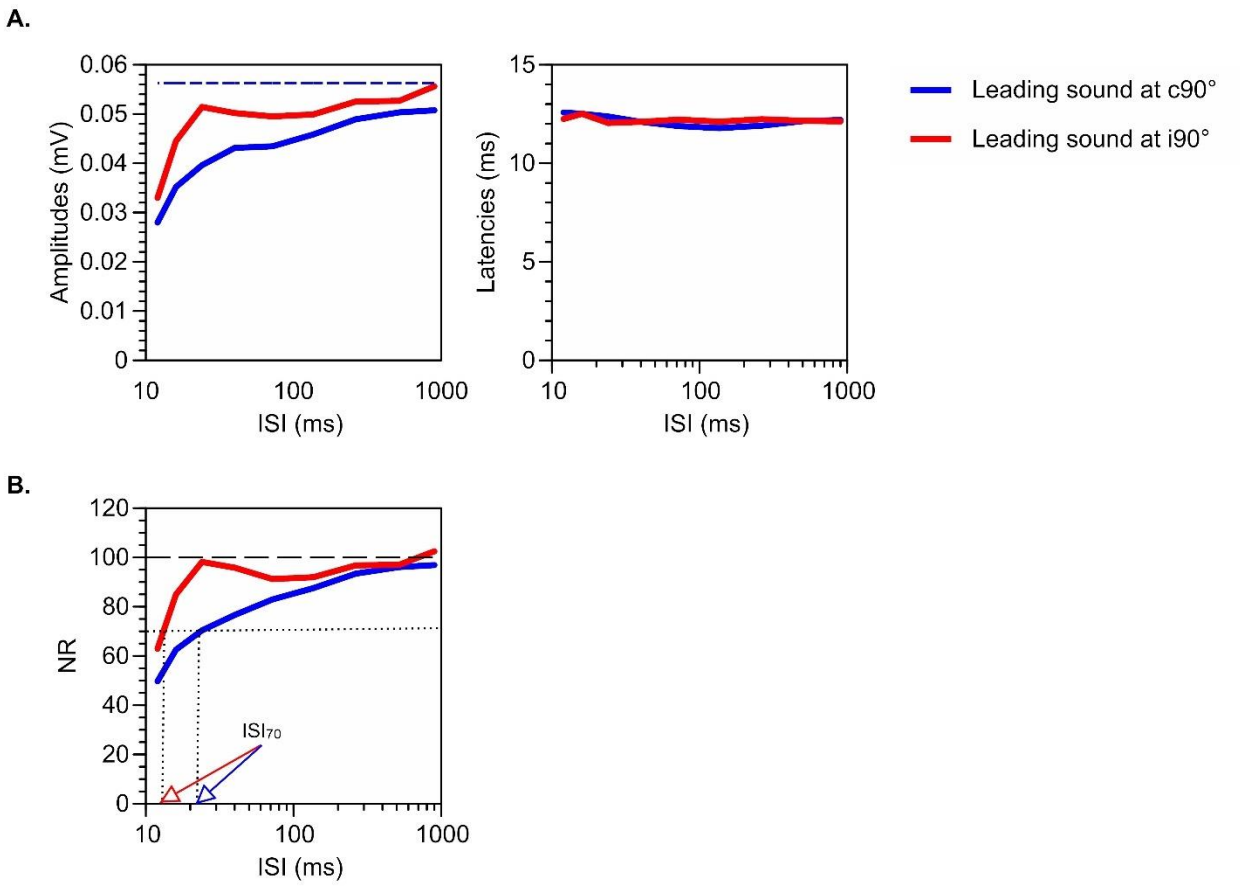


**Figure 23.** An example showing the effect of the relocation of a leading sound from c90° (blue lines) to i90° (red lines) on the suppressive effect on the response to a trailing sound. **A.** The ISI dependence of the absolute amplitude (left panel) and the latency (right panel) of the negative peak of an LFP elicited by a trailing sound. The blue dashed line in the left panel shows the amplitude of the trailing sound alone. **B.** The ISI dependence of the normalized amplitude of the response elicited by a trailing sound. The red and blue arrows indicate the $ISI_{70}$ time points of the trailing sound response NRs when the leading sound was at i90° versus c90° respectively.

Group results indicate that relocating a leading sound from c90° to i90° significantly changed the amplitude of response to a trailing sound (Figure 24, Friedman's test, $\chi^2$ (15) = 185.694, $p < 0.001$). Wilcoxon-signed rank *post hoc* test showed that there was a significantly

stronger suppression of the response to a trailing sound when a leading sound was at c90° than when it was at i90° at a few ISIs. These ISIs included 16 ms ($Z$ = -3.412, $p$ = 0.037), 24 ms ($Z$ = -4.824, $p$ = 0.003), and 40 ms ($Z$ = -3.882, $p$ = 0.017). Relocating a leading sound from c90° to i90° did not significantly changed the latency of the negative peak of the LFP elicited by a trailing sound based on Wilcoxon-signed rank *post hoc* test at specific ISIs between the two curves. However, the initial Friedman's test showed that there was a significant difference ($\chi^2$ (15) = 63.909, $p$ < 0.001) but this difference was at different ISIs between the two curves or within the same curve.

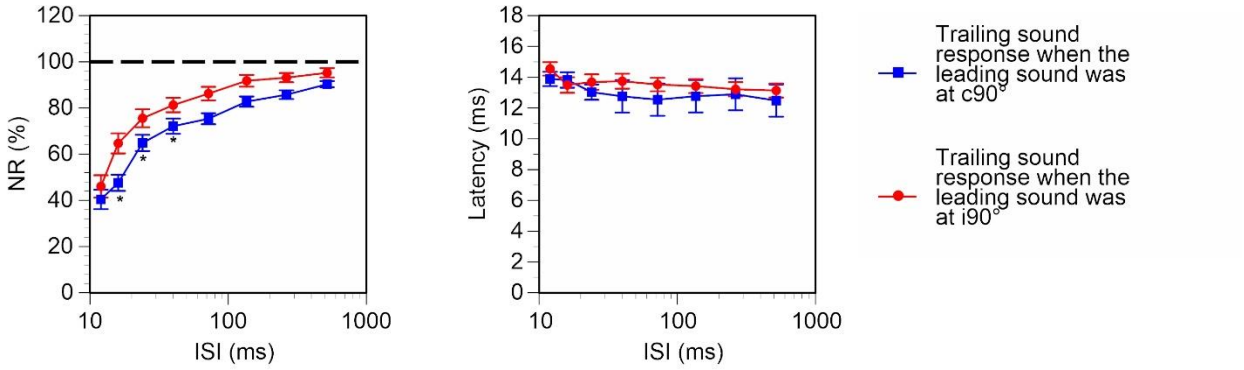


**Figure 24.** Group results showing responses to a trailing sound when a leading sound was at c90° (blue lines) and i90° (red lines) azimuths. The left and right panels show the amplitude and the latency of the negative peak of the LFP elicited by a trailing sound respectively. The dashed line in the left panel shows NR of 100. The error bars show SEM. The ISIs at which the data points significantly differ between the two curves are shown by "*".

Two $ISI_{70}$ values, based on the response to a trailing sound that was preceded by a leading sound at c90° and i90°, were obtained from the same 17 cases (Figure 25). The median $ISI_{70}$ value was 32.21 ms (SEM = 6.73 ms) when a leading sound was at c90° and 18.27 ms (SEM = 3.54 ms) when a leading sound was at i90°. The Wilcoxon-signed rank test showed a

significant difference between the $ISI_{70}$ values obtained when a leading sound was at c90° vs. i90° ( $Z = -3.527$, $p < 0.001$).

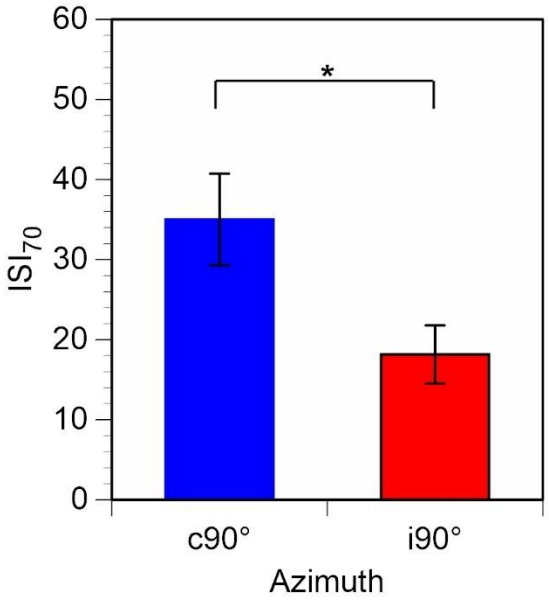


**Figure 25.** $ISI_{70}$ values of the c90° and i90° trailing sound response curves. The error bars show SEM.

### 3.5 Effects of gabazine

#### *3.5.1 Effects of gabazine on a response elicited by a single tone*

The specific antagonist of the $GABA_A$ receptor, gabazine, was used to block the inhibitory neurotransmission mediated by the receptor. The effect of the drug was revealed by LFP elicited by a single tone burst that was presented at c90° and i90°. As shown by an example in Figure 26, Gabazine enhanced the LFP regardless of the location where the sound was presented (Figure 26). It was noted that the enhancement occurred only after the initial falling phase of the trough of the LFP, which resulted in the widening of the waveform and a minor increase in the latency of the negative peak. The effect of gabazine was reversible. The

waveform of an LFP including its amplitude typically returned to its pre-drug levels 60 mins after the cessation of the drug injection.

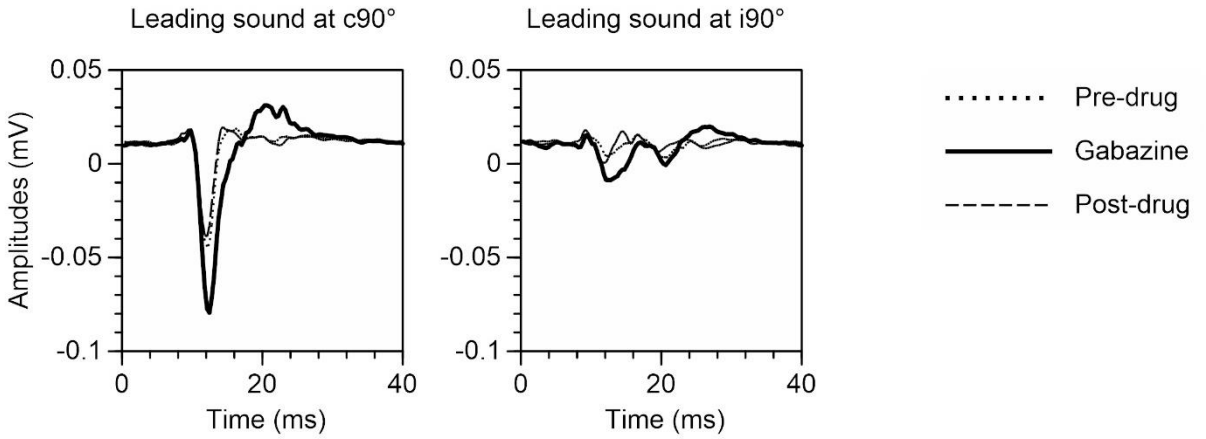


**Figure 26.** Effect of gabazine on an LFP elicited by a single tone presented at c90° and i90°.The CF of the recording site: 12 kHz; the frequency of the tone burst: 11,591.236 Hz.

The enhancement of the amplitude was observed over a wide range of supra-threshold stimulus intensities. Shown in Figure 27 is the AIF curves obtained before, during, and after injection of gabazine. The drug produced a proportional increase in the amplitude of the negative peak of an LFP over the entire range of intensities at which a tone burst was presented. Furthermore, the recovery of the response is observed.

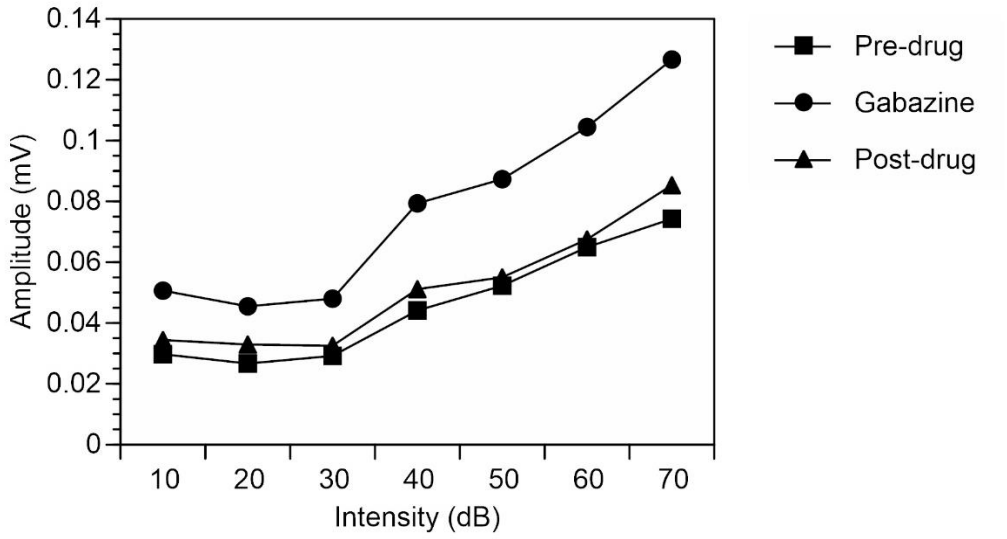


**Figure 27.** Gabazine changed the amplitude-intensity function of the negative peak of an LFP. In this case, LFPs were elicited by a tone burst at the CF of the recording site (12 kHz) presented at c90° before, during, and after injection of gabazine.

The effect of gabazine on the LFP elicited by a single tone burst was examined in 8 cases. Changes similar to those shown in Figure 27 were observed in all the 8 cases. These cases displayed increases in the amplitude of the negative peak of the LFP at all supra-threshold intensities. Based on trailing sound alone (presented at 30 dB above threshold) responses at c90°, the percentage increase in the amplitude ranged between 54.02% and 195.19% after drug injection. The median increase was 97.87% (SEM = 17.19%). The current used ranged from 10 to 91 nA (median 15 nA ± 16.13 nA (SEM).

### *3.5.2 Effects of gabazine on responses elicited by a pair of leading-trailing sounds*

The effects of gabazine on responses to a pair of leading-trailing sounds were evaluated in 6 cases. As shown by an example in Figure 28, gabazine enhanced responses to both a leading and a trailing sound (Figure 28A and B). The drug also caused an increase in the latency of

response (Figure 28A and B). The drug changed the time course of the suppressive effect produced by a leading sound. During the drug injection, the response to a trailing sound was less suppressed at short ISIs when a leading sound was presented at c90° (Figure 28C). The suppressive effect produced by a leading sound was not affected at large ISIs. Furthermore, the drug didn't substantially change the suppressive effect produced by a leading sound at any ISI when the leading sound was presented at i90° (Figure 28C). The $ISI_{70}$ value obtained based on responses recorded before and during injection of gabazine was 26.63 ms and 13.27 ms when a leading sound was presented at c90°. It was 13.28 ms and 14.41 ms, respectively, when a leading sound was presented at i90°.

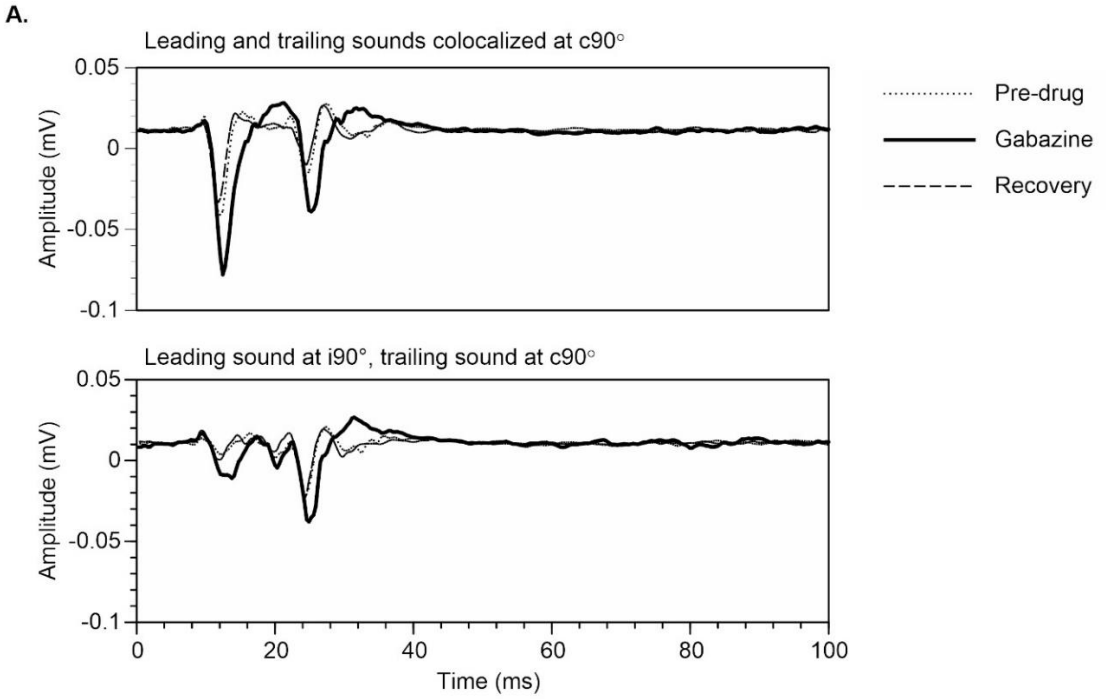

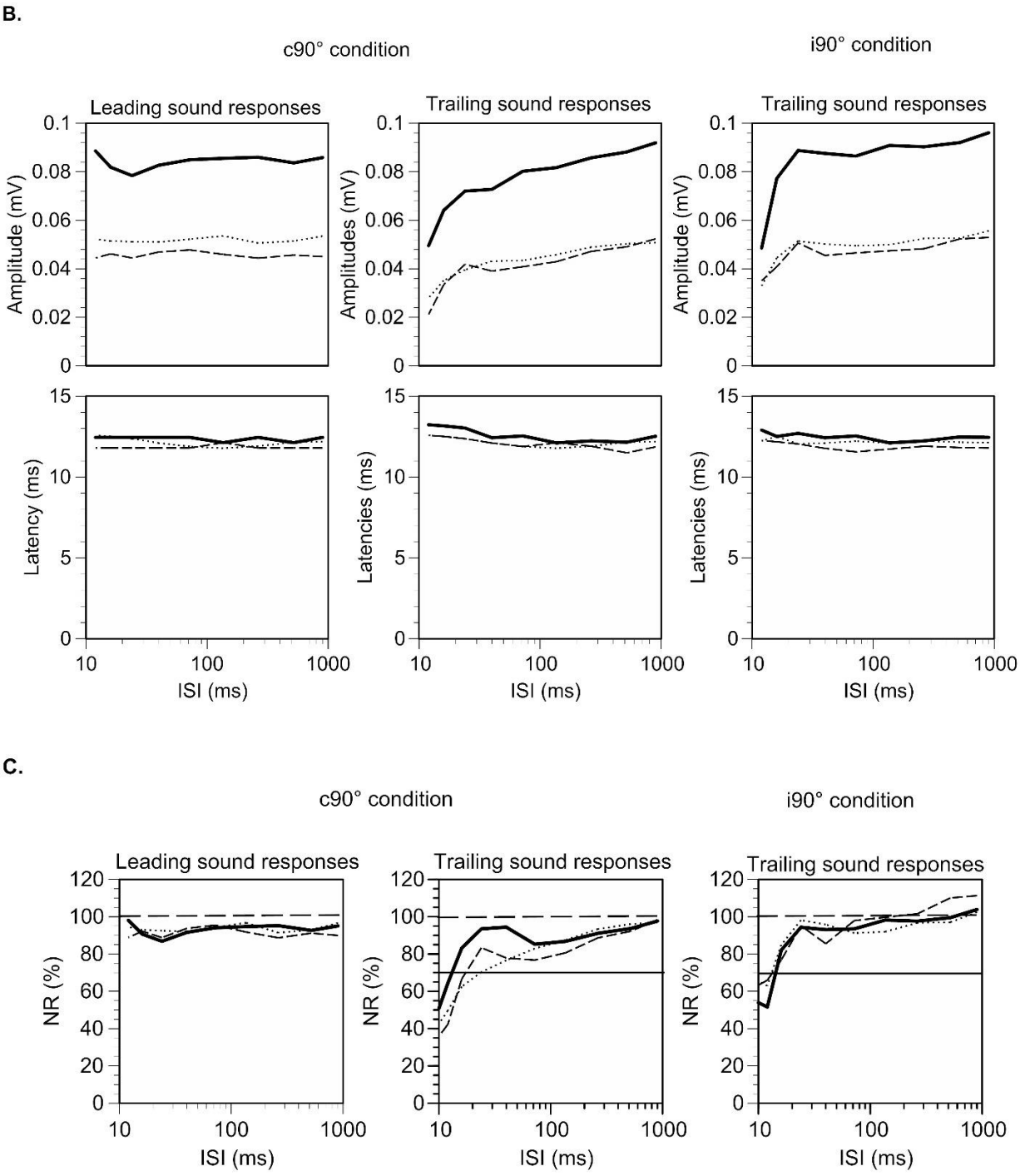


**Figure 28.** An example showing the effects of gabazine on responses to a pair of leading-trailing sounds. A. The top panel shows results obtained when the leading sound was at c90° while the bottom panel shows results obtained when the leading sound was at i90°. The ISI between the

leading and trailing sounds was 12 ms. B. Line charts showing the amplitude (top panels) and latency (bottom panels) of the negative peaks of LFPs elicited by a leading and a trailing sound over a wide range of ISIs. The two left column panels show responses to a leading sound and trailing sound when they were colocalized at c90°. The right panels show responses to a trailing sound when the leading sound was at i90°. C. Line charts showing normalized response to a leading sound at c90° (left panel), a trailing sound at c90° that was colocalized by a leading sound (middle panel), and a trailing sound at c90° when a leading sound was at i90° (right panel), respectively. In all panels, the horizontal dashed line indicates an NR of 100%. The horizontal solid line indicates an NR of 70%.

Group results based on six cases supported results from the example shown in Figure 29. Only responses at ISIs 12, 16, 24, 40, 72, and 520 ms were used in the evaluation since some cases were missing data points at other ISIs. These results indicate that when leading and trailing sounds were colocalized at c90° the normalized amplitude of the negative peak of an LFP elicited by a leading sound was constant across the entire range of ISIs both before and during the application of gabazine (Figure 29A top left panel). The normalized amplitudes and latencies of the response to a leading sound obtained before and during drug application were similar to each other (Friedman's test, $\chi^2$ (11) = 9.667, $p$ = 0.561 and $\chi^2$ (11) = 7.713, $p$ = 0.739 respectively).

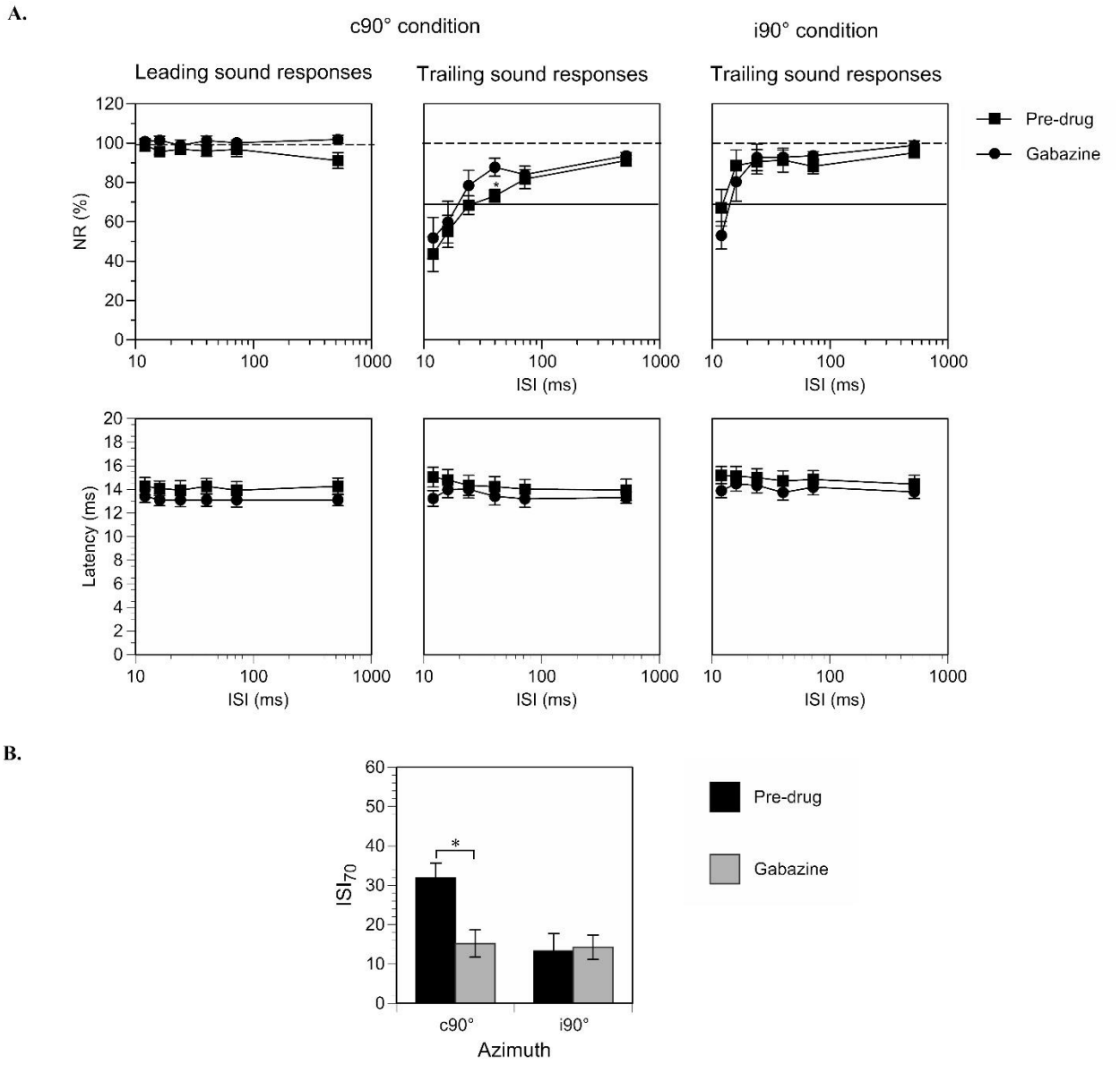


**Figure 29.** Group results showing the effects of gabazine on responses to leading and trailing sounds in a sound pair. A. Line charts showing normalized amplitude (top panels) and latency (bottom panels) of the negative peak of an LFP elicited by a leading sound (first column) or a trailing sound (second and third columns). The first two columns show responses to a leading sound (first column) and a trailing sound (second column) when the two sounds were colocalized at the c90°. The third column shows the response to a trailing sound (located at i90°) when a leading sound was at i90°. B. $ISI_{70}$ values based on responses to a trailing sound obtained before

and during the application of gabazine. Results were obtained when a leading sound was at c90° and i90°, respectively. The error bars show SEM.

When a leading sound was at c90°, the median normalized amplitude of the negative peak of an LFP elicited by a trailing sound was increased by gabazine at short ISIs (Figure 29A top middle panel) (Friedman's test, $\chi^2$ (11) = 40.282, $p < 0.001$). A Wilcoxon-signed rank *post-hoc* test showed that there was a significant difference between the pre-drug and gabazine curve at ISI 40 ms ($Z$ = -4.167, $p$ = 0.045). The $ISI_{70}$ value was significantly reduced (Wilcoxon-signed rank test, $Z$ = -2.028, $p$ = 0.043) (Figure 29B left panel). The $ISI_{70}$ value was 31.83 ms (SEM = 3.80 ms) obtained before gabazine injection and it was 15.20 ms (SEM = 3.48 ms) during the application of gabazine. When comparing the latency of trailing sound colocalized with the leading sound at c90°, there were no significant difference of latencies between pre-drug and gabazine curves at specific ISIs based on Wilcoxon-signed rank post hoc tests. However, the initial Friedman's test showed that there was a significant difference ($\chi^2$ (11) = 19.965, $p$ = 0.046) but this difference was at different ISIs between the two curves or within the same curve based on the *post hoc* test. When the leading sound was at i90°, there were no differences at the same ISIs between the normalized amplitudes of the negative peak of an LFP elicited by a trailing sound. Concomitantly, the $ISI_{70}$ value was not affected by the drug when a leading sound was at i90° ($Z$ = -2.280, $p$ = 0.866) (Figure 29B right panel). When comparing the trailing sound latencies between pre-drug and gabazine curves, there were no significant differences of normalized amplitudes at specific ISIs.

## 3.6 Effects of CGP35348

### *3.6.1 The effect of CGP35348 on response elicited by a single tone*

The effect of CGP35348 on an LFP elicited by a single tone burst was evaluated in five cases. As shown by the example in Figure 30, the drug minimally affected the responses. The waveforms obtained before, during, and after application of the drug overlapped with each other substantially.

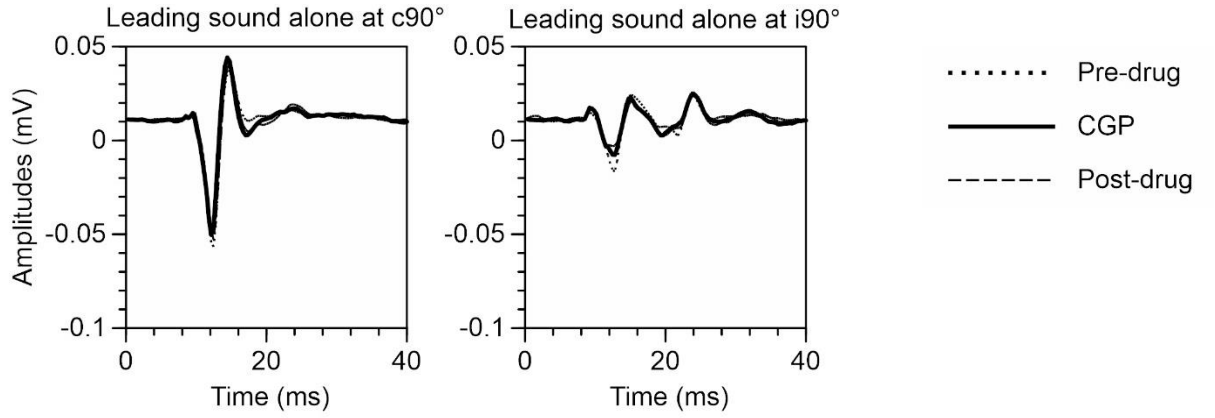


**Figure 30.** An example showing the effect of CGP35348 on the response to a single tone burst (serving as a leading sound in a leading-trailing sound pair) at c90° and i90°. The CF of the recording site: 10 kHz; the frequency of the tone burst: 10.352 kHz.

For the same case, as shown in Figure 30, CGP35348 minimally affected responses to a single tone burst over a wide range of stimulus intensity. Thus, an AIF curve based on these responses was not affected by the drug (Figure 31).

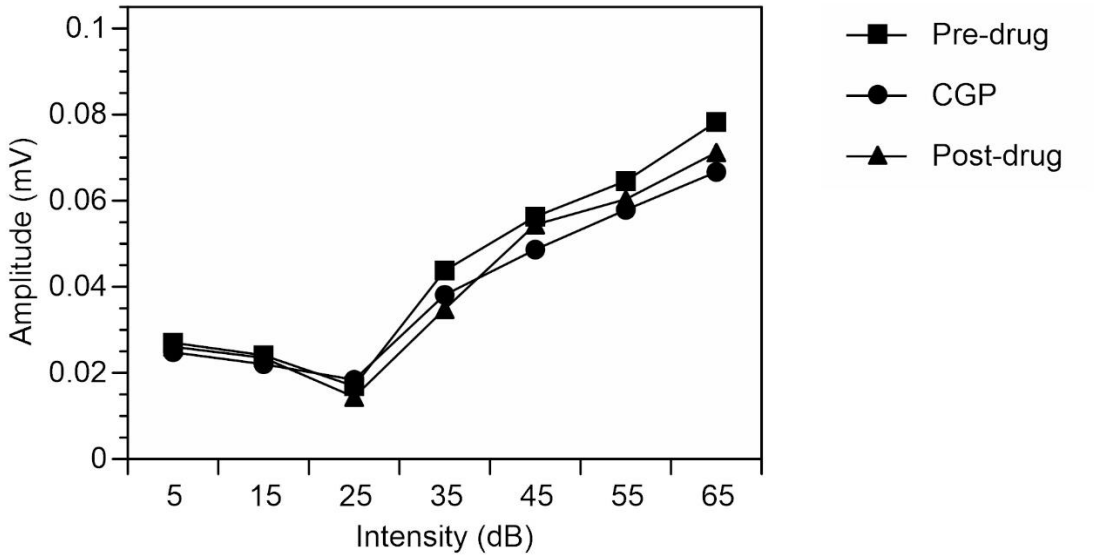


**Figure 31.** An example showing the effect of CGP35348 on an amplitude-intensity function based on the negative peak of an LFP. LFP responses were elicited by a tone burst at the CF of the recording site (10 kHz).

Group results from the 5 cases supported that CGP35348 minimally affected LFP responses elicited by a single tone burst.

### *3.6.2 Effects of CGP35348 on responses elicited by a pair of leading-trailing sound*

CGP35348 minimally affected LFPs elicited by a leading and a trailing sound in a sound pair regardless of the location of the leading sound. There were no significant differences of the normalized amplitudes between the pre-drug and CGP conditions both when the leading sound was presented at c90° and i90° at specific ISIs. There were no significant differences between the latencies of the trailing sound responses obtained before and during application of CGP35348 regardless of whether the leading sound was at c90° (Friedman's test, $\chi^2$ (17) = 18.848, $p$ = 0.337) or when it was at i90° (Friedman's test, $\chi^2$ (13) = 14.120, $p$ = 0.365). Thus, the normalized amplitude-ISI and latency-ISI curves based on the negative peak of the LFP elicited by a trailing

sound were not affected by the drug no matter whether a leading sound was presented at c90° or i90° (Figure 32A). Although the $ISI_{70}$ value was reduced during the CGP when the leading sound was at c90° (Median = 28.71 ms, SD = 9.24 ms) compared to the pre-drug condition (Median = 43.96 ms, SD = 16.58 ms), this reduction was not statistically significant (Wilcoxon-signed rank test, $Z = 0.000$, $p = 0.068$). Similarly, there were no significant differences between the $ISI_{70}$ values obtained during (median = 18.58 ms, SD = 4.25 ms) and before (median = 18.27 ms, SD = 9.07) application of CGP35348 when the leading sound was at i90° (Wilcoxon-signed rank test, $Z = 6.000$, $p = 0.686$).

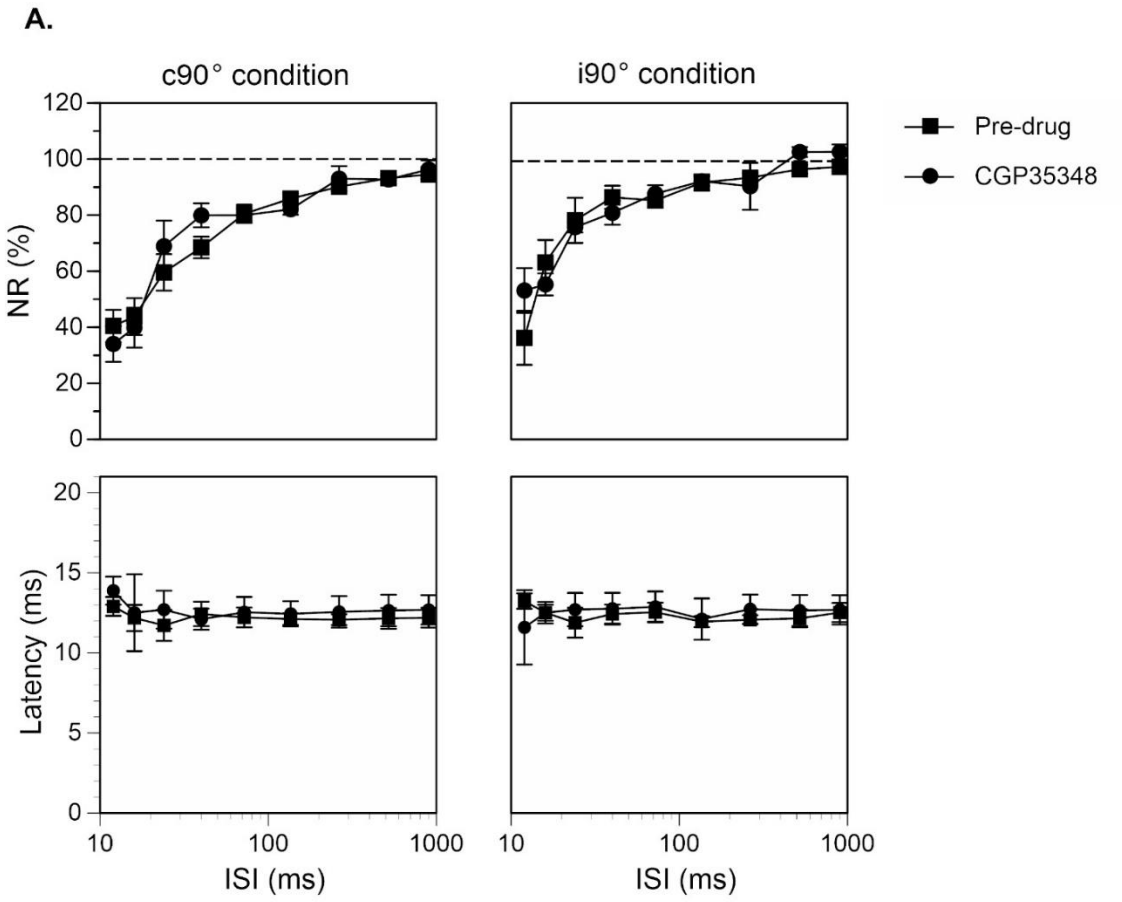

**B.**

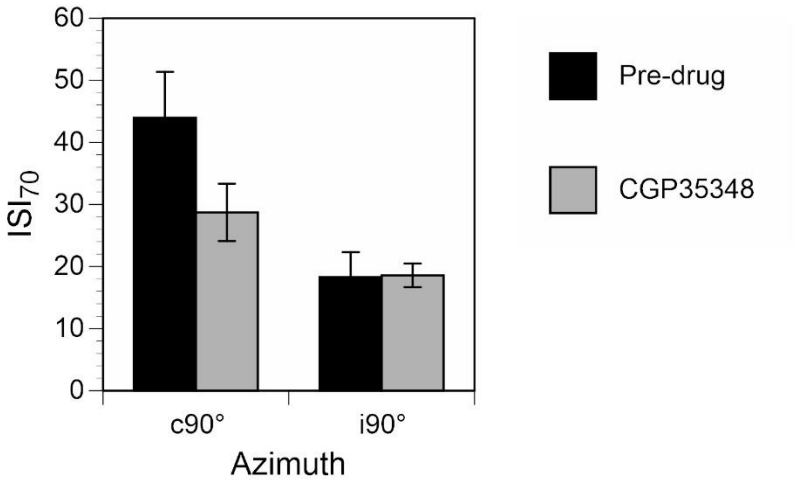


**Figure 32.** Group results showing a lack of effect of CGP35348 on the suppression produced by a leading sound. The suppression was revealed by the response to a trailing sound at a wide range of ISIs. A. Line chart showing normalized amplitude (top panels) and latency (bottom panels) of the negative peak of an LFP elicited by a trailing sound when a leading sound was at c90° (left column) and i90° (right column). The trailing sound was always presented at c90°. B. $ISI_{70}$ values based on responses to a trailing sound obtained before and during the application of CGP35348. Results were obtained when a leading sound was at c90° and i90°, respectively. The error bars show SEM.

### 3.7 Effects of strychnine.

#### *3.7.1 The effect of strychnine on a response elicited by a single tone*

The effect of strychnine was examined in 7 cases. As shown by the example in Figure 33, the drug-enhanced the response to a single tone.

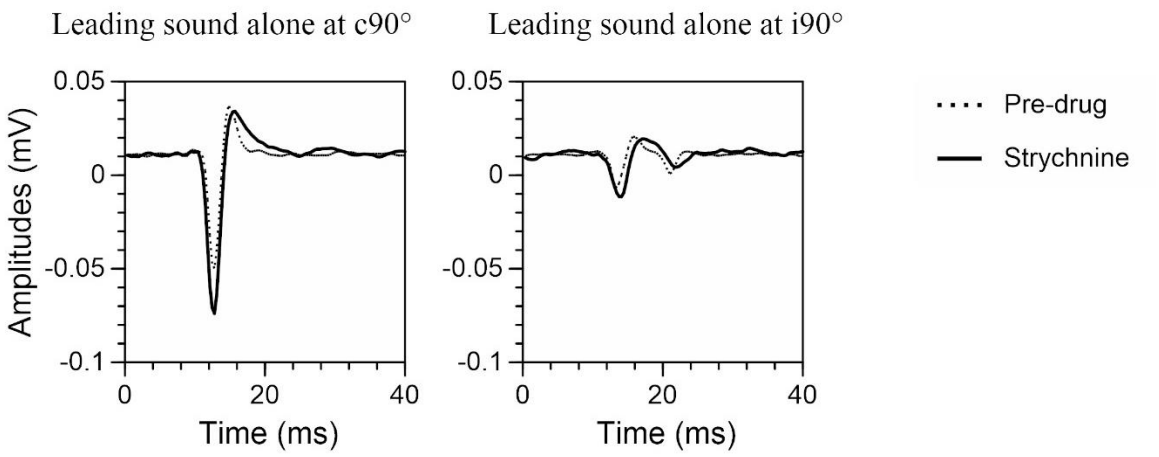


**Figure 33.** An example showing the effect of strychnine on a response to a single tone burst at c90° and i90°. The CF of the recording site: 13 kHz; the frequency of the tone burst: 13,458.44 Hz.

Strychnine produced an effect on the amplitude of the negative peak of an LFP over a wide rate of stimulus intensities. Thus, an AIF curve was proportionally elevated during drug injection (Figure 34). Group results from 7 cases indicated that the increase of response caused by strychnine ranged from 25.99% and 99.03% (Median 40.76% ± 31.46% (SD)).

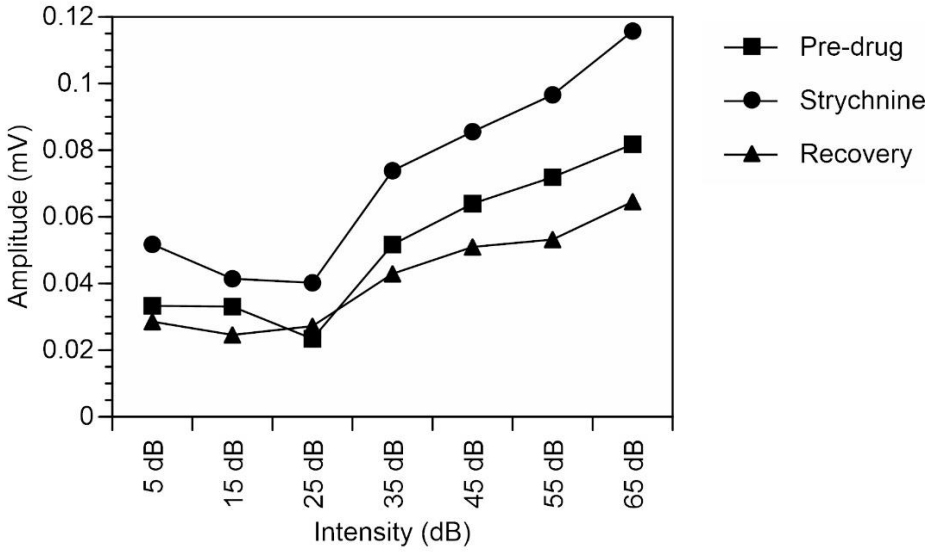

**Figure 34.** An example showing the effect of strychnine on an amplitude-intensity function based on the negative peak of an LFP. LFP responses were elicited by a tone burst at the CF of the recording site (13 kHz) presented at c90°.

### *3.7.2 Effects of strychnine on responses elicited by a pair of leading-trailing sound*

As shown by an example in Figure 35, strychnine increased responses to both leading and trailing sounds in a pair of sound no matter whether the leading sound was presented from c90° or i90° (Figure 35A). The amplitudes of the LFPs elicited by the two sounds were substantially increased during the drug injection (Figure 35B top panels). The latencies were slightly increased during the strychnine condition (Figure 35B bottom panels). A comparison of the leading sound normalized responses shows that there was no increase during the shorter ISIs, however, there was an increase during the longer ISIs. The $ISI_{70}$ value obtained based on responses recorded before and during injection of gabazine was 38.93 ms and 19.92 ms when a leading sound was presented at c90°. It was 21.60 ms and 17.88 ms, respectively, when a leading sound was presented at i90° (Figure 35C). The normalized post-drug response to the leading sound are not shown because a baseline response to a leading sound alone at c90 was not collected during the post-drug condition. Moreover, the animals condition declined drastically during the i90° post-drug condition and responses were excluded from the presentation below.

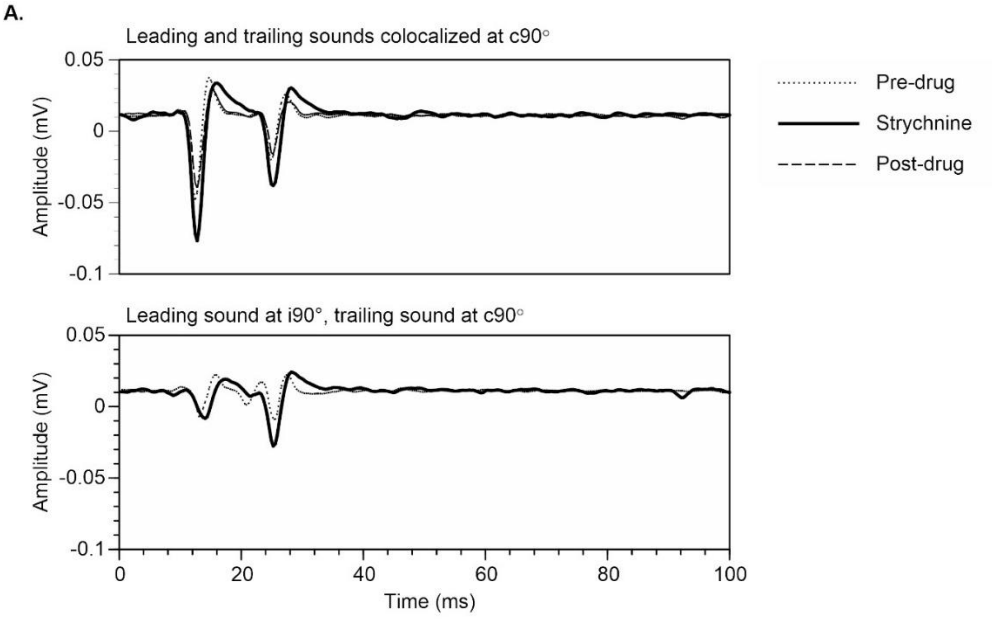
A.
Leading and trailing sounds colocalized at c90°
Amplitude (mV)
0.05
0
-0.05
-0.1
Pre-drug
Strychnine
Post-drug
Leading sound at i90°, trailing sound at c90°
Amplitude (mV)
0.05
0
-0.05
-0.1
0
20
40
60
80
100
Time (ms)

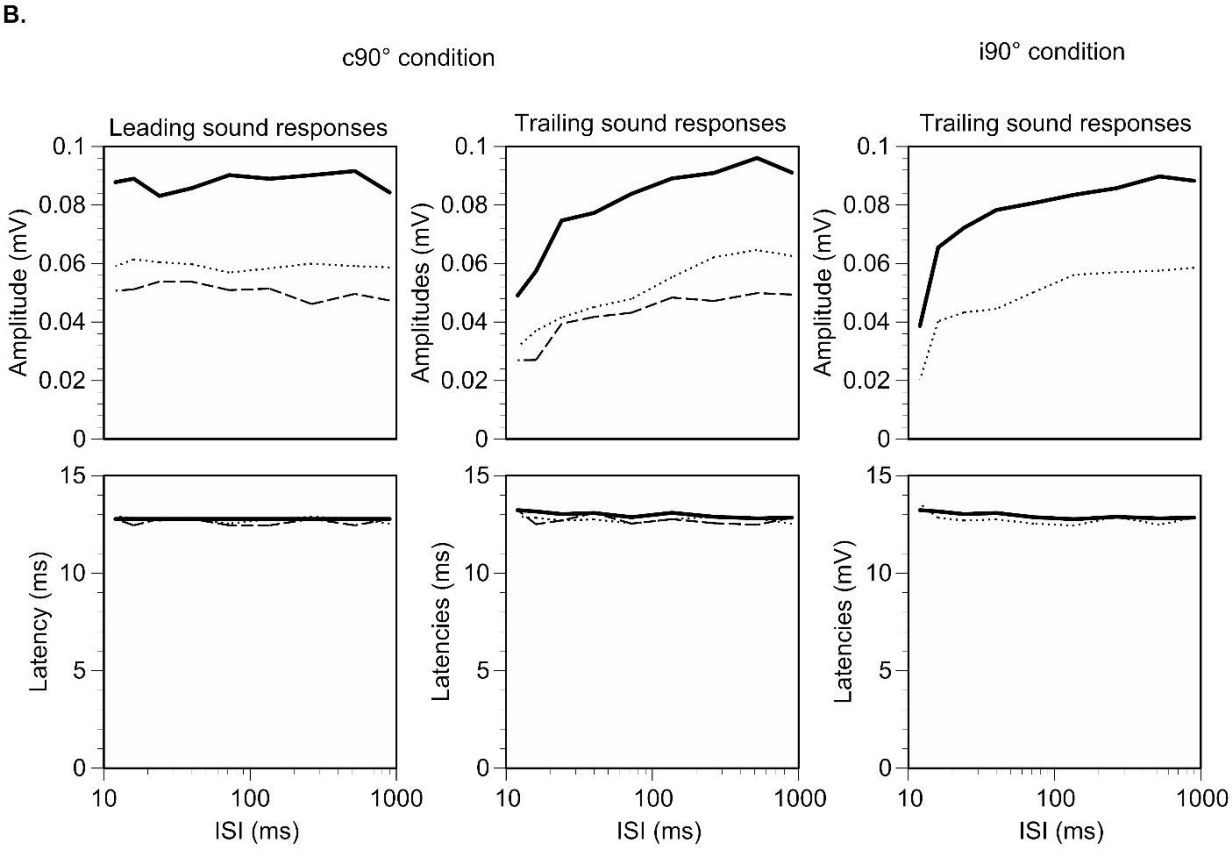
B.
c90° condition
i90° condition
Leading sound responses
Trailing sound responses
Trailing sound responses
Amplitude (mV)
Amplitudes (mV)
Amplitude (mV)
0.1
0.08
0.06
0.04
0.02
0
Latency (ms)
Latencies (ms)
Latencies (mV)
15
10
5
0
10
100
1000
ISI (ms)

C.

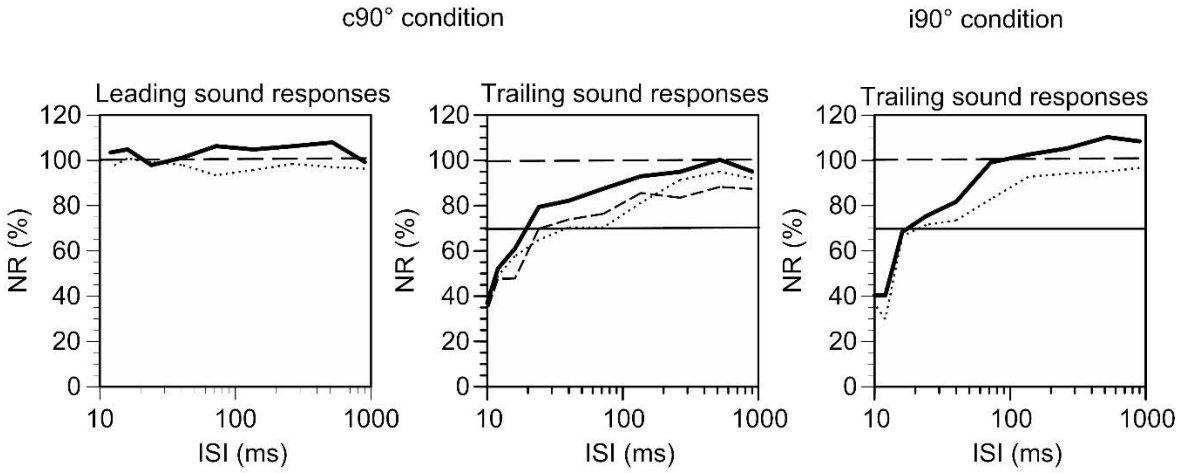


**Figure 35.** An example showing the effects of strychnine on responses to a pair of leading-trailing sounds. A. Effects of strychnine on waveforms of responses to a pair of leading-trailing sounds when a leading sound was presented at c90° and i90°. A trailing sound was at a fixed location at c90°. B. Line charts showing the absolute amplitude (top panels) and latency (bottom panels) of the negative peak of an LFP elicited by a trailing sound obtained before, during, and after application of strychnine. The first two columns show the response to the leading sound (left panels) and trailing sound (middle panels) when the sound was colocalized at c90°. The third column panels show the response to the trailing sound (located at c90°) when the leading sound was at i90°. C. Line charts showing the normalized amplitude of the leading and trailing sound responses. The extreme left panel shows the NR of the leading sound responses when it was at c90°. The middle panel shows the normalized amplitudes of the trailing sound resposnes when the leading sound was at c90°. The extreme left panels shows the normalized amplitudes of the trailing sound responses when the leading sound was at i90°. Horizontal dashed lines indicate NR value of 100%. The solid lines indicate the NR value of of 70%.

Group results indicated that strychnine did not change NR-ISI and latency-ISI curves that were based on responses to a leading sound that was presented at c90° (Friedman's test, $\chi 2$ (17) = 19.961, $p$ = 0.276) and (Friedman's test, $\chi 2$ (17) = 15.162, $p$ = 0.584) respectively (Figure 36A). In contrast, the normalized amplitudes of the trailing sound responses during the strychnine condition were significantly different when a leading sound was at the c90° (Friedman's test, $\chi 2$ (17) = 105.336, $p < 0.001$) and when it was at the i90° azimuth (Friedman test, $\chi 2$ (17) = 70.347, $p < 0.001$). Wilcoxon-signed rank *post-hoc* that when the leading sound was at c90°, strychnine significantly increased the NR at ISIs of 16 ms ($Z$ = -2.197, $p$ = 0.028), 24 ms ($Z$ = -2.366, $p$ = 0.018), 40 ms ($Z$ = -2.197, $p$ = 0.028) and 264 ms ($Z$ = -2.028, $p$ = 0.043). When the leading sound was at i90°, strychnine increased the NR at ISIs of 24 ms ($Z$ = -2.201, $p$ = 0.028), and 40 ms ($Z$ = -2.366, $p$ = 0.018). Strychnine did not increase the latency of the negative peak of an LFP elicited by a trailing sound at specific ISIs when a leading sound was at c90° or i90°. The Friedman's test showed a significant difference in the trailing sound latencies when the leading sound was at c90° ($\chi 2$ (17) = 33.424, $p$ = 0.010) and i90° (Friedman's test, $\chi 2$ (17) = 35.837, $p$ = 0.005), however, these differences were across different ISIs between the pre-drug and strychnine curves or within the same curve but different ISIs based on the *post hoc* analysis. Due to an increase of the median NR values at short ISIs, the $ISI_{70}$ value was significantly decreased from 41.86 ms (SD = 16.90 ms) to 20.46 ms (SD = 2.61 ms) during the application of strychnine when a leading sound was at c90° (Wilcoxon signed-rank test, $Z$ = -2.366, $p$ = 0.018) (Figure 36B). When a leading sound was at i90°, the value decreased from 27.34 (SD = 10.27) to 17.02 (SD = 3.76) (Wilcoxon signed-rank test, $Z$ = -2.197, $p$ = 0.028) (Figure 36B).

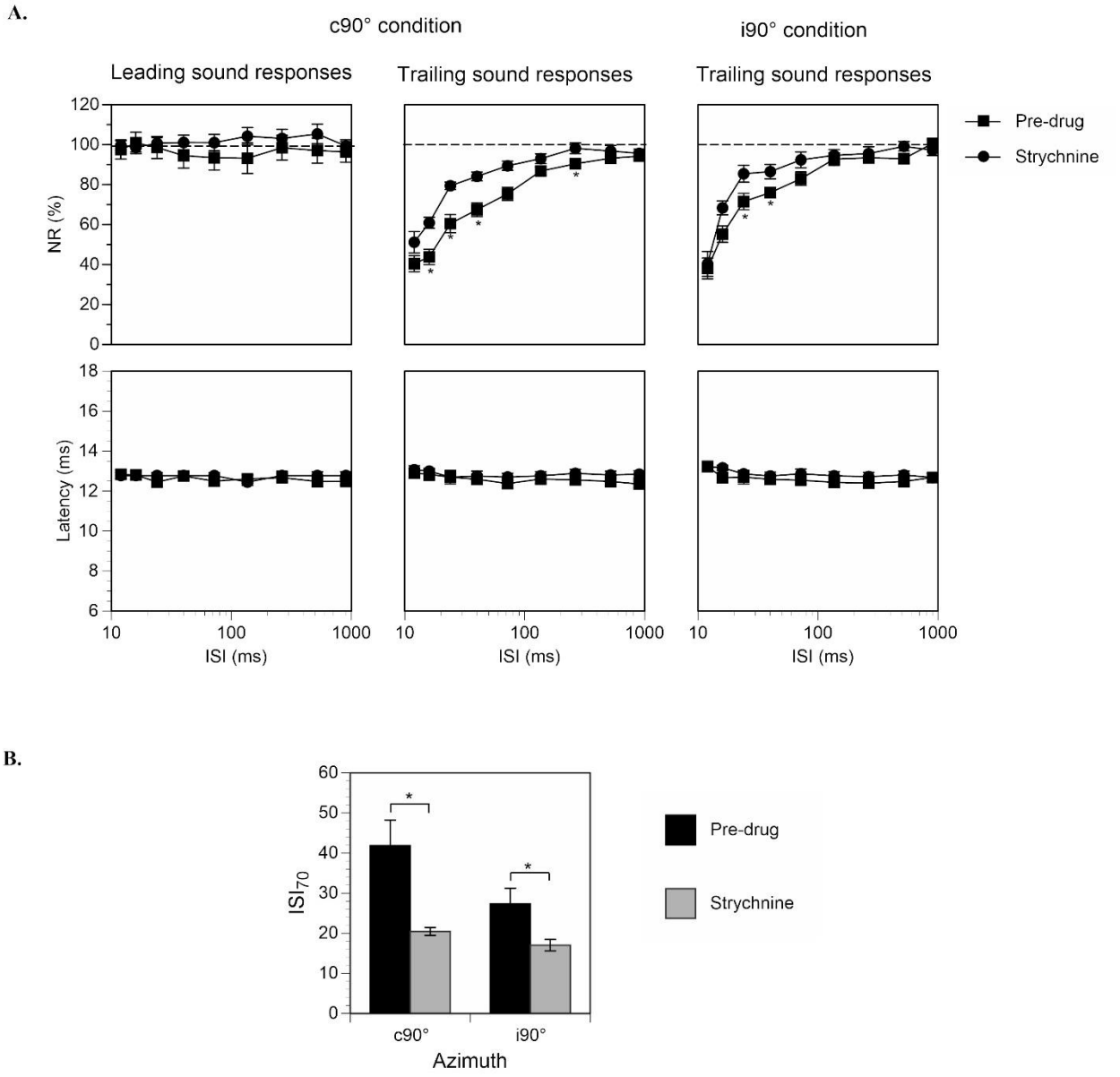


**Figure 36.** Group results showing the effects of strychnine on responses to leading and trailing sounds in a sound pair. A. Line charts showing normalized amplitude (top panels) and latency (bottom panels) of the negative peak of an LFP elicited by a leading sound (first column) and a trailing sound (second and third columns). The first two columns show responses to a leading sound (first column) and a trailing sound (second column) when the two sounds were colocalized at the c90°. The third column shows the response to a trailing sound (located at i90°) when a

leading sound was at i90°. B. ISI70 values based on responses to a trailing sound obtained before and during the application of strychnine. Results were obtained when a leading sound was at c90° and i90°, respectively. The error bars show SEM.

# CHAPTER IV. DISCUSSION

## 4.1 Directional dependence of a response in the CIC to a single-tone

This study showed that an LFP response elicited by a single tone burst in the CIC was directionally dependent. Such a response had a reduced amplitude and an increased latency when the tone was relocated from the contralateral ear to the ipsilateral ear. This finding is in agreement with results from single neurons in the same structure showing that firing of an action potential elicited by a single tone burst was stronger when the tone burst was at the contralateral rather than the ipsilateral ear (Cant 2005; Flammino and Clopton 1975; Kelly et al. 1991). Moreover, studies have shown that the response latencies are shorter for contralateral sound in comparison to ipsilateral sound (Flammino and Clopton 1975). The major difference between these previous studies and our study is that our study used free-field sound stimulation (sound delivered through location changeable speakers) instead of dichotic stimulation (sound delivered through earphones). Therefore, our acoustic stimulation better reflects the natural acoustic environment. Other studies that have used free-field stimulation to study the directional dependence of IC neurons used other animal models instead of the rat such as bats (Fuzessery et al. 1990; Fuzessery and Pollak 1985), frogs (Gooler et al. 1996; Xu et al. 1996) and cats (Semple et al. 1983).

The directional dependence of the responses in the CIC could be related to the integration of contralateral excitatory inputs and the inhibitory ipsilateral inputs. A large amplitude and a short latency of responses to the single sound at the contralateral ear maybe because the CIC receives direct excitatory inputs from the contralateral cochlear nucleus, a major source of the excitatory inputs to the CIC (Malmierca 2015). The contralateral cochlear nucleus sends frequency-specific excitatory signals to the CIC (Coleman and Clerici 1987; Malmierca 2003, 2015). In contrast, a

decrease in response amplitudes and a long latency of responses to the single sound at the ipsilateral ear maybe be explained by the inhibitory inputs into the CIC by LSO (Glendenning et al. 1992; Helfert et al. 1989; Marie et al. 1989; Vater et al. 1992b). LSO receives excitatory inputs from the ipsilateral CN and sends inhibitory inputs to the ipsilateral CIC (Cant and Benson 2006). Another explanation could be a reduction in the excitatory inputs when the sound was presented from the i90° azimuth.

**4.2 The suppressive effect produced by a leading sound in a leading-trailing sound pair**

The amplitude and latency of response to leading sound in a pair of leading-trailing sounds that were colocalized at c90° were the same as the response elicited by the leading sound presented alone. This indicates that between multiple presentations of leading-trailing sound pairs, the trailing sound of one pair did not affect the response to a leading sound of the subsequent pair. This ensured that only a leading sound could affect the response to a trailing sound over multiple presentations of leading-trailing sound pairs.

When the trailing sound was colocalized with the leading sound, group results showed that the strongest suppression of the trailing sound response was at the lowest ISI of 12 ms. The responses recovered by at least 70% at an ISI value of 38.93 ms. A previous study used a forward masking paradigm to examine responses to a probe-test (or leading-trailing) sound pair under a monaural contralateral condition (Finlayson and Adam 1997). They observed that CIC neurons were suppressed by 83.1%  in response to a trailing sound delayed by 8 ms after the offset of the leading sound (Finlayson and Adam 1997). Moreover, the trailing sound responses recovered by at least 75% when the trailing sound was delayed by 226.9 ms (Finlayson and Adam 1997). The general finding of this study agrees with our study because the trailing sound was strongly suppressed at shorter delays and gradually recovered at higher delays. However, the

recovery time points differ substantially. This is because the previous study used a modified form of forward masking paradigm and the sound stimuli used in this study were different from our study. For instance, the probe tone (or the leading sound) was 200 ms in duration and the test tone (or the trailing sound) was 30 ms in duration and both were delivered through dichotic stimulation at the best frequency of the neuron (Finlayson and Adam 1997). In contrast, we evaluated LFPs elicited by leading and trailing sounds that were 8 ms long and had frequency differences.

The results showed that the suppressive effect generated by a leading sound on the response to a trailing sound at c90° is dependent on the location of the leading sound. This dependence was significant when the ISI between two sounds was 16 ms and 24 ms. There was a significant increase in the trailing sound response NR when the leading sound was relocated to i45° and i90° from the c90° azimuth. There was also a gradual increase in the latency of the trailing sound responses as the leading sound was moved away from the c90° azimuth and towards the ipsilateral side. However, no significant differences were found. Our findings are in general agreement with a previous finding showing that relocation of one of the two sounds that were colocalized at c90° to another angle increased the response to the second sound (Chot et al. 2019). However, the study by Chot et al. 2019 used tones that were 100 ms in duration in comparison to the 8 ms duration tones in our study. This study also studied single neuron response rather than LFPs.

The time course of the suppressive effect produced by a leading sound was evaluated when the leading sound was at c90° and when it was at i90°. The $ISI_{70}$ value of the trailing sound responses was significantly lower when the leading sound was at i90° compared to c90°. This indicates that the suppressive effect of the leading sound on the trailing sound responses lasted

longer when both sounds were colocalized at the c90° azimuth compared to when the leading sound was separated to the i90° azimuth.

The suppressive effect of the leading sound on the responses to a trailing sound can be due to three mechanisms. One of the mechanisms could be the local adaption of the excitatory response. The excitation resulting from the leading sound response may deplete glutamate in CIC neurons which prevents the trailing sound from eliciting an equally strong response. Another possible mechanism of suppression could be the interaction between the local excitatory/inhibitory projections received by the CIC from other structures. Most of the previous studies related to binaural inhibition were conducted with the contralateral and ipsilateral stimulation presented simultaneously. Zhang and Kelly 2010 indicated that the degree of binaural interaction changes throughout the dichotic stimulation. Zhang and Kelly 2009 indicated that an ipsilateral stimulation could generate a long lasting inhibitory aftereffect even after the offset of the ipsilateral stimulation. These results suggest that a leading sound can generate different effects on the response to a trailing sound when the leading sound is presented at different locations. Another mechanism responsible for the suppressive effect could be that the inheritance of response characteristics by the CIC neurons. Through this mechanism, the binaural responses are integrated in lower brainstem nuclei which process binaural inputs such as the SOC or DNLL and are then sent through projections to converge on the CIC neurons. The pharmacological manipulations in our study asesssed the degree of suppression that was dependent on the excitatory/inhibitory projections received by the CIC.

## 4.3 Contributions of local inhibitory interaction in shaping responses to a pair of leading-trailing sounds

Gabazine substantially increased the amplitude of the LFP elicited by a single tone burst. The median of the increase was 97.87%. Similarly, strychnine increased the amplitude of the LFP elicited by a single tone burst by a median of 40.76%. This finding is in agreement with previous studies showing that both $GABA_A$ receptors and glycine receptors play an inhibitory role in the CIC (Brandão et al. 1988; Kelly and Caspary 2005; Milbrandt et al. 1996; Moore et al. 1998; Xu et al. 2004).

CGP35348 minimally affected the response amplitudes. This lack of effect supports results from previous studies (Vaughn et al. 1996). This lack of effect could be explained by the low abundance of $GABA_B$ receptors in the CIC (Jamal et al. 2012). However, within the CIC, the $GABA_B$ receptors are more abundant in the dorsal regions (Jamal et al. 2012). The responses to trailing sound alone showed a median decrease in absolute amplitudes by 35.03%. Moreover, the raw amplitudes failed to recover to pre-drug levels during the post-drug conditions and decreased even further. The CGP results were mainly collected at the very end of the long experiments (more than 8 hours after the start of the experiment) and they may have been influenced by the decline in animals condition.

### *4.3.1 Involvement of the $GABA_A$ receptor*

The main GABAergic inputs to the CIC are from the ipsilateral SPON and contralateral DNLL (Malmierca 2015). The ipsilateral SPON is excited by contralateral sound stimulus and sends inhibitory inputs to the ipsilateral CIC neurons (Choy Buentello et al. 2015; Kulesza et al. 2003). DNLL receives major excitatory inputs from the contralateral dorsal cochlear nucleus and sends inhibitory projections to the contralateral CIC (Kelly et al. 2009). Our results indicated that

gabazine did not completely eliminate the long-lasting inhibitory effect produced by a leading sound. This result seemingly contradicts previous findings because previous studies have indicated that SPON is contralaterally driven and neurons in this structure show offset firing (i.e they fire after a sound stops) (Behrend et al. 2002; Choy Buentello et al. 2015; Kulesza et al. 2003; Saldaña et al. 2009). The finding that the trailing sound responses are still suppressed when the leading sound is at the i90° suggests there may be other inhibitory inputs responsible for the suppression. There was, however, a significant decrease in the $ISI_{70}$ value of the trailing sound responses when the leading-trailing sound pair was colocalized at c90° during the gabazine condition. In contrast, there were no significant differences between trailing sound $ISI_{70}$ values between the pre-drug and gabazine conditions when the leading sound was presented at i90°. This finding suggests that the suppression of the responses when the leading sound was at c90° may have been predominantly driven by $GABA_A$ receptors.

### *4.3.2 Involvement of the $GABA_B$ receptor*

Postsynaptic $GABA_B$ receptors activate the G protein-coupled inwardly-rectifying potassium channel (GIRK) ion channels which leads to the efflux of potassium (Lüscher et al. 1997). Antagonizing these channels would result in the excitatory effect (Lüscher et al. 1997). Presynaptic $GABA_B$ receptors regulate the release of GABA and glutamate neurotransmitters (Ma et al. 2002). If the presynaptic terminal releases GABA, the $GABA_B$ receptors will act to decrease the further release of GABA (Ma et al. 2002). If the presynaptic terminal releases glutamate, the $GABA_B$ receptors will act to decrease further glutamate release (Ma et al. 2002). Antagonizing these receptors will release more GABA or glutamate depending on the neurotransmitter released at the presynaptic terminal (Ma et al. 2002).

Our results showed that there were no apparent changes in the LFP waveforms after the application of CGP 35348. In most cases, the responses were weaker during the CGP condition compared to the pre-drug condition. However, the evaluation of the NR curve when the leading sound was at c90° showed that the median NRs at ISI 24 ms and 40 ms were higher than the pre-drug condition, however, there was no statistical significance between the median NRs and latencies between the same ISIs of the pre-drug and CGP curve in any condition. Similarly, a previous single-unit study which examined the role of $GABA_B$ receptors on paired-pulse stimulation comprised of two tones, showed that CGP did not significantly reduce the inhibition of the second sound separated by an interpulse interval of 200 ms (Vaughn et al. 1996).

In those cases where CGP results were collected relatively early during the experiment, the general lack of effect of CGP can be explained by the lack of relative abundance of these receptors in the CIC compared to other inhibitory neurotransmitter receptors (Jamal et al. 2012). The antagonizing effect of CGP on presynaptic receptors may have resulted in the increase in both glutamate and GABA from presynaptic terminals of the CIC neurons which may have led to no net change in the responses.

### *4.3.3 Involvement of the glycine receptor*

The CIC receives glycinergic inputs from the ipsilateral ventral nucleus of the lateral lemniscus (VNLL) (Choy Buentello et al. 2015; Riquelme et al. 2001; Vater et al. 1997) and the ipsilateral LSO (Glendenning et al. 1992; Helfert et al. 1989; Marie et al. 1989; Vater et al. 1992b). The ipsilateral VNLL is excited by contralateral stimulation (Kelly et al. 2009; Saldaña et al. 2009). LSO is excited by ipsilateral stimulation (Shu Hui Wu and Kelly 1992).

Our results show that there was a significant increase in the trailing sound median NRs during the strychnine condition when the leading sound was colocalized at c90°. There was a

significant difference at ISIs: 16 ms, 24 ms, 40 ms, and 264 ms between the pre-drug and strychnine NRs of the trailing sound response. There was also a significant increase in the median NRs of the trailing sound response during the strychnine condition when the leading sound was at the i90° azimuth. The ISIs with a significant difference were 24 ms and 40 ms. The $ISI_{70}$ values were significantly lower during the strychnine condition whether the leading sound was at c90° and i90°. Thus, it is a possibility that leading sound at c90° may have excited VNLL neurons which may have inhibited CIC responses to the subsequent trailing sound through glycinergic inhibition. This inhibition may have been antagonized by the strychnine thus increasing the NR values of the trailing sound response significantly at lower ISIs and the $ISI_{70}$ value when the leading sound was at c90°. When the leading sound was at i90°, it may have excited ipsilateral LSO neurons which may then have inhibited CIC responses to the subsequent trailing sound. The application of strychnine may have antagonized glycinergic innervations to the CIC which may have increased the NR values and the $ISI_{70}$ value when the leading sound was at i90. It should be noted that it is not yet evident whether VNLL and LSO produce long-lasting inhibitory effects.

### 4.4 Technical limitations

The interpretation of the LFP signals can be difficult due to technical limitations. For instance, activity from distant sources may be picked up if the activity of the local source is weak (Herreras 2016). Our LFP responses may have been contaminated with activity from the lateral nucleus, dorsal nucleus, and the rostral cortex of the inferior colliculus.

The microiontophoresis method has several pitfalls. For instance, the exact concentration of the drugs at the recordings site is indirectly controlled by the ejections current, however, the exact concentration cannot be determined (Vater et al. 1992a). Moreover, previous studies have

shown that the drug spread can be hundreds of micrometers from the electrode tip which is between 10-15 μm in diameter.

### 4.5 Implications and future directions

Future studies should examine single neuron responses in the CIC using dichotic stimulation and pharmacological manipulation to evaluate the excitatory-inhibitory binaural interaction in the CIC. Studying single neurons will give the temporal resolution of the binaural excitatory/inhibitory interactions at an individual neuron level. Pharmacological manipulations using the same inhibitory neurotransmitter antagonists as our study should also be done to evaluate the changes in excitation and inhibition over different ISI conditions. Additionally, using a glutamate agonist can provide insight as to whether local adaptation within the CIC neurons contributes to the suppression of the trailing sound in a leading-trailing pair.

To test whether response characteristics in the CIC neurons are inherited from lower brainstem nuclei, pharmacological agents can be applied to these nuclei to see how CIC responses are affected. For instance, directly antagonizing SPON and LSO neurons while observing CIC responses can give insight as to how much these nuclei contribute to the trailing sound response suppression.

# CHAPTER V. CONCLUSIONS

Results from the present study indicate that the responses of a population of neurons in the CIC to a sound is suppressed by a preceding sound. The suppressive effect is strong when the two sounds are colocalized at the ear contralateral to the neurons being studied and separated by a small temporal gap. The suppressive effect is reduced when the two sounds are temporally and spatially separated. Two inhibitory neurotransmitter receptors, the $GABA_A$ receptor, and the glycine receptor are partially involved in the generation of the suppressive effect of a leading sound. Other mechanisms such as the adaptation of excitatory response or inheritance of response characteristics likely play a major role in generating the suppressive effect of the leading sound.

## REFERENCES

**Adams JC**. Cytology of periolivary cells and the organization of their projections in the cat. *J Comp Neurol* , 1983. doi:10.1002/cne.902150304.

**Van Adel BA**, **Kelly JB**. Kainic acid lesions of the superior olivary complex: Effects on sound localization by the albino rat. *Behav Neurosci* , 1998. doi:10.1037/0735-7044.112.2.432.

**Ahveninen J**, **Kopčo N**, **Jääskeläinen IP**. Psychophysics and neuronal bases of sound localization in humans. *Hear. Res.* 2014.

**Aitkin LM**, **Anderson DJ**, **Brugge JF**. Tonotopic organization and discharge characteristics of single neurons in nuclei of the lateral lemniscus of the cat. *J Neurophysiol* , 1970. doi:10.1152/jn.1970.33.3.421.

**Alho K**, **Sainio K**, **Sajaniemi N**, **Reinikainen K**, **Näätänen R**. Event-related brain potential of human newborns to pitch change of an acoustic stimulus. *Electroencephalogr Clin Neurophysiol Evoked Potentials* , 1990. doi:10.1016/0168-5597(90)90031-8.

**Alibardi L**. Ultrastructural and immunocytochemical characterization of neurons in the rat ventral cochlear nucleus projecting to the inferior colliculus. *Ann Anat* , 1998. doi:10.1016/S0940-9602(98)80102-7.

**Arcelli P**, **Frassoni C**, **Regondi MC**, **Biasi S De**, **Spreafico R**. GABAergic neurons in mammalian thalamus: A marker of thalamic complexity? *Brain Res Bull* , 1997. doi:10.1016/S0361-9230(96)00107-4.

**Asaba A**, **Hattori T**, **Mogi K**, **Kikusui T**. Sexual attractiveness of male chemicals and

vocalizations in mice. *Front. Neurosci.* 2014.

**Astl J**, **Popelář J**, **Kvašňák E**, **Syka J**. Comparison of response properties of neurons in the inferior colliculus of guinea pigs under different anesthetics. *Int J Audiol* , 1996. doi:10.3109/00206099609071954.

**Bajo VM**, **Merchán MA**, **López DE**, **Rouiller EM**. Neuronal morphology and efferent projections of the dorsal nucleus of the lateral lemniscus in the rat. *J Comp Neurol* , 1993. doi:10.1002/cne.903340207.

**Bajo VM**, **Villa AEP**, **De Ribaupierre F**, **Rouiller EM**. Discharge properties of single neurons in the dorsal nucleus of the lateral lemniscus of the rat. *Brain Res Bull* , 1998. doi:10.1016/S0361-9230(98)00127-0.

**Banks MI**, **Smith PH**. Intracellular recordings from neurobiotin-labeled cells in brain slices of the rat medial nucleus of the trapezoid body. *J Neurosci* , 1992. doi:10.1523/jneurosci.12-07-02819.1992.

**Bartlett EL**, **Smith PH**. Anatomic, intrinsic, and synaptic properties of dorsal and ventral division neurons in rat medial geniculate body. *J Neurophysiol* , 1999a. doi:10.1152/jn.1999.81.5.1999.

**Bartlett EL**, **Smith PH**. Anatomic, intrinsic, and synaptic properties of dorsal and ventral division neurons in rat medial geniculate body. *J Neurophysiol* 1999–2016, 1999b.

**Bartlett EL**, **Stark JM**, **Guillery RW**, **Smith PH**. Comparison of the fine structure of cortical and collicular terminals in the rat medial geniculate body. *Neuroscience* , 2000.

doi:10.1016/S0306-4522(00)00340-7.

**Bauer EE**, **Klug A**, **Pollak GD**. Features of contralaterally evoked inhibition in the inferior colliculus. *Hear Res* , 2000. doi:10.1016/S0378-5955(99)00206-3.

**Beecher MD**, **Harrison JM**. RAPID ACQUISITION OF AN AUDITORY LOCALIZATION DISCRIMINATION BY RATS 1 . *J Exp Anal Behav* , 1971. doi:10.1901/jeab.1971.16-193.

**Behrend O**, **Brand A**, **Kapfer C**, **Grothe B**. Auditory response properties in the superior paraolivary nucleus of the gerbil. *J Neurophysiol* , 2002. doi:10.1152/jn.2002.87.6.2915.

**Bernstein LR**. The normalized interaural correlation: Accounting for NoSπ thresholds obtained with Gaussian and “low-noise” masking noise. *J Acoust Soc Am* , 1999.

**Beyerl BD**. Afferent projections to the central nucleus of the inferior colliculus in the rat. *Brain Res* , 1978. doi:10.1016/0006-8993(78)90858-2.

**Blackburn CC**, **Sachs MB**. Classification of unit types in the anteroventral cochlear nucleus: PST histograms and regularity analysis. *J Neurophysiol* , 1989. doi:10.1152/jn.1989.62.6.1303.

**Bordi F**, **LeDoux JE**. Response properties of single units in areas of rat auditory thalamus that project to the amygdala - I. Acoustic discharge patterns and frequency receptive fields. *Exp Brain Res* , 1994a. doi:10.1007/BF00228414.

**Bordi F**, **LeDoux JE**. Response properties of single units in areas of rat auditory thalamus that project to the amygdala - II. Cells receiving convergent auditory and somatosensory inputs and cells antidromically activated by amygdala stimulation. *Exp Brain Res* , 1994b. doi:10.1007/BF00228415.

**Brand A**, **Urban A**, **Grothe B**. Duration tuning in the mouse auditory midbrain. *J Neurophysiol* , 2000. doi:10.1152/jn.2000.84.4.1790.

**Brandão ML**, **Tomaz C**, **Leão Borges PC**, **Coimbra NC**, **Bagri A**. Defense reaction induced by microinjections of bicuculline into the inferior colliculus. *Physiol Behav* , 1988. doi:10.1016/0031-9384(88)90038-8.

**Brodal A**. Brodal, A., Neurological anatomy in relation to clinical medicine. Third edition. New York, Oxford University Press, 1981, 1,053 pages, $35.00. *Ann Neurol* , 1981. doi:10.1002/ana.410100629.

**Bronkhorst AW**. The cocktail party phenomenon: A review of research on speech intelligibility in multiple-talker conditions. *Acustica* 2000.

**Brugge JF**, **Anderson DJ**, **Aitkin LM**. Responses of neurons in the dorsal nucleus of the lateral lemniscus of cat to binaural tonal stimulation. *J Neurophysiol* , 1970. doi:10.1152/jn.1970.33.3.441.

**Burghardt H**. UEBER DIE SUBJEKTIVE DAUER VON SCHALLIMPULSEN UND SCHALLPAUSEN. *Acustica* , 1973.

**Caicedo A**, **Herbert H**. Topography of descending projections from the inferior colliculus to auditory brainstem nuclei in the rat. *J Comp Neurol* , 1993. doi:10.1002/cne.903280305.

**Cant NB**. Projections from the cochlear nuclear complex to the inferior colliculus. In: *The Inferior Colliculus*. 2005.

**Cant NB**, **Benson CG**. Organization of the inferior colliculus of the gerbil (Meriones

unguiculatus): Differences in distribution of projections from the cochlear nuclei and the superior olivary complex. *J Comp Neurol* , 2006. doi:10.1002/cne.20888.

**Casseday JH**, **Ehrlich D**, **Covey E**. Neural tuning for sound duration: Role of inhibitory mechanisms in the inferior colliculus. *Science (80- )* , 1994. doi:10.1126/science.8171341.

**Chen L**, **Kelly JB**, **Wu SH**. The commissure of Probst as a source of GABAergic inhibition. *Hear Res* , 1999. doi:10.1016/S0378-5955(99)00156-2.

**Chernock ML**, **Winer JA**. Organization of bilateral projections from the inferior colliculus to the medial geniculate body. *Soc Neurosci Abstr* 27, 2001.

**Chot MG**, **Tran S**, **Zhang H**. Responses of neurons in the rat's inferior colliculus to a sound are affected by another sound in a space-dependent manner. *Sci Rep* , 2019. doi:10.1038/s41598-019-50297-8.

**Choy Buentello D**, **Bishop DC**, **Oliver DL**. Differential distribution of GABA and glycine terminals in the inferior colliculus of rat and mouse. *J Comp Neurol* , 2015. doi:10.1002/cne.23810.

**Clarkson C**, **Herrero-Turrión MJ**, **Merchán MA**. Cortical auditory deafferentation induces long-term plasticity in the inferior colliculus of adult rats: Microarray and qPCR analysis. *Front Neural Circuits* , 2012. doi:10.3389/fncir.2012.00086.

**Clarkson C**, **Juíz JM**, **Merchán MA**. Transient down-regulation of sound-induced c-Fos protein expression in the inferior colliculus after ablation of the auditory cortex. *Front Neuroanat* , 2010a. doi:10.3389/fnana.2010.00141.

**Clarkson C**, **Juíz JM**, **Mercḥan MÁ**. Long-term regulation in calretinin staining in the rat inferior colliculus after unilateral auditory cortical ablation. *J Comp Neurol* , 2010b. doi:10.1002/cne.22453.

**Clerici WJ**, **Coleman JR**. Anatomy of the rat medial geniculate body: I. Cytoarchitecture, myeloarchitecture, and neocortical connectivity. *J Comp Neurol* , 1990. doi:10.1002/cne.902970103.

**Clerici WJ**, **McDonald AJ**, **Thompson R**, **Coleman JR**. Anatomy of the rat medial geniculate body: II. Dendritic morphology. *J Comp Neurol* , 1990. doi:10.1002/cne.902970104.

**Coleman JR**, **Clerici WJ**. Sources of projections to subdivisions of the inferior colliculus in the rat. *J Comp Neurol* , 1987. doi:10.1002/cne.902620204.

**Cowles JT**, **Pennington LA**. An Improved Conditioning Technique for Determining Auditory Acuity of the Rat. *J Psychol Interdiscip Appl* , 1943. doi:10.1080/00223980.1943.9917135.

**Crocker MJ**. *Encyclopedia of Acoustics, Volume Three.* 3rd ed. John Wiley & Sons, Ltd, 1997.

**Davis KA**. Evidence of a functionally segregated pathway from dorsal cochlear nucleus to inferior colliculus. *J Neurophysiol* , 2002. doi:10.1152/jn.00769.2001.

**Doron NN**, **Ledoux JE**. Organization of projections to the lateral amygdala from auditory and visual areas of the thalamus in the rat. *J Comp Neurol* , 1999. doi:10.1002/(SICI)1096-9861(19990927)412:3<383::AID-CNE2>3.0.CO;2-5.

**Doucet JR**, **Ross AT**, **Gillespie MB**, **Ryugo DK**. Glycine immunoreactivity of multipolar neurons in the ventral cochlear nucleus which project to the dorsal cochlear nucleus. *J Comp*

*Neurol* , 1999. doi:10.1002/(sici)1096-9861(19990614)408:4<515::aid-cne6>3.3.co;2-f.

**Doucet JR**, **Ryugo DK**. Projections from the ventral cochlear nucleus to the dorsal cochlear nucleus in rats. *J Comp Neurol* , 1997. doi:10.1002/(SICI)1096-9861(19970825)385:2<245::AID-CNE5>3.0.CO;2-1.

**Doucet JR**, **Ryugo DK**. Axonal pathways to the lateral superior olive labeled with biotinylated dextran amine injections in the dorsal cochlear nucleus of rats. *J Comp Neurol* , 2003. doi:10.1002/cne.10722.

**Egorova M**, **Ehret G**, **Vartanian I**, **Esser KH**. Frequency response areas of neurons in the mouse inferior colliculus. I. Threshold and tuning characteristics. *Exp Brain Res* , 2001. doi:10.1007/s002210100786.

**Ehret G**, **Schreiner CE**. Spectral and intensity coding in the auditory midbrain. In: *The Inferior Colliculus*. 2005.

**Faingold CL**, **Boersma Anderson CA**, **Caspary DM**. Involvement of GABA in acoustically-evoked inhibition in inferior colliculus neurons. *Hear Res* , 1991. doi:10.1016/0378-5955(91)90200-S.

**Faingold CL**, **Gehlbach G**, **Caspary DM**. On the role of GABA as an inhibitory neurotransmitter in inferior colliculus neurons: iontophoretic studies. *Brain Res* , 1989. doi:10.1016/0006-8993(89)90326-0.

**Fastl H**, **Zwicker E**. Psychoacoustics: Facts and models. 2007.

**Fay RR**, **Popper AN**. *Comparative Hearing: Mammals*. Springer-Verlag, 1994.

**Faye-Lund H**. The neocortical projection to the inferior colliculus in the albino rat. *Anat Embryol (Berl)* , 1985. doi:10.1007/BF00707304.

**Faye-Lund H**. Projection from the inferior colliculus to the superior olivary complex in the albino rat. *Anat Embryol (Berl)* , 1986. doi:10.1007/BF00315454.

**Faye-Lund H**, **Osen KK**. Anatomy of the inferior colliculus in rat. *Anat Embryol (Berl)* , 1985. doi:10.1007/BF00319050.

**Feliciano M**, **Saldana E**, **Mugnaini E**. Direct projections from the rat primary auditory neocortex to nucleus sagulum, paralemniscal regions, superior olivary complex and cochlear nuclei. *Audit Neurosci* , 1995.

**Finlayson PG**, **Adam TJ**. Short-term adaptation of excitation and inhibition shapes binaural processing. In: *Acta Oto-Laryngologica*. 1997.

**Flammino F**, **Clopton BM**. Neural responses in the inferior colliculus of albino rat to binaural stimuli. *J Acoust Soc Am* , 1975. doi:10.1121/1.380494.

**Frey JD**, **Wendt M**, **Jacobsen T**. Automatic detection of unattended changes in room acoustics. *Neurosci Lett* , 2015. doi:10.1016/j.neulet.2014.09.050.

**Freyman RL**, **Helfer KS**, **McCall DD**, **Clifton RK**. The role of perceived spatial separation in the unmasking of speech. *J Acoust Soc Am* , 1999. doi:10.1121/1.428211.

**Friauf E**. Tonotopic Order in the Adult and Developing Auditory System of the Rat as Shown by c-fos Immunocytochemistry. *Eur J Neurosci* , 1992. doi:10.1111/j.1460-9568.1992.tb00190.x.

**Friauf E**, **Ostwald J**. Divergent projections of physiologically characterized rat ventral cochlear nucleus neurons as shown by intra-axonal injection of horseradish peroxidase. *Exp Brain Res* , 1988. doi:10.1007/BF00248219.

**Fubara BM**, **Casseday JH**, **Covey E**, **Schwartz-Bloom RD**. Distribution of GABAA, GABAB, and glycine receptors in the central auditory system of the big brown bat, Eptesicus fuscus. *J Comp Neurol* , 1996. doi:10.1002/(SICI)1096-9861(19960520)369:1<83::AID-CNE6>3.0.CO;2-G.

**Fuzessery ZM**, **Pollak GD**. Determinants of sound location selectivity in bat inferior colliculus: A combined dichotic and free-field stimulation study. *J Neurophysiol* , 1985. doi:10.1152/jn.1985.54.4.757.

**Fuzessery ZM**, **Wenstrup JJ**, **Pollak GD**. Determinants of horizontal sound location selectivity of binaurally excited neurons in an isofrequency region of the mustache bat inferior colliculus. *J Neurophysiol* , 1990. doi:10.1152/jn.1990.63.5.1128.

**Games KD**, **Winer JA**. Layer V in rat auditory cortex: Projections to the inferior colliculus and contralateral cortex. *Hear Res* , 1988. doi:10.1016/0378-5955(88)90047-0.

**Glendenning KK**, **Baker BN**. Neuroanatomical distribution of receptors for three potential inhibitory neurotransmitters in the brainstem auditory nuclei of the cat. *J Comp Neurol* , 1988. doi:10.1002/cne.902750210.

**Glendenning KK**, **Baker BN**, **Hutson KA**, **Masterton RB**. Acoustic chiasm V: Inhibition and excitation in the ipsilateral and contralateral projections of LSO. *J Comp Neurol* , 1992. doi:10.1002/cne.903190110.

**Goldberg JM**, **Brown PB**. Response of binaural neurons of dog superior olivary complex to dichotic tonal stimuli: some physiological mechanisms of sound localization. *J Neurophysiol* , 1969. doi:10.1152/jn.1969.32.4.613.

**González-Hernández T**, **Mantolán-Sarmiento B**, **González-González B**, **Pérez-González H**. Sources of GABAergic input to the inferior colliculus of the rat. *J Comp Neurol* , 1996. doi:10.1002/(SICI)1096-9861(19960819)372:2<309::AID-CNE11>3.0.CO;2-E.

**González-Hernández TH**, **Galindo-Mireles D**, **Castañeyra-Perdomo A**, **Ferres-Torres R**. Divergent projections of projecting neurons of the inferior colliculus to the medial geniculate body and the contralateral inferior colliculus in the rat. *Hear Res* , 1991. doi:10.1016/0378-5955(91)90184-B.

**Gooler DM**, **Xu J**, **Feng AS**. Binaural inhibition is important in shaping the free-field frequency selectivity of single neurons in the inferior colliculus. *J Neurophysiol* , 1996. doi:10.1152/jn.1996.76.4.2580.

**Gourevitch G**. Auditory Masking in the Rat. *J Acoust Soc Am* , 1965. doi:10.1121/1.1909348.

**Gourevitch G**, **Cole B**. A MANIPULANDUM FOR USE WITH RATS RESPONDING TO AUDITORY STIMULI. *J Exp Anal Behav* , 1963. doi:10.1901/jeab.1963.6-413.

**Gourevitch G**, **Hack MH**, **Hawkins JE**. Auditory thresholds in the rat measured by an operant technique. *Science (80- )* , 1960. doi:10.1126/science.131.3406.1046.

**Grothe B**, **Neuweiler G**. The function of the medial superior olive in small mammals: Temporal receptive fields in auditory analysis. *J. Comp. Physiol. - A Sensory, Neural, Behav. Physiol.*

2000.

**Hack MH**. Auditory intensity discrimination in the rat. *J Comp Physiol Psychol* , 1971. doi:10.1037/h0030356.

**Harrison JM**, **Beecher MD**. CONTROL OF RESPONDING BY THE LOCATION OF AN AUDITORY STIMULUS: ROLE OF RISE TIME OF THE STIMULUS 1 . *J Exp Anal Behav* , 1969. doi:10.1901/jeab.1969.12-217.

**Harrison JM**, **Warr WB**. A study of the cochlear nuclei and ascending auditory pathways of the medulla. *J Comp Neurol* , 1962. doi:10.1002/cne.901190306.

**Heffner RS**, **Masterton RB**. Sound localization in mammals: Brain-stem mechanisms. *Comp perception1* , 1990.

**Hefti BJ**, **Smith PH**. Anatomy, physiology, and synaptic responses of rat layer V auditory cortical cells and effects of intracellular GABA(A) blockade. *J Neurophysiol* , 2000. doi:10.1152/jn.2000.83.5.2626.

**Helfert RH**, **Bonneau JM**, **Wenthold RJ**, **Altschuler RA**. GABA and glycine immunoreactivity in the guinea pig superior olivary complex. *Brain Res* , 1989. doi:10.1016/0006-8993(89)90644-6.

**Henkel CK**, **Gabriele ML**. Organization of the disynaptic pathway from the anteroventral cochlear nucleus to the lateral superior olivary nucleus in the ferret. *Anat Embryol (Berl)* , 1999. doi:10.1007/s004290050216.

**Herbert H**, **Aschoff A**, **Ostwald J**. Topography of projections from the auditory cortex to the

inferior colliculus in the rat. *J Comp Neurol* , 1991. doi:10.1002/cne.903040108.

**Hernández O**, **Rees A**, **Malmierca MS**. A GABAergic component in the commissure of the inferior colliculus in rat. *Neuroreport* , 2006. doi:10.1097/01.wnr.0000236857.70715.be.

**Herreras O**. Local Field Potentials: Myths and Misunderstandings. *Front Neural Circuits* , 2016. doi:10.3389/fncir.2016.00101.

**Hoeffding V**, **Harrison JM**. AUDITORY DISCRIMINATION: ROLE OF TIME AND INTENSITY IN THE PRECEDENCE EFFECT. *J Exp Anal Behav* , 1979. doi:10.1901/jeab.1979.32-157.

**Huffman RF**, **Henson OW**. The descending auditory pathway and acousticomotor systems: connections with the inferior colliculus. *Brain Res. Rev.* 1990.

**Inbody SB**, **Feng AS**. Binaural response characteristics of single neurons in the medial superior olivary nucleus of the albino rat. *Brain Res* , 1981. doi:10.1016/0006-8993(81)90910-0.

**Irfan N**, **Zhang H**, **Shu HW**. Synaptic transmission mediated by ionotropic glutamate, glycine and GABA receptors in the rat's ventral nucleus of the lateral lemniscus. *Hear Res* , 2005. doi:10.1016/j.heares.2004.11.021.

**Irvine DR.**, **Gago G**. Binaural interaction in high-frequency neurons in inferior colliculus of the cat: Effects of variations in sound pressure level on sensitivity to interaural intensity differences. *Hear Res* 127–141, 1990.

**Irvine DRF**, **Park VN**, **Mattingley JB**. Responses of neurons in the inferior colliculus of the rat to interaural time and intensity differences in transient stimuli: Implications for the latency

hypothesis. *Hear Res* , 1995. doi:10.1016/0378-5955(95)00040-B.

**Ito M**, **Van Adel B**, **Kelly JB**. Sound localization after transection of the commissure of Probst in the albino rat. *J Neurophysiol* , 1996. doi:10.1152/jn.1996.76.5.3493.

**Jacobsen T**, **Schröger E**. Measuring duration mismatch negativity. *Clin Neurophysiol* , 2003. doi:10.1016/S1388-2457(03)00043-9.

**Jamal L**, **Khan AN**, **Butt S**, **Patel CR**, **Zhang H**. The level and distribution of the GABABRI and GABABR2 receptor subunits in the rat's inferior colliculus. *Front Neural Circuits* , 2012. doi:10.3389/fncir.2012.00092.

**Kadner A**, **Berrebi AS**. Encoding of temporal features of auditory stimuli in the medial nucleus of the trapezoid body and superior paraolivary nucleus of the rat. *Neuroscience* , 2008. doi:10.1016/j.neuroscience.2007.11.008.

**Kaukoranta E**, **Sams M**, **Hari R**, **Hämäläinen M**, **Näätänen R**. Reactions of human auditory cortex to a change in tone duration. *Hear Res* , 1989. doi:10.1016/0378-5955(89)90174-3.

**Kelly JB**. Effects of auditory cortical lesions on sound localization by the rat. *J Neurophysiol* , 1980. doi:10.1152/jn.1980.44.6.1161.

**Kelly JB**, **Van Adel BA**, **Ito M**. Anatomical projections of the nuclei of the lateral lemniscus in the Albino rat (Rattus norvegicus). *J Comp Neurol* , 2009. doi:10.1002/cne.21929.

**Kelly JB**, **Buckthought AD**, **Kidd SA**. Monaural and binaural response properties of single neurons in the rat's dorsal nucleus of the lateral lemniscus. *Hear Res* , 1998. doi:10.1016/S0378-5955(98)00082-3.

**Kelly JB**, **Caspary DM**. Pharmacology of the inferior colliculus. In: *The Inferior Colliculus*. 2005.

**Kelly JB**, **Glazier SJ**. Auditory cortex lesions and discrimination of spatial location by the rat. *Brain Res* , 1978. doi:10.1016/0006-8993(78)90865-X.

**Kelly JB**, **Glenn SL**, **Beaver CJ**. Sound frequency and binaural response properties of single neurons in rat inferior colliculus. *Hear Res* , 1991. doi:10.1016/0378-5955(91)90177-B.

**Kelly JB**, **Judge PW**. Effects of medial geniculate lesions on sound localization by the rat. *J Neurophysiol* , 1985. doi:10.1152/jn.1985.53.2.361.

**Kelly JB**, **Judge PW**, **Fraser IH**. Development of the auditory orientation response in the albino rat (Rattus norvegicus). *J Comp Psychol* , 1987. doi:10.1037/0735-7036.101.1.60.

**Kelly JB**, **Kidd SA**. NMDA and AMPA receptors in the dorsal nucleus of the lateral lemniscus shape binaural responses in rat inferior colliculus. *J Neurophysiol* , 2000. doi:10.1152/jn.2000.83.3.1403.

**Kelly JB**, **Li L**, **Van Adel B**. Sound localization after kainic acid lesions of the dorsal nucleus of the lateral lemniscus in the albino rat. *Behav Neurosci* , 1996. doi:10.1037/0735-7044.110.6.1445.

**Kelly JB**, **Masterton B**. Auditory sensitivity of the albino rat. *J Comp Physiol Psychol* , 1977. doi:10.1037/h0077356.

**King J**, **Insanally M**, **Jin M**, **Martins ARO**, **D'amour JA**, **Froemke RC**. Rodent auditory perception: Critical band limitations and plasticity. *Neuroscience* 2015.

**Klug A**, **Park TJ**, **Pollak GD**. Glycine and GABA influence binaural processing in the inferior colliculus of the mustache bat. *J Neurophysiol* , 1995. doi:10.1152/jn.1995.74.4.1701.

**Kopp-Scheinpflug C**, **Tolnai S**, **Malmierca MS**, **Rübsamen R**. The medial nucleus of the trapezoid body: Comparative physiology. *Neuroscience* , 2008. doi:10.1016/j.neuroscience.2008.01.088.

**Kulesza Jr. RJ**, **Berrebi AS**. Superior paraolivary nucleus of the rat is a GABAergic nucleus. *J Assoc Res Otolaryngol* , 2000.

**Kulesza RJ**. Cytoarchitecture of the human superior olivary complex: Nuclei of the trapezoid body and posterior tier. *Hear Res* , 2008. doi:10.1016/j.heares.2008.04.010.

**Kulesza RJ**, **Spirou GA**, **Berrebi AS**. Physiological response properties of neurons in the superior paraolivary nucleus of the rat. *J Neurophysiol* , 2003. doi:10.1152/jn.00547.2002.

**LeBeau FEN**, **Malmierca MS**, **Rees A**. Iontophoresis in vivo demonstrates a key role for GABAA and glycinergic inhibition in shaping frequency response areas in the inferior colliculus of guinea pig. *J Neurosci* , 2001. doi:10.1523/jneurosci.21-18-07303.2001.

**Ledoux JE**, **Ruggiero DA**, **Forest R**, **Stornetta R**, **Reis DJ**. Topographic organization of convergent projections to the thalamus from the inferior colliculus and spinal cord in the rat. *J Comp Neurol* , 1987. doi:10.1002/cne.902640110.

**LeDoux JE**, **Ruggiero DA**, **Reis DJ**. Projections to the subcortical forebrain from anatomically defined regions of the medial geniculate body in the rat. *J Comp Neurol* , 1985a. doi:10.1002/cne.902420204.

**LeDoux JE**, **SAKAGUCHI A**, **IWATA J**, **REIS DJ**. Auditory Emotional Memories: Establishment by Projections from the Medial Geniculate Nucleus to the Posterior Neostriatum and/or Dorsal Amygdala. *Ann N Y Acad Sci* , 1985b. doi:10.1111/j.1749-6632.1985.tb37611.x.

**LeDoux JE**, **Sakaguchi A**, **Reis DJ**. Subcortical efferent projections of the medial geniculate nucleus mediate emotional responses conditioned to acoustic stimuli. *J Neurosci* , 1984. doi:10.1523/jneurosci.04-03-00683.1984.

**Leppänen PHT**, **Eklund KM**, **Lyytinen H**. Event-Related Brain Potentials to Change in Rapidly Presented Acoustic Stimuli in Newborns. *Dev Neuropsychol* , 1997. doi:10.1080/87565649709540677.

**Li L**, **Kelly JB**. Inhibitory influence of the dorsal nucleus of the lateral lemniscus on binaural responses in the rat's inferior colliculus. *J Neurosci* , 1992.

**Li Y**, **Evans MS**, **Faingold CL**. In vitro electrophysiology of neurons in subnuclei of rat inferior colliculus. *Hear Res* , 1998. doi:10.1016/S0378-5955(98)00066-5.

**Lima JP**, **Ariga S**, **Velasco I**, **Schochat E**. Effect of the ketamine/xylazine anesthetic on the auditory brainstem response of adult gerbils. *Brazilian J Med Biol Res* , 2012. doi:10.1590/S0100-879X2012007500144.

**Lindsey BG**. Fine structure and distribution of axon terminals from cochlear nucleus on neurons in the medial superior olivary nucleus of the cat. *J Comp Neurol* , 1975. doi:10.1002/cne.901600106.

**Litovsky RY**. Speech intelligibility and spatial release from masking in young children. *J Acoust*

*Soc Am* , 2005. doi:10.1121/1.1873913.

**Litovsky RY**. Spatial Release from Masking. *Acoust Today* , 2012. doi:10.1121/1.4729575.

**Loftus WC**, **Malmierca MS**, **Bishop DC**, **Oliver DL**. The cytoarchitecture of the inferior colliculus revisited: A common organization of the lateral cortex in rat and cat. *Neuroscience* , 2008. doi:10.1016/j.neuroscience.2008.01.019.

**Lüscher C**, **Jan LY**, **Stoffel M**, **Malenka RC**, **Nicoll RA**. G protein-coupled inwardly rectifying K+ channels (GIRKs) mediate postsynaptic but not presynaptic transmitter actions in hippocampal neurons. *Neuron* , 1997. doi:10.1016/S0896-6273(00)80381-5.

**Ma CL**, **Kelly JB**, **Wu SH**. Presynaptic modulation of GABAergic inhibition by GABAB receptors in the rat's inferior colliculus. *Neuroscience* , 2002. doi:10.1016/S0306-4522(02)00130-6.

**Malmierca MS**. The structure and physiology of the rat auditory system: An overview. *Int. Rev. Neurobiol.* 2003.

**Malmierca MS**. Auditory System. In: *The Rat Nervous System: Fourth Edition*. 2015.

**Malmierca MS**, **Blackstad TW**, **Osen KK**, **Karagülle T**, **Molowny RL**. The central nucleus of the inferior colliculus in rat: A Golgi and computer reconstruction study of neuronal and laminar structure. *J Comp Neurol* , 1993. doi:10.1002/cne.903330102.

**Malmierca MS**, **Cristaudo S**, **Pérez-González D**, **Covey E**. Stimulus-specific adaptation in the inferior colliculus of the anesthetized rat. *J Neurosci* , 2009. doi:10.1523/JNEUROSCI.4153-08.2009.

**Malmierca MS**, **Hernández O**, **Rees A**. Intercollicular commissural projections modulate neuronal responses in the inferior colliculus. *Eur J Neurosci* , 2005a. doi:10.1111/j.1460-9568.2005.04103.x.

**Malmierca MS**, **Saint Marie RL**, **Merchan MA**, **Oliver DL**. Laminar inputs from dorsal cochlear nucleus and ventral cochlear nucleus to the central nucleus of the inferior colliculus: Two patterns of convergence. *Neuroscience* , 2005b. doi:10.1016/j.neuroscience.2005.04.040.

**Malmierca MS**, **Merchán M**. Computer-assisted 3-D reconstructions of Golgi-impregnated cells in the rat inferior colliculus. *Dpt. Cell Biol. Pathol.* 1991.

**Malmierca MS**, **Merchán MA**, **Henkel CK**, **Oliver DL**. Direct projections from cochlear nuclear complex to auditory thalamus in the rat. *J Neurosci* , 2002. doi:10.1523/jneurosci.22-24-10891.2002.

**Malmierca MS**, **Ryugo DK**. Descending connections of auditory cortex to the midbrain and brain stem. In: *The Auditory Cortex*. 2011.

**Malmierca MS**, **Seip KL**, **Osen KK**. Morphological classification and identification of neurons in the inferior colliculus: a multivariate analysis. *Anat Embryol (Berl)* , 1995. doi:10.1007/BF00534687.

**Saint Marie RL**, **Baker RA**. Neurotransmitter-specific uptake and retrograde transport of [3H]glycine from the inferior colliculus by ipsilateral projections of the superior olivary complex and nuclei of the lateral lemniscus. *Brain Res* , 1990. doi:10.1016/0006-8993(90)90698-B.

**Marie RLS**, **Ostapoff E -Michael**, **Morest DK**, **Wenthold RJ**. Glycine-immunoreactive

projection of the cat lateral superior olive: Possible role in midbrain ear dominance. *J Comp Neurol* , 1989. doi:10.1002/cne.902790305.

**May BJ**. Role of the dorsal cochlear nucleus in the sound localization behavior of cats. *Hear Res* , 2000. doi:10.1016/S0378-5955(00)00142-8.

**McCabe RT**, **Wamsley JK**, **Yezuita JP**, **Olsen RW**. A novel GABAA antagonist [3H]SR 95531: Microscopic analysis of binding in the rat brain and allosteric modulation by several benzodiazepine and barbiturate receptor ligands. *Synapse* , 1988. doi:10.1002/syn.890020208.

**Merchán MA**, **Berbel P**. Anatomy of the ventral nucleus of the lateral lemniscus in rats: A nucleus with a concentric laminar organization. *J Comp Neurol* , 1996. doi:10.1002/(SICI)1096-9861(19960819)372:2<245::AID-CNE7>3.0.CO;2-3.

**Merchán MA**, **Saldaña E**, **Plaza I**. Dorsal nucleus of the lateral lemniscus in the rat: Concentric organization and tonotopic projection to the inferior colliculus. *J Comp Neurol* , 1994. doi:10.1002/cne.903420209.

**Milbrandt JC**, **Albin RL**, **Caspary DMC**. Age-related decrease in GABAB receptor binding in the Fischer 344 rat i inferior colliculus. *Neurobiol Aging* , 1994. doi:10.1016/0197-4580(94)90051-5.

**Milbrandt JC**, **Albin RL**, **Turgeon SM**, **Caspary DM**. GABAA receptor binding in the aging rat inferior colliculus. *Neuroscience* , 1996. doi:10.1016/0306-4522(96)00050-4.

**Moore DR**, **Kotak VC**, **Sanes DH**. Commissural and lemniscal synaptic input to the gerbil inferior colliculus. *J Neurophysiol* , 1998. doi:10.1152/jn.1998.80.5.2229.

**Moore JK**, **Moore RY**. A comparative study of the superior olivary complex in the primate brain. *Folia Primatol* , 1971. doi:10.1159/000155390.

**Moore MJ**, **Caspary DM**. Strychnine blocks binaural inhibition in lateral superior olivary neurons. *J Neurosci* , 1983. doi:10.1523/jneurosci.03-01-00237.1983.

**Moriizumi T**, **Hattori T**. Pyramidal cells in rat temporoauditory cortex project to both striatum and inferior colliculus. *Brain Res Bull* , 1991. doi:10.1016/0361-9230(91)90297-W.

**Näätänen R**, **Gaillard AWK**, **Mäntysalo S**. Early selective-attention effect on evoked potential reinterpreted. *Acta Psychol (Amst)* , 1978. doi:10.1016/0001-6918(78)90006-9.

**Näätänen R**, **Paavilainen P**, **Alho K**, **Reinikainen K**, **Sams M**. The mismatch negativity to intensity changes in an auditory stimulus sequence. *Electroencephalogr Clin Neurophysiol Suppl* , 1987.

**Nadol JB**. Comparative anatomy of the cochlea and auditory nerve in mammals. *Hear Res* , 1988. doi:10.1016/0378-5955(88)90006-8.

**Nayagam DAX**, **Clarey JC**, **Paolini AG**. Powerful, onset inhibition in the ventral nucleus of the lateral lemniscus. *J Neurophysiol* , 2005. doi:10.1152/jn.00167.2005.

**Okoyama S**, **Ohbayashi M**, **Ito M**, **Harada S**. Neuronal organization of the rat inferior colliculus participating in four major auditory pathwaystle. *Hear Res* 218: 72–80, 2006.

**Oliver D**, **Ostapoff E**, **Beckius GE**. Direct innervation of identified tectothalamic neurons in the inferior colliculus by axons from the cochlear nucleus. *Neuroscience* 93: 643–658, 1999.

**Oliver DL**, **Beckius GE**, **Bishop DC**, **Kuwada S**. Simultaneous anterograde labeling of axonal

layers from lateral superior olive and dorsal cochlear nucleus in the inferior colliculus of cat. *J Comp Neurol* , 1997. doi:10.1002/(SICI)1096-9861(19970602)382:2<215::AID-CNE6>3.0.CO;2-6.

**Oliver DL**, **Shneiderman A**. An EM study of the dorsal nucleus of the lateral lemniscus: Inhibitory, commissural, synaptic connections between ascending auditory pathways. *J Neurosci* , 1989. doi:10.1523/jneurosci.09-03-00967.1989.

**Olpe HR**, **Karlsson G**, **Pozza MF**, **Brugger F**, **Steinmann M**, **Van Riezen H**, **Fagg G**, **Hall RG**, **Froestl W**, **Bittiger H**. CGP 35348: a centrally active blocker of GABAB receptors. *Eur J Pharmacol* , 1990. doi:10.1016/0014-2999(90)90337-6.

**Osen KK**, **Mugnaini E**, **Dahl AL**, **Christiansen AH**. Histochemical localization of acetylcholinesterase in the cochlear and superior olivary nuclei. A reappraisal with emphasis on the cochlear granule cell system. *Arch Ital Biol* , 1984. doi:10.4449/aib.v122i3.3223.

**Ottersen OP**, **Ben-Ari Y**. Afferent connections to the amygdaloid complex of the rat and cat. I. Projections from the thalamus. *J Comp Neurol* , 1979. doi:10.1002/cne.901870209.

**Paavilainen P**, **Karlsson ML**, **Reinikainen K**, **Näätänen R**. Mismatch negativity to change in spatial location of an auditory stimulus. *Electroencephalogr Clin Neurophysiol* , 1989. doi:10.1016/0013-4694(89)90192-2.

**Palmer AR**, **Kuwada S**. Binaural and spatial coding in the inferior colliculus. In: *The Inferior Colliculus*. 2005.

**Pérez-González D**, **Hernández O**, **Covey E**, **Malmierca MS**. GABA A-mediated inhibition

modulates stimulus-specific adaptation in the inferior colliculus. *PLoS One* , 2012. doi:10.1371/journal.pone.0034297.

**Pérez-González D**, **Malmierca MS**, **Moore JM**, **Hernández O**, **Covey E**. Duration selective neurons in the inferior colliculus of the rat: Topographic distribution and relation of duration sensitivity to other response properties. *J Neurophysiol* , 2006. doi:10.1152/jn.00741.2005.

**Peruzzi D**, **Bartlett E**, **Smith PH**, **Oliver DL**. A monosynaptic GABAergic input from the inferior colliculus to the medial geniculate body in rat. *J Neurosci* , 1997. doi:10.1523/jneurosci.17-10-03766.1997.

**Peruzzi D**, **Sivaramakrishnan S**, **Oliver DL**. Identification of cell types in brain slices of the inferior colliculus. *Neuroscience* , 2000. doi:10.1016/S0306-4522(00)00382-1.

**Plomp R**, **Mimpen AM**. EFFECT OF THE ORIENTATION OF THE SPEAKER'S HEASPEECHD AND THE AZIMUTH OF A NOISE SOURCE ON THE -RECEPTION THRESHOLD FOR SENTENCES. *Acustica* , 1981.

**Polley DB**, **Read HL**, **Storace DA**, **Merzenich MM**. Multiparametric auditory receptive field organization across five cortical fields in the albino rat. *J Neurophysiol* , 2007. doi:10.1152/jn.01298.2006.

**Potash M**, **Kelly J**. Development of directional responses to sounds in the rat (Rattus norvegicus). *J Comp Physiol Psychol* , 1980. doi:10.1037/h0077819.

**Pulkki V**, **Karjalainen M**. *Communication Acoustics an Introduction to Speech, Audio and Psychoacoustics*. John Wiley & Sons, Ltd, 2015.

**Regan D**. Evoked Potentials in Psychology, Sensory Physiology and Clinical Medicine. 1972.

**Rietzel HJ**, **Friauf E**. Neuron types in the rat lateral superior olive and developmental changes in the complexity of their dendritic arbors. *J Comp Neurol* , 1998. doi:10.1002/(SICI)1096-9861(19980105)390:1<20::AID-CNE3>3.0.CO;2-S.

**Riquelme R**, **Saldaña E**, **Osen KK**, **Ottersen OP**, **Merchán MA**. Colocalization of GABA and glycine in the ventral nucleus of the lateral lemniscus in rat: An in situ hybridization and semiquantitative immunocytochemical study. *J Comp Neurol* , 2001. doi:10.1002/cne.1111.

**Romanski LM**, **LeDoux JE**. Equipotentiality of thalamo-amygdala and thalamo-cortico-amygdala circuits in auditory fear conditioning. *J Neurosci* , 1992. doi:10.1523/jneurosci.12-11-04501.1992.

**Saldaña E**. Descending projections from the inferior colliculus to the cochlear nuclei in mammals. In: *The Mammalian Cochlear Nuclei, Organization and Function*, edited by M. Merchán JJ, Godfrey DA, Muganini E. New York: Plenum Press, 1993, p. 153–166.

**Saldaña E**, **Aparicio MA**, **Fuentes-Santamaría V**, **Berrebi AS**. Connections of the superior paraolivary nucleus of the rat: projections to the inferior colliculus. *Neuroscience* , 2009. doi:10.1016/j.neuroscience.2009.06.030.

**Saldaña E**, **Feliciano M**, **Mugnaini E**. Distribution of descending projections from primary auditory neocortex to inferior colliculus mimics the topography of intracollicular projections. *J Comp Neurol* , 1996. doi:10.1002/(SICI)1096-9861(19960715)371:1<15::AID-CNE2>3.0.CO;2-O.

**Saldaña E**, **Merchán MA**. Intrinsic and commissural connections of the inferior colliculus. In: *The Inferior Colliculus*. 2005.

**Sally SL**, **Kelly JB**. Effects of superior olivary comples lesions on binaural responses in rat inferior colliculus. *Brain Res* , 1992. doi:10.1016/0006-8993(92)90444-E.

**Sams M**, **Paavilainen P**, **Alho K**, **Näätänen R**. Auditory frequency discrimination and event-related potentials. *Electroencephalogr Clin Neurophysiol Evoked Potentials* , 1985. doi:10.1016/0168-5597(85)90054-1.

**Schröger E**, **Wolff C**. Mismatch response of the human brain to changes in sound location. *Neuroreport* , 1996. doi:10.1097/00001756-199611250-00041.

**Semple MN**, **Aitkin LM**, **Calford MB**, **Pettigrew JD**, **Phillips DP**. Spatial receptive fields in the cat inferior colliculus. *Hear Res* , 1983. doi:10.1016/0378-5955(83)90054-0.

**Senatorov V V.**, **Hu B**. Extracortical descending projections to the rat inferior colliculus. *Neuroscience* , 2002. doi:10.1016/S0306-4522(02)00316-0.

**Shneiderman A**, **Henkel CK**. Banding of lateral superior olivary nucleus afferents in the inferior colliculus: A possible substrate for sensory integration. *J Comp Neurol* , 1987. doi:10.1002/cne.902660406.

**Shneiderman A**, **Oliver DL**, **Henkel CK**. Connections of the dorsal nucleus of the lateral lemniscus: An inhibitory parallel pathway in the ascending auditory system? *J Comp Neurol* , 1988. doi:10.1002/cne.902760204.

**Shu Hui Wu**, **Kelly JB**. Binaural interaction in the lateral superior olive: Time difference

sensitivity studied in mouse brain slice. *J Neurophysiol* , 1992. doi:10.1152/jn.1992.68.4.1151.

**Small AM**. Pure-Tone Masking. *J Acoust Soc Am* , 1959. doi:10.1121/1.1907670.

**Smith PH**. Structural and functional differences distinguish principal from nonprincipal cells in the guinea pig MSO slice. *J Neurophysiol* 73: 1653–1667, 1995.

**Smith PH**, **Uhlrich DJ**, **Manning KA**, **Banks MI**. Thalamocortical projections to rat auditory cortex from the ventral and dorsal divisions of the medial geniculate nucleus. *J Comp Neurol* 34–51, 2012.

**Sommer I**, **Lingenhöhl K**, **Friauf E**. Principal cells of the rat medial nucleus of the trapezoid body: an intracellular in vivo study of their physiology and morphology. *Exp Brain Res* , 1993. doi:10.1007/BF00229781.

**Spangler KM**, **Warr WB**. The descending auditory system. New York: Raven Press, 1991, p. 27–45.

**Storace DA**, **Higgins NC**, **Read HL**. Thalamic label patterns suggest primary and ventral auditory fields are distinct core regions. *J Comp Neurol* 1630–1646, 2010.

**Talwar SK**, **Gerstein GL**. Auditory frequency discrimination in the white rat. *Hear Res* , 1998. doi:10.1016/S0378-5955(98)00162-2.

**Tan ML**, **Theeuwes HP**, **Feenstra L**, **Borst JGG**. Membrane properties and firing patterns of inferior colliculus neurons: An in vivo patch-clamp study in rodents. *J Neurophysiol* , 2007. doi:10.1152/jn.01273.2006.

**Thompson AM**, **Schofield BR**. Afferent projections of the superior olivary complex. *Microsc*

*Res Tech* , 2000. doi:10.1002/1097-0029(20001115)51:4<330::AID-JEMT4>3.0.CO;2-X.

**Tolnai S**, **Hernandez O**, **Englitz B**, **Rübsamen R**, **Malmierca MS**. The medial nucleus of the trapezoid body in rat: Spectral and temporal properties vary with anatomical location of the units. *Eur J Neurosci* , 2008. doi:10.1111/j.1460-9568.2008.06228.x.

**Vater M**, **Covey E**, **Casseday JH**. The columnar region of the ventral nucleus of the lateral lemniscus in the big brown bat (Eptesicus fuscus): Synaptic arrangements and structural correlates of feedforward inhibitory function. *Cell Tissue Res* , 1997. doi:10.1007/s004410050869.

**Vater M**, **Habbicht H**, **Kössl M**, **Grothe B**. The functional role of GABA and glycine in monaural and binaural processing in the inferior colliculus of horseshoe bats. *J Comp Physiol A* , 1992a. doi:10.1007/BF00194587.

**Vater M**, **Kössl M**, **Horn AKE**. GAD- and GABA-immunoreactivity in the ascending auditory pathway of horseshoe and mustached bats. *J Comp Neurol* , 1992b. doi:10.1002/cne.903250205.

**Vaughn MD**, **Pozza MF**, **Lingenhöhl K**. Excitatory acoustic responses in the inferior colliculus of the rat are increased by GABA(B) receptor blockade. *Neuropharmacology* , 1996. doi:10.1016/S0028-3908(96)00143-8.

**Warr WB**. Fiber degeneration following lesions in the anterior ventral cochlear nucleus of the cat. *Exp Neurol* , 1966. doi:10.1016/0014-4886(66)90130-0.

**Weedman DL**, **Ryugo DK**. Projections from auditory cortex to the cochlear nucleus in rats: Synapses on granule cell dendrites. *J Comp Neurol* , 1996. doi:10.1002/(SICI)1096-

9861(19960722)371:2<311::AID-CNE10>3.3.CO;2-U.

**Wenstrup JJ**, **Fuzessery ZM**, **Pollak GD**. Binaural neurons in the mustache bat's inferior colliculus. II. Determinants of spatial responses among 60-kHz EI units. *J Neurophysiol* , 1988a. doi:10.1152/jn.1988.60.4.1384.

**Wenstrup JJ**, **Fuzessery ZM**, **Pollak GD**. Binaural neurons in the mustache bat's inferior colliculus. I. Responses of 6-kHz EI units to dichotic sound stimulation. *J Neurophysiol* , 1988b. doi:10.1152/jn.1988.60.4.1369.

**Whitley JM**, **Henkel CK**. Topographical organization of the inferior collicular projection and other connections of the ventral nucleus of the lateral lemniscus in the cat. *J Comp Neurol* , 1984. doi:10.1002/cne.902290210.

**Winer JA**. The Functional Architecture of the Medial Geniculate Body and the Primary Auditory Cortex. 1992.

**Winer JA**, **Kelly JB**, **Larue DT**. Neural architecture of the rat medial geniculate body. *Hear Res* , 1999a. doi:10.1016/S0378-5955(98)00216-0.

**Winer JA**, **Larue DT**. Patterns of reciprocity in auditory thalamocortical and corticothalamic connections: Study with horseradish peroxidase and autoradiographic methods in the rat medial geniculate body. *J Comp Neurol* , 1987. doi:10.1002/cne.902570212.

**Winer JA**, **Larue DT**, **Kelly JB**. Neural architecture of the rat medial geniculate body. *Hear Res* 130: 19–41, 1999b.

**Winer JA**, **Saint Marie RL**, **Larue DT**, **Oliver DL**. GABAergic feedforward projections from

the inferior colliculus to the medial geniculate body. *Proc Natl Acad Sci U S A* , 1996. doi:10.1073/pnas.93.15.8005.

**Wu GK**, **Li P**, **Tao HW**, **Zhang LI**. Nonmonotonic Synaptic Excitation and Imbalanced Inhibition Underlying Cortical Intensity Tuning. *Neuron* , 2006. doi:10.1016/j.neuron.2006.10.009.

**Xu H**, **Zhou KQ**, **Huang YN**, **Chen L**, **Xu T Le**. Taurine activates strychnine-sensitive glycine receptors in neurons of the rat inferior colliculus. *Brain Res* , 2004. doi:10.1016/j.brainres.2004.07.001.

**Xu J**, **Cooler DM**, **Feng AS**. Effects of sound direction on the processing of amplitude-modulated signals in the frog inferior colliculus. *J Comp Physiol A Sensory, Neural, Behav Physiol* , 1996. doi:10.1007/BF00190174.

**Yan W**, **Suga N**. Corticofugal modulation of the midbrain frequency map in the bat auditory system. *Nat Neurosci* , 1998. doi:10.1038/255.

**Young ED**, **Robert JM**, **Shofner WP**. Regularity and latency of units in ventral cochlear nucleus: Implications for unit classification and generation of response properties. *J Neurophysiol* , 1988. doi:10.1152/jn.1988.60.1.1.

**Young ED**, **Spirou GA**, **Rice JJ**, **Voigt HF**. Neural organization and responses to complex stimuli in the dorsal cochlear nucleus. *Philos. Trans. R. Soc. Lond. B. Biol. Sci.* 1992.

**Zhang DX**, **Li L**, **Kelly JB**, **Wu SH**. GABAergic projections from the lateral lemniscus to the inferior colliculus of the rat. *Hear Res* , 1998. doi:10.1016/S0378-5955(97)00202-5.

**Zhang H**, **Kelly JB**. Responses of neurons in the rat's ventral nucleus of the lateral lemniscus to monaural and binaural tone bursts. *J Neurophysiol* , 2006a. doi:10.1152/jn.01215.2005.

**Zhang H**, **Kelly JB**. Responses of neurons in the rat's ventral nucleus of the lateral lemniscus to amplitude-modulated tones. *J Neurophysiol* , 2006b. doi:10.1152/jn.00481.2006.

**Zhang H**, **Kelly JB**. Time-dependent effects of ipsilateral stimulation on contralaterally elicited responses in the rat's central nucleus of the inferior colliculus. *Brain Res* , 2009. doi:10.1016/j.brainres.2009.09.059.

**Zhang H**, **Kelly JB**. Time dependence of binaural responses in the rat's central nucleus of the inferior colliculus. *Hear Res* , 2010. doi:10.1016/j.heares.2010.06.010.

**Zhang Y**, **Wu SH**. Long-term potentiation in the inferior colliculus studied in rat brain slice. *Hear Res* , 2000. doi:10.1016/S0378-5955(00)00123-4.

**Zhao M**, **Wu SH**. Morphology and physiology of neurons in the ventral nucleus of the lateral lemniscus in rat brain slices. *J Comp Neurol* , 2001. doi:10.1002/cne.1139.

**Zilles K**, **Zilles B**, **Schleicher A**. A quantitative approach to cytoarchitectonics - VI. The Areal Pattern of the Cortex of the Albino Rat. *Anat Embryol (Berl)* , 1980. doi:10.1007/BF00317655.

# APPENDIX

**Calculation of drug dosages:**

Weight of the rat: 0.3 kg

**Ketamine dosage calculation for the initial injection:**

$$dosage(mL) = \frac{60mg}{kg} x \frac{10^{-3}mL}{1mg} x\ (weight\ of\ the\ rat\ in\ kg)$$

$$dosage(mL) = \frac{60mg}{kg} x \frac{10^{-3}mL}{1mg} x\ (0.3\ kg)$$

$$dosage(mL) = 0.018\ mL$$

**Ketamine dosage calculation for supplementary injection:**

$$\text{Supplementary dosage } = \frac{\text{intial dosage}}{3}$$

$$\text{Supplementary dosage } = \frac{0.018\ mL}{3}$$

$$\text{Supplementary dosage } = 0.006\ \text{mL}$$

**Xylazine dosage calculation for the initial injection:**

$$dosage(mL) = \frac{10\ mg}{kg} x \frac{10^{-3}mL}{1mg} x\ (weight\ of\ the\ rat\ in\ kg)$$

$$dosage(mL) = \frac{10\ mg}{kg} x \frac{10^{-3}mL}{1mg} x\ (0.3\ kg)$$

$$dosage(mL) = 0.003\ mL$$

**Xylazine dosage calculation for the supplementary injection:**

$$\text{Supplementary dosage } = \frac{\text{initial dosage}}{3}$$

$$\text{Supplementary dosage } = \frac{0.003\ mL}{3}$$

$$\text{Supplementary dosage } = 0.001\ \text{mL}$$

**Pentobarbital dosage calculation for euthanasia:**

$$dosage(mL) = \frac{\left[\frac{300\ mL}{540\ kg}\ x\ (0.3\ kg)\right]}{3}$$

$$dosage(mL) = \frac{\left[\frac{300mL}{540kg}\ x\ (0.3\ kg)\right]}{3}$$

$$dosage(mL) = 0.167\ mL$$

**Atropine dosage calculations:** same as xylazine supplemental dosage calculation

**Calculation of fH and fL:**

CF = 2000 Hz

Octaves between fH and fL= 0.1

Octaves between CF and fL= 0.05

Octaves between CF and fH = 0.05

**Sample Calculation of fH:**

$$Octaves = \log\left(\frac{fH}{CF}\right)$$

$$2^{Octaves} = \frac{\mathrm{fH}}{\mathrm{CF}}$$

$$2^{Octaves}CF = fH$$

**Sample Calculation of fL:**

$$Octaves = \log\left(\frac{CF}{fL}\right)$$

$$2^{Octaves} = \frac{\mathrm{CF}}{\mathrm{fL}}$$

$$fL = \frac{CF}{2^{Octaves}}$$

$2^{0.05}(2000Hz) = fH$

$2^{0.05}(2000Hz) = fH$

$2070.53\ Hz = fH$

$fL = \frac{2000}{2^{0.05}}$

$fL = \frac{2000}{2^{0.05}}$

$fL = 1931.87\ Hz$

**Sample calculation of NR and trough latencies**

**Sample calculation of NR**

$A_0$ is the trough amplitude of the leading sound presented alone.

$A_1$ is the trough amplitude of the trailing sound presented after one leading sound with an ISI of 24 ms.

$A_0$ = 0.060925423 mV

$A_1$ = 0.060466577 mV

**Sample calculation of trough latencies**

$T_0$ is the time when the trailing sound was presented to the rat at an ISI of 24 ms.

$T_1$ is a time when the trough of the trailing sound was observed.

Trough latency = $T_1 - T_0$

Trough latency = 37.03 ms – 24 ms

Trough latency = 13.03 ms

$$NR = \frac{A_1}{A_0}\ x\ 100$$

$$NR = \frac{0.060466577}{0.060925423}\ x\ 100$$

$$NdR = 99\%$$

**Sample calculation of the $ISI_{70}$ value:**

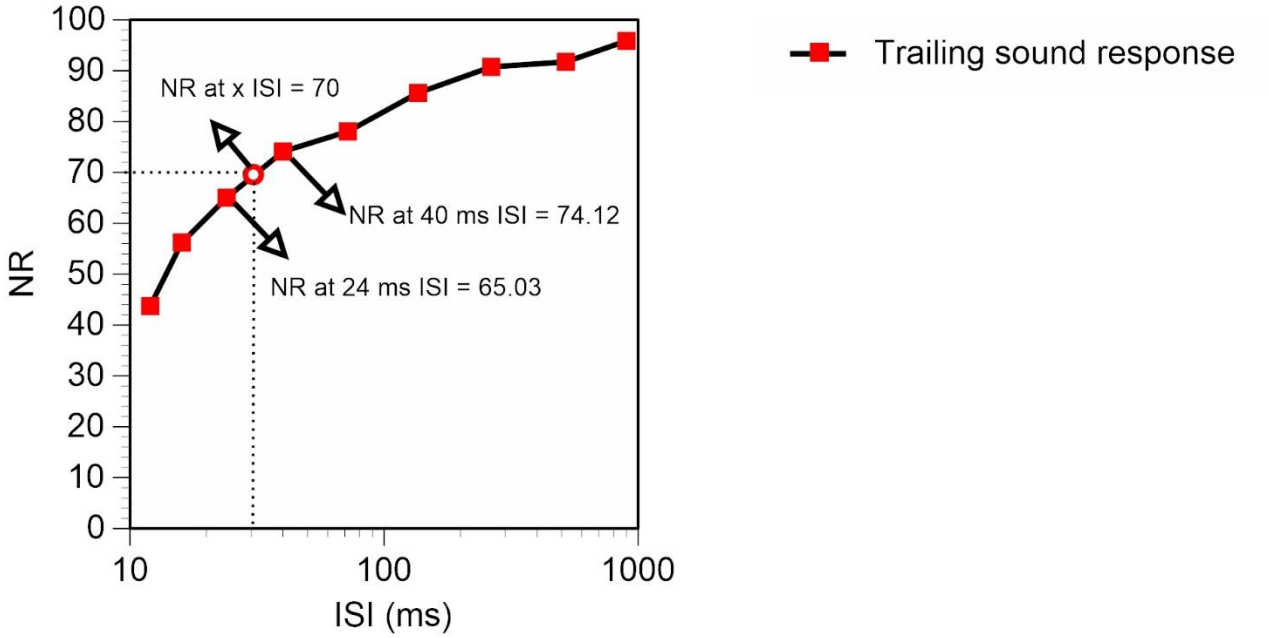


$(x_1, y_1) = (24, 65.03)$

$(x_2, y_2) = (40, 74.12)$

$(x, y) = (x, 70)$

$$x = \frac{(y - y_1)(x_2 - x_1)}{(y_2 - y_1)} + x_1$$

$$x = \frac{(70 - 65.03)(40 - 24)}{(74.12 - 65.03)} + 24$$

$$x = 32.75$$

Therefore, the ISI value at which NR is 70 is 32.75 ms.

# VITA AUCTORIS

Syed Anam Asim was born in Riyadh, Saudi Arabia. He moved to Canada in 2010 and completed his high school at Vincent Massey Secondary School in 2015. From there he studied Behaviour, Cognition, and Neuroscience at the University of Windsor and graduated with Great Distinction. He is currently completing his masters in Biological Sciences at the University of Windsor and hopes to graduate in the Fall of 2020.